

SUPPORTING MATERIAL FOR

Coumarin luciferins and mutant luciferases for robust multicomponent bioluminescence imaging

Zi Yao^{1,‡}, Donald R. Caldwell^{4,‡}, Anna C. Love^{1,‡}, Bethany Kolbaba-Kartchner^{5,6}, Jeremy H. Mills^{5,6}, Martin J. Schnermann^{4,*}, Jennifer A. Prescher^{1,2,3,*}

Departments of ¹Chemistry, ²Molecular Biology & Biochemistry, and ³Pharmaceutical Sciences, University of California, Irvine, Irvine CA, United States

⁴Chemical Biology Laboratory, Center for Cancer Research, National Cancer Institute, Frederick MD, United States

⁵School of Molecular Sciences, and ⁶The Biodesign Center for Molecular Design and Biomimetics, Arizona State University, Tempe AZ, United States

*Correspondence should be addressed to martin.schnermann@nih.gov and jpresche@uci.edu

‡These authors contributed equally to the work.

TABLE OF CONTENTS

Figures S1-S20	S2-15
Materials and Methods	S16-22
Rosetta Methods	S22-36
Synthetic Procedures	S36-41
References	S41-42
NMR Spectra	S43-60

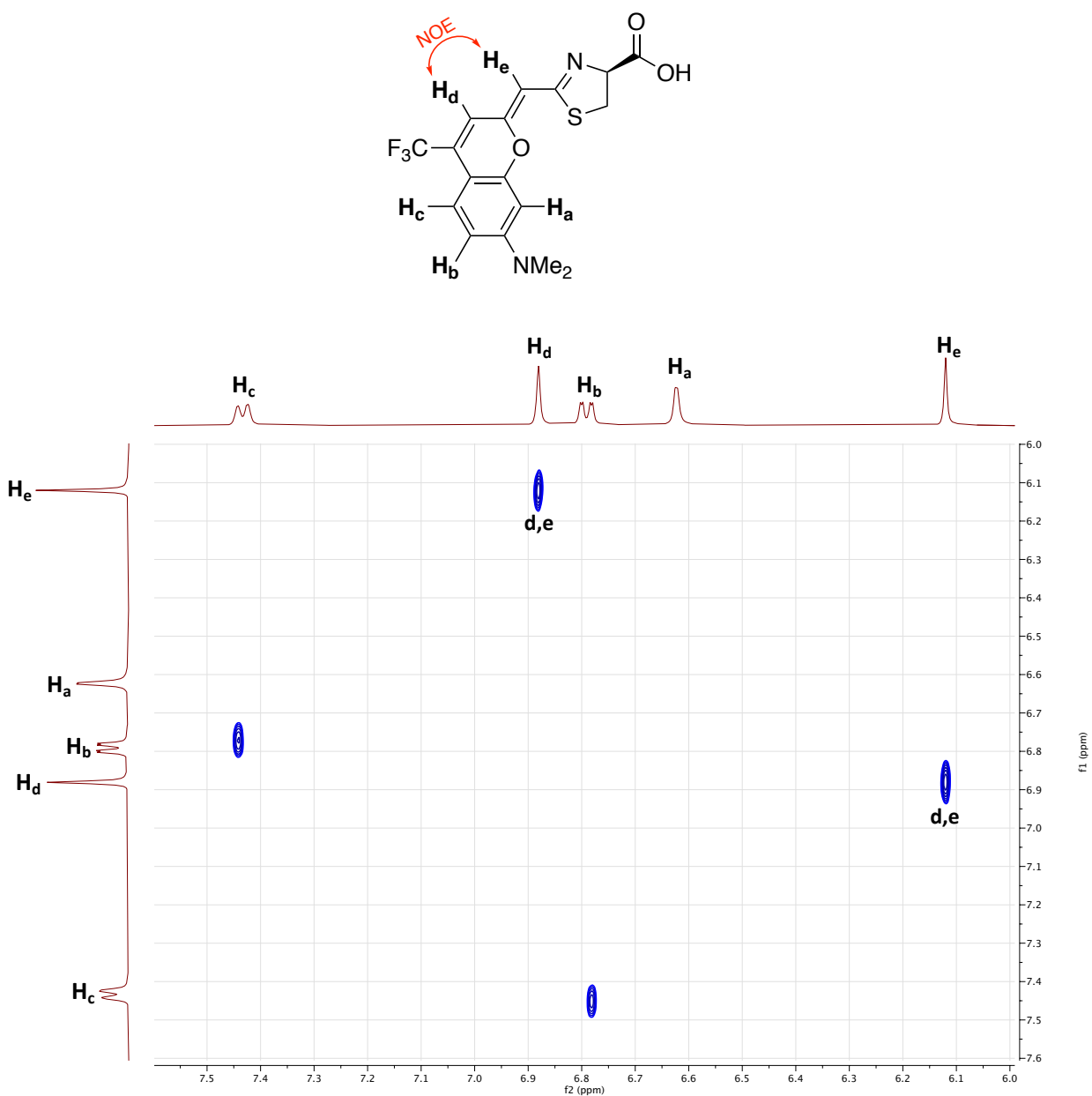


Figure S1. 2D NOESY spectrum (diagonal peak suppression) of CouLuc-1-NMe₂ in DMSO-*d*₆ showing the correlation of H_d and H_e.

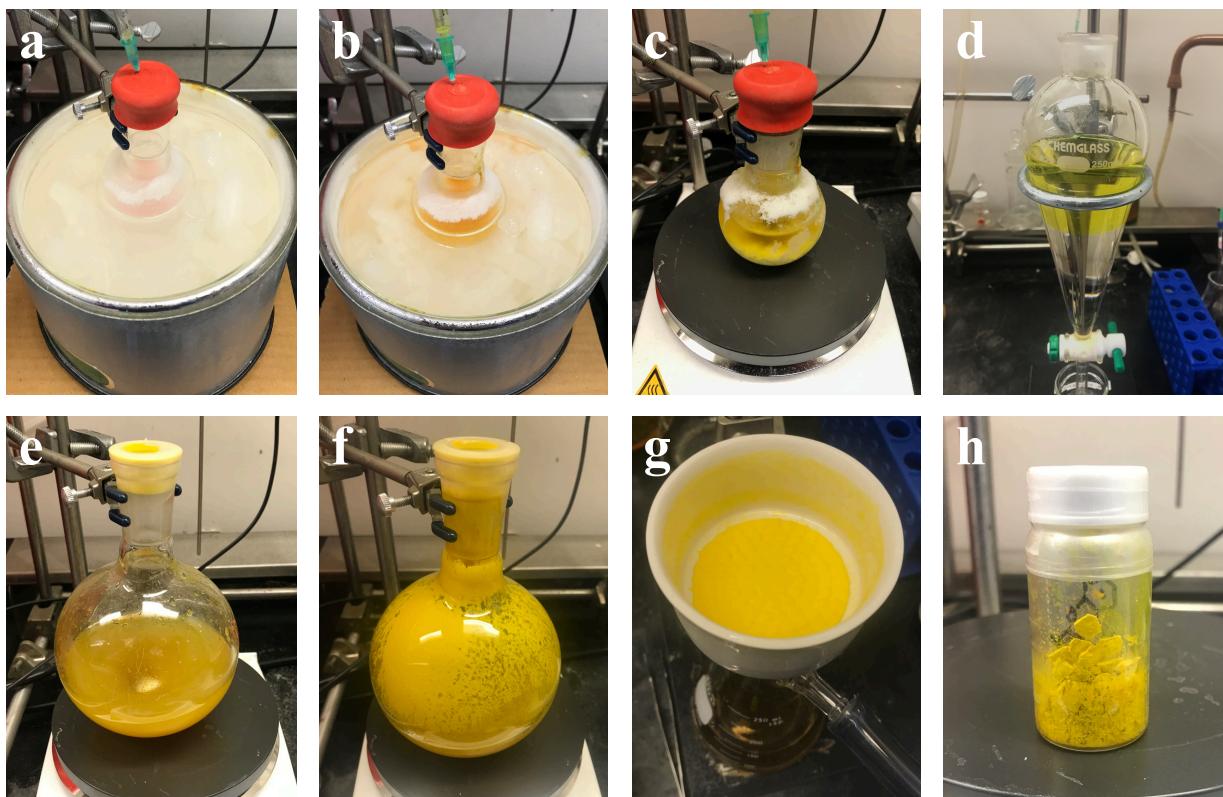
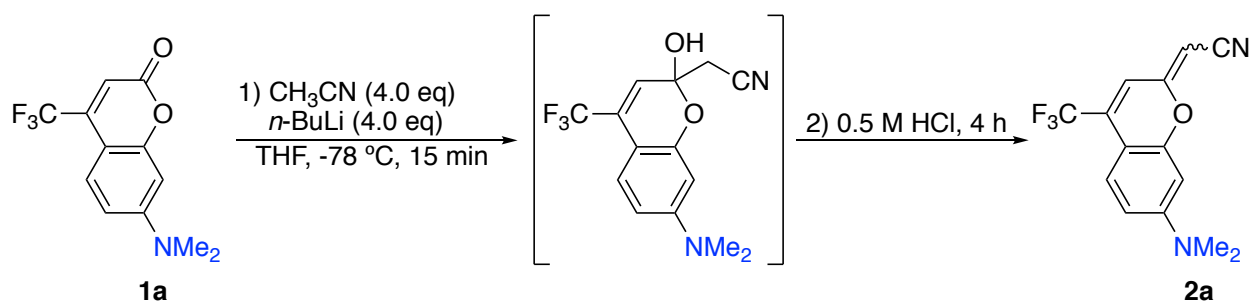


Figure S2. Chromatography-free synthesis of cyanomethylene coumarin 2a from commercial coumarin. Starting from a flame-dried round-bottom flask under nitrogen; (a) The flask was charged with THF, CH₃CN, and *n*-BuLi at $-78\text{ }^{\circ}\text{C}$; (b) After addition of coumarin **1a** in THF; (c) Reaction quenched with aqueous NH₄Cl solution and the $-78\text{ }^{\circ}\text{C}$ bath was removed; (d) Extraction with EtOAc; (e) Addition of 0.5 M HCl and stirred at 1000 rpm; (f) Precipitation of cyanomethylene coumarin **2a** as a yellow solid; (g) Vacuum filtration; (h) Isolated cyanomethylene coumarin **2a**.

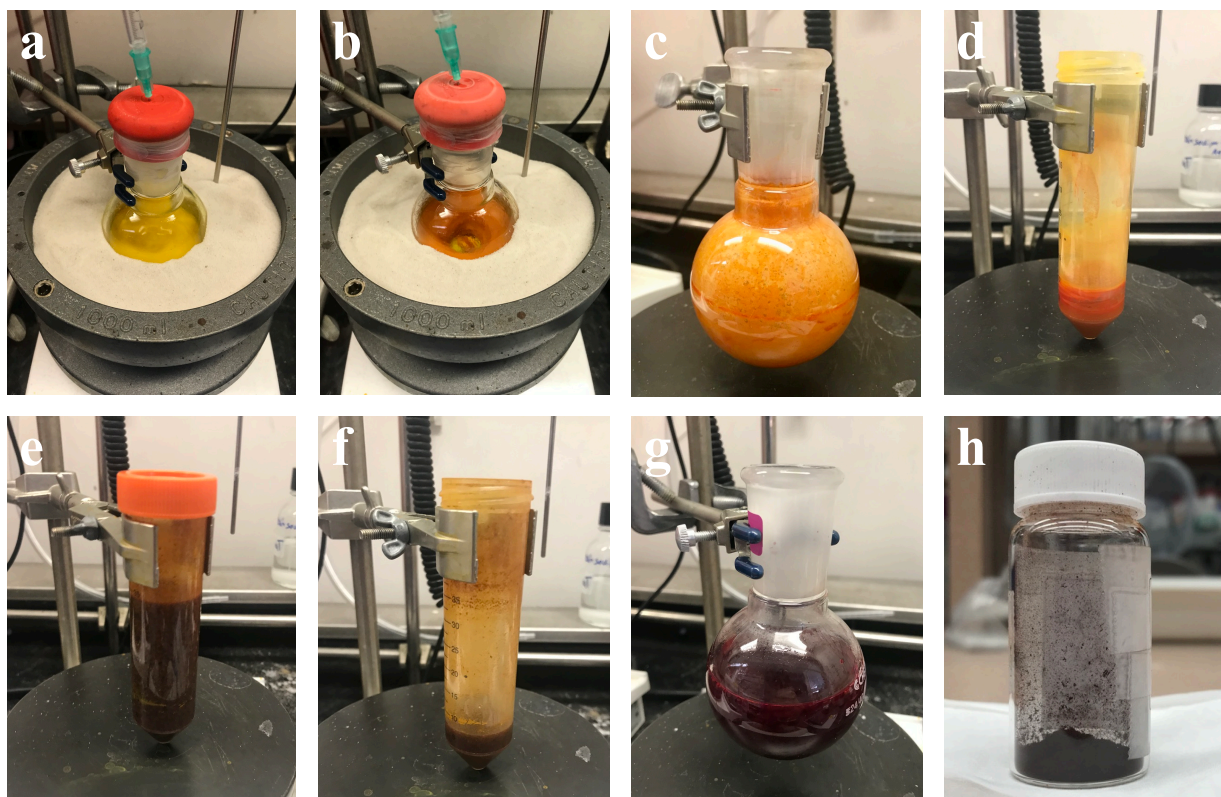
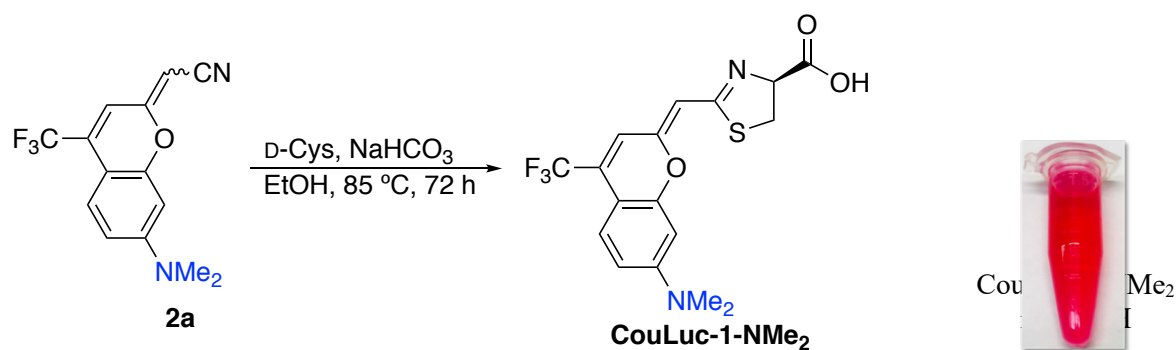


Figure S3. Chromatography-free synthesis of CouLuc-1-NMe₂ from cyanomethylene coumarin. Starting from a flame-dried round-bottom flask under nitrogen; (a) Flask charged with **2a**, D-cysteine, NaHCO₃ and degassed EtOH; (b) Reaction after >75% conversion; (c) Crude mixture after removing EtOH; (d) After triturating with EtOAc; (e) Color change after acidifying with 1.0 M HCl; (f) After centrifugation and supernatant removal; (g) Transferred product to round-bottomed flask with MeOH/H₂O, red color change; (h) Lyophilized CouLuc-1-NMe₂.

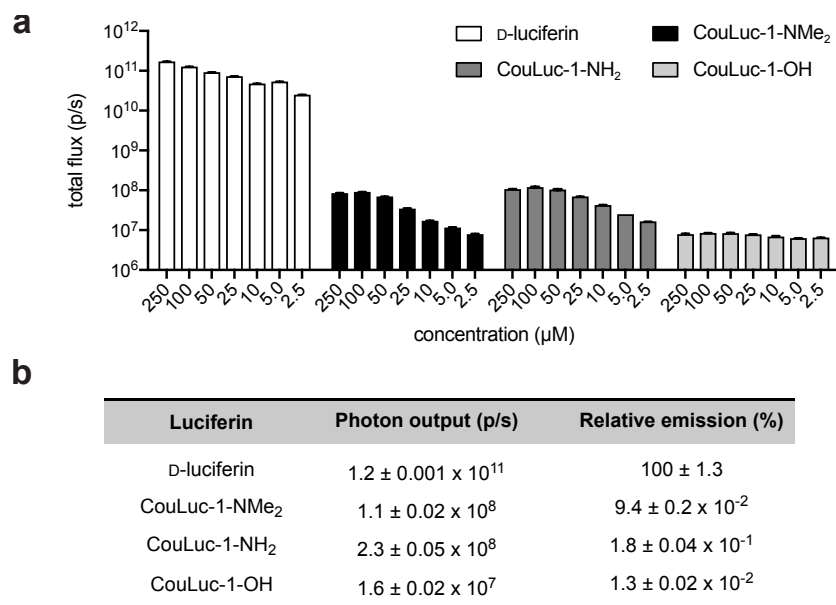


Figure S4. CouLuc-1 analogs are competent, albeit weak, emitters with Fluc. (a) Light emission of CouLuc-1 analogs (2.5–250 μ M) or D-luc (2.5–250 μ M) when incubated with ATP (1 mM), coenzyme A (1 mM) and recombinant Fluc (160 nM). Emission intensities are plotted as total photon flux values. Error bars represent the standard error of the mean for $n = 3$ experiments. (b) Tabulated photon outputs from (a). Relative emission values for each analog (compared to D-luc) at 100 μ M are also listed

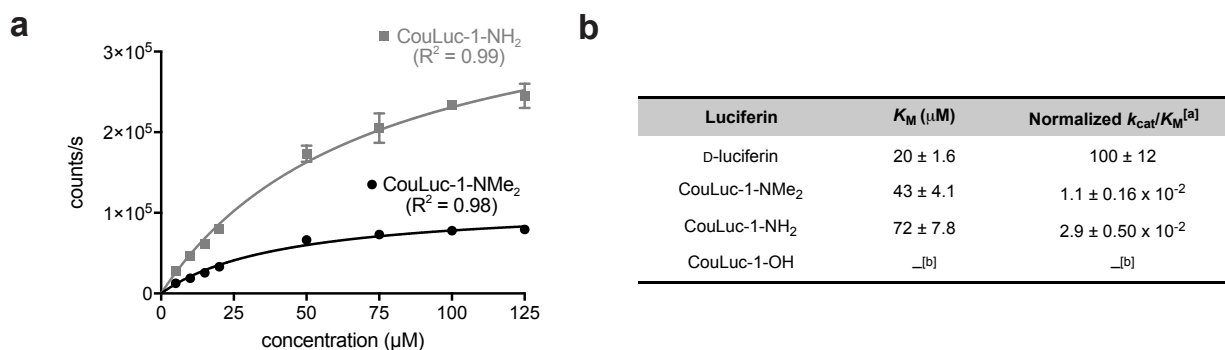


Figure S5. Biochemical analyses of Fluc with CouLuc-1 analogs. (a) Kinetics studies revealed CouLuc-1 analogs were poor binders of Fluc. (b) Kinetic constants shown are apparent values, determined via measurements of the initial rates of light emission over a range of substrate concentrations. ^[a]Values were normalized to emission of Fluc/D-luciferin. Error bars represent the standard error of the mean for $n = 3$ experiments. ^[b]Kinetic parameters could not be determined due to low levels of light production.

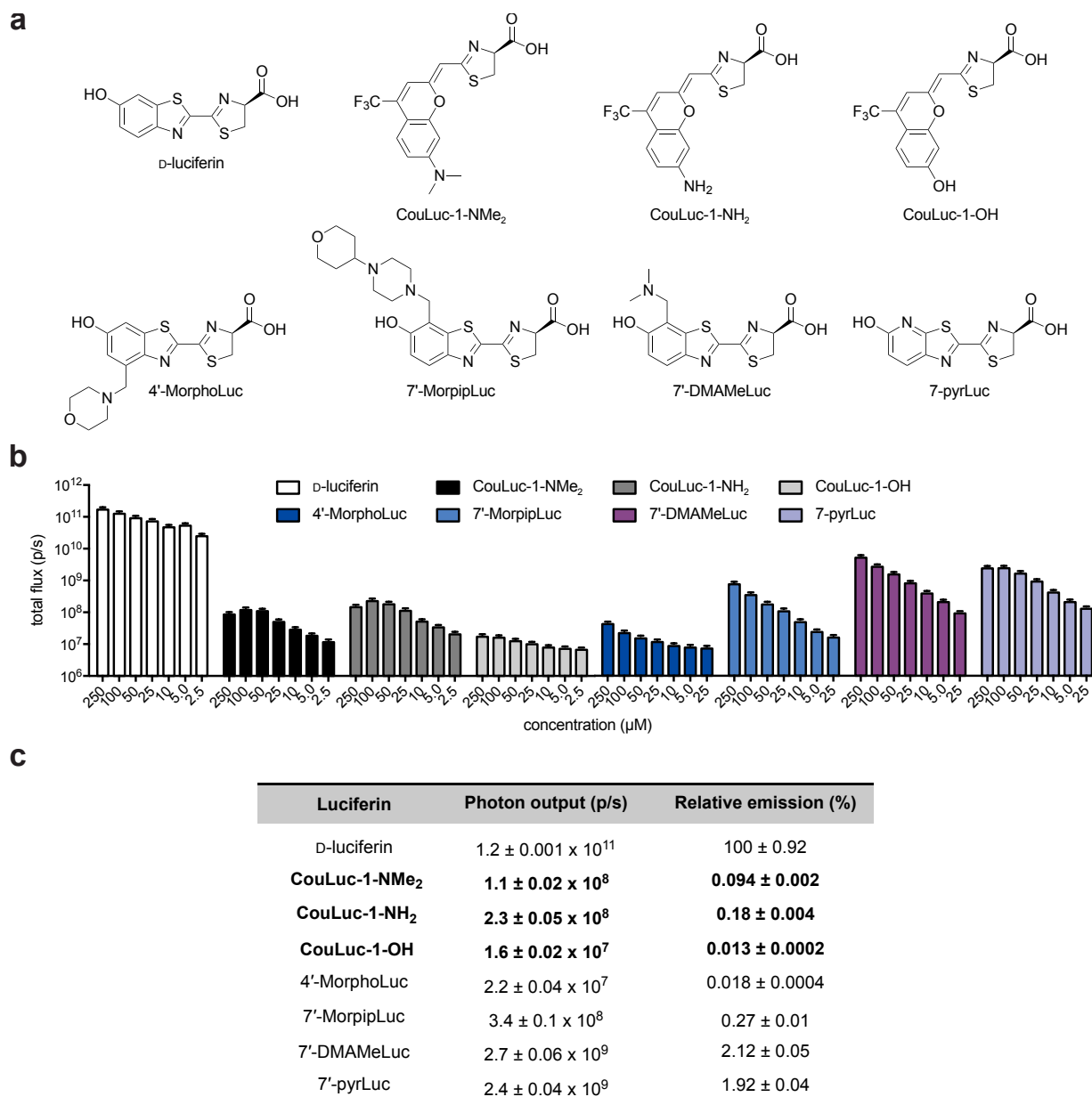


Figure S6. Comparison of CouLuc-1 analogs to other synthetic luciferins. (a) Chemical structures of the synthetic luciferins tested. (b) CouLuc-1 analogs or synthetic luciferins (2.5–250 μ M) were incubated with ATP (1 mM), coenzyme A (1 mM) and recombinant Fluc (160 nM). Emission intensities are plotted as total photon flux values. Error bars represent the standard error of the mean for $n = 3$ experiments. (c) Tabulated photon outputs from (b) with [luciferin] = 100 μ M. Relative emission values for each analog (compared to D-luciferin) are also listed.

Table S1. Bioluminescence and fluorescence emission of CouLuc-1 analogs.

Luciferin	BL λ_{max} (nm) (with Fluc)	FL λ_{max} (nm)		
		pH 7.4 PBS	MeOH	DMF
CouLuc-1-NMe ₂	620	627	650	609
CouLuc-1-NH ₂	597	593	588	476
CouLuc-1-OH	625	600	541	644

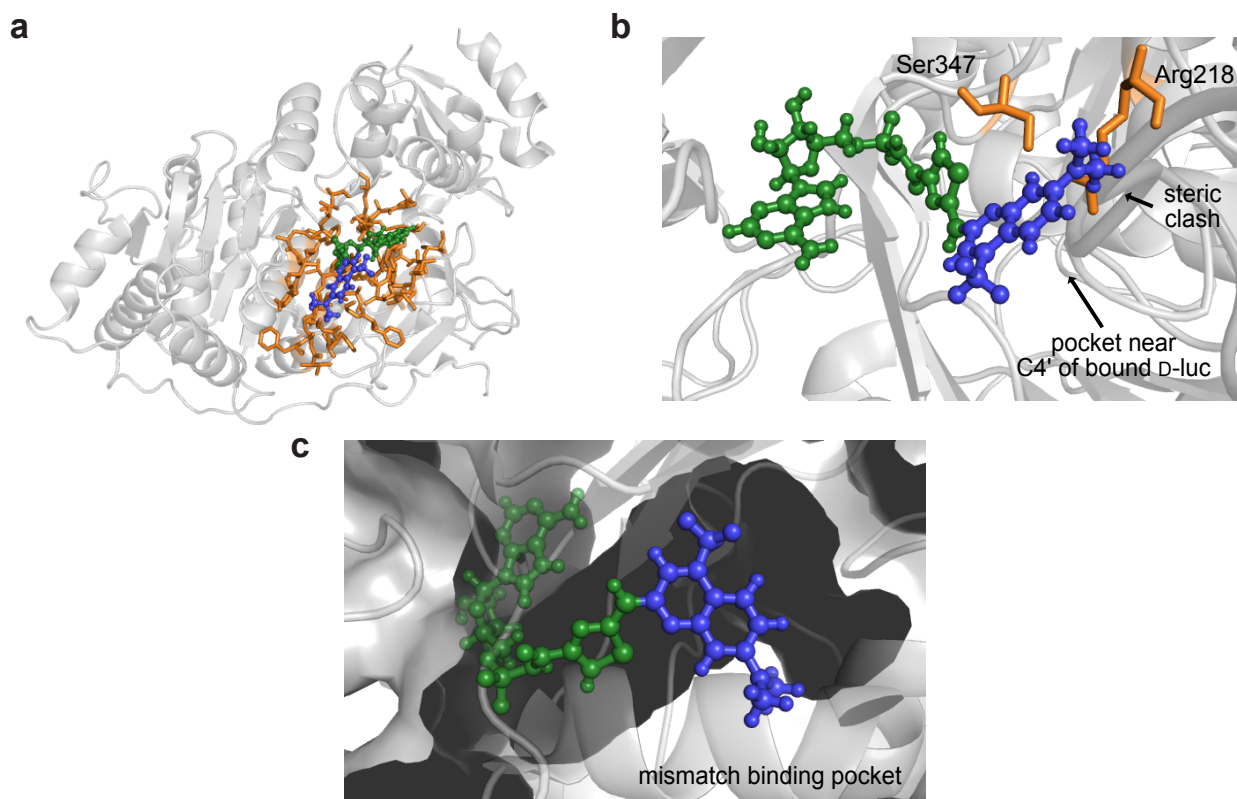


Figure S7. The binding pocket of Fluc does not accommodate the CouLuc-1 architecture. (a) CouLuc-1-NMe₂ was docked into the Fluc active site (PDB: 4G36) using the RosettaMatch algorithm.¹⁻² Residues within 5 Å of the bound luciferin are highlighted in orange. (b-c) Zoom-in view of (a). The coumarin portion of the luciferin is located near residues adjacent to C4' in bound D-luc.

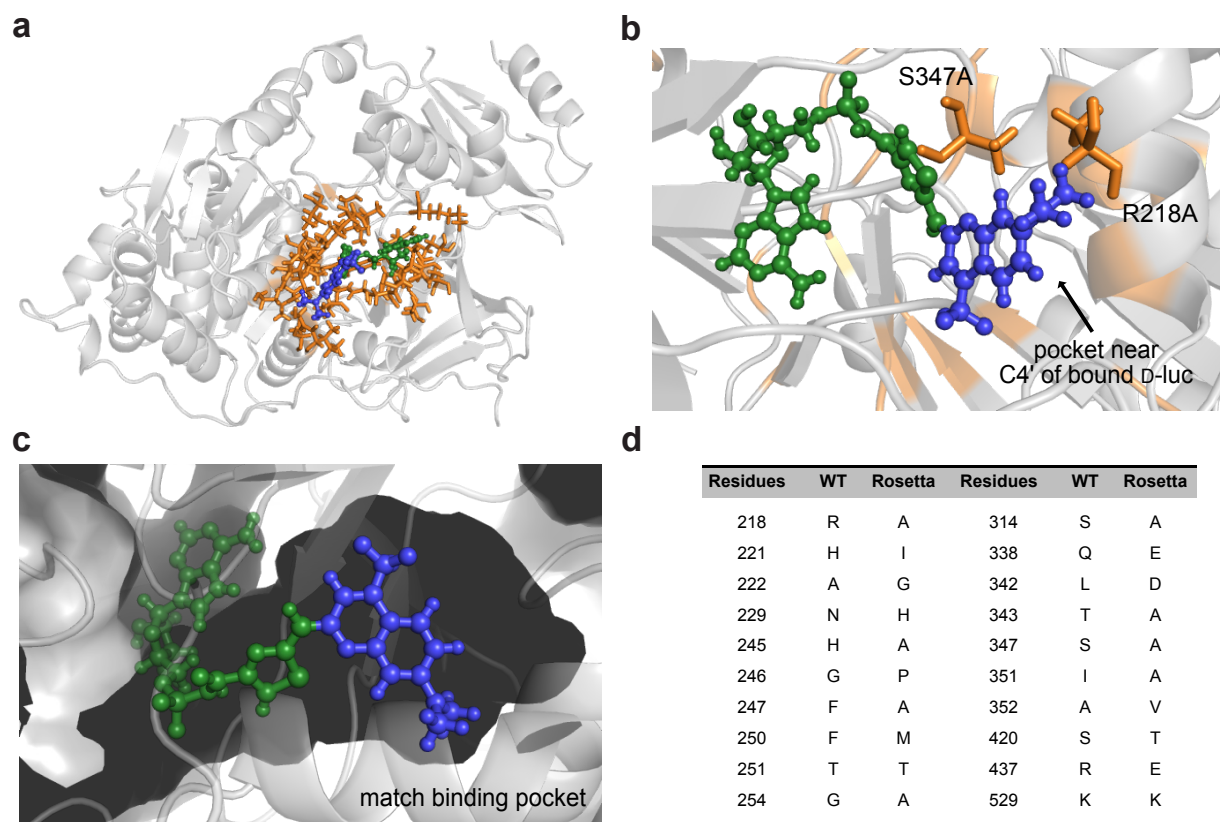


Figure S8. Searching for a complementary luciferase via Rosetta-guided library design. (a) Residues within 6 Å of the docked CouLuc-1-NMe₂ scaffold were subjected to RosettaDesign.¹⁻² From the analysis, 40 residues were mutated (orange). (b-c) Zoom-in view of (a). Active site residues sculpted to accommodate the CouLuc-1 structures mitigating the steric clash observed in Figure S7b was mitigated. (d). From the analysis, 20 of the 40 residues mutated by Rosetta were targeted for library construction.

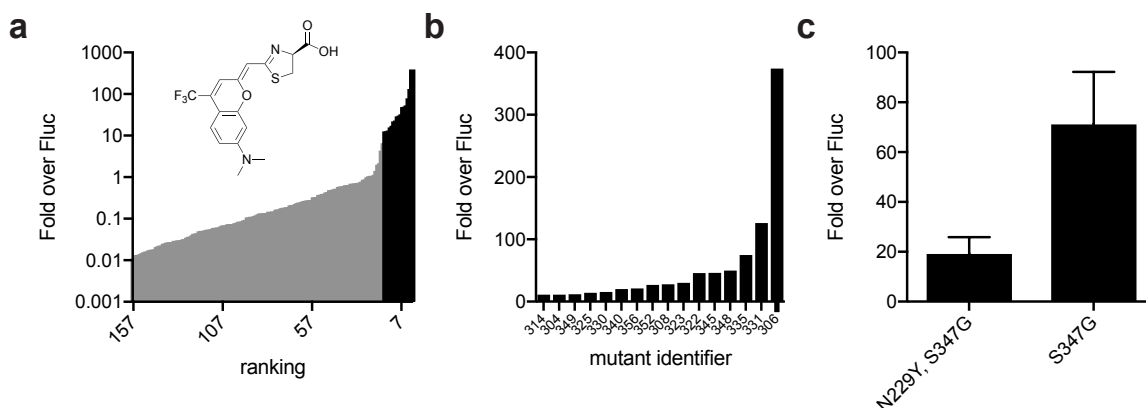


Figure S9. Evolving a brighter luciferase for CouLuc-1-NMe₂ via RosettaDesign. (a) Functional mutants identified from on-plate screens were picked and subjected to two secondary screens. In the first round, luciferase expression was auto-induced³ and mutants with >10-fold light emission (compared to Fluc) were re-examined via IPTG induction. (b) Variants with reproducible improvements were considered hits and sequenced. (c) Unique sequences identified from (b). Plasmids encoding mutant hits were isolated and re-introduced to *E. coli*. The magnitude of improvement was re-analyzed in a final assay using IPTG induction. Relative light emissions are plotted as fold over the native enzyme. Error bars represent the standard error of the mean for n = 3 experiments.

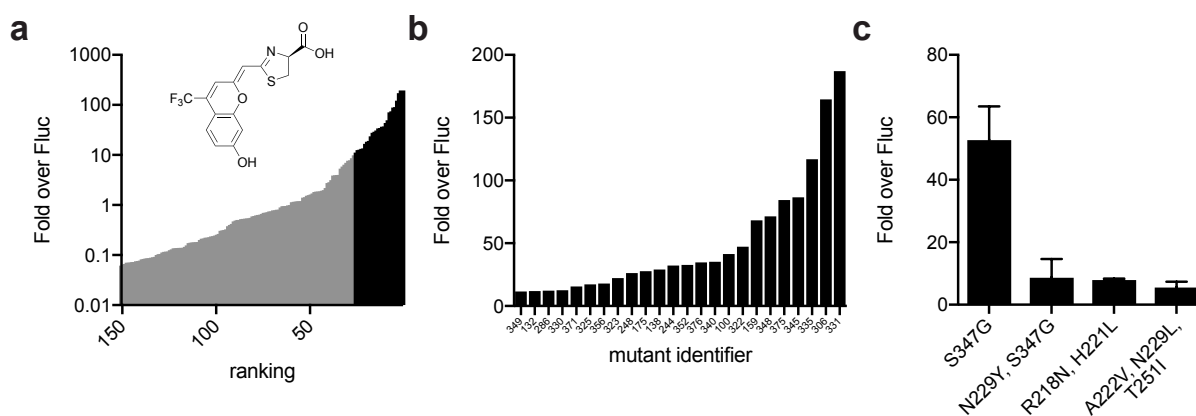


Figure S10. Evolving a brighter luciferase for CouLuc-1-OH via RosettaDesign. (a) Functional mutants identified from on-plate screens were picked and subjected to two secondary screens. In the first round, luciferase expression was autoinduced³ and mutants with >10-fold light emission (compared to Fluc) were re-examined via IPTG induction. (b) Variants with reproducible improvements were considered hits and sequenced. (c) Unique sequences identified from (b). Plasmids encoding these mutants were isolated and re-introduced to *E. coli*. The magnitude of improvement was re-analyzed in a final assay using IPTG induction. Relative light emissions are plotted as fold over the native enzyme. Error bars represent the standard error of the mean for n = 3 experiments.

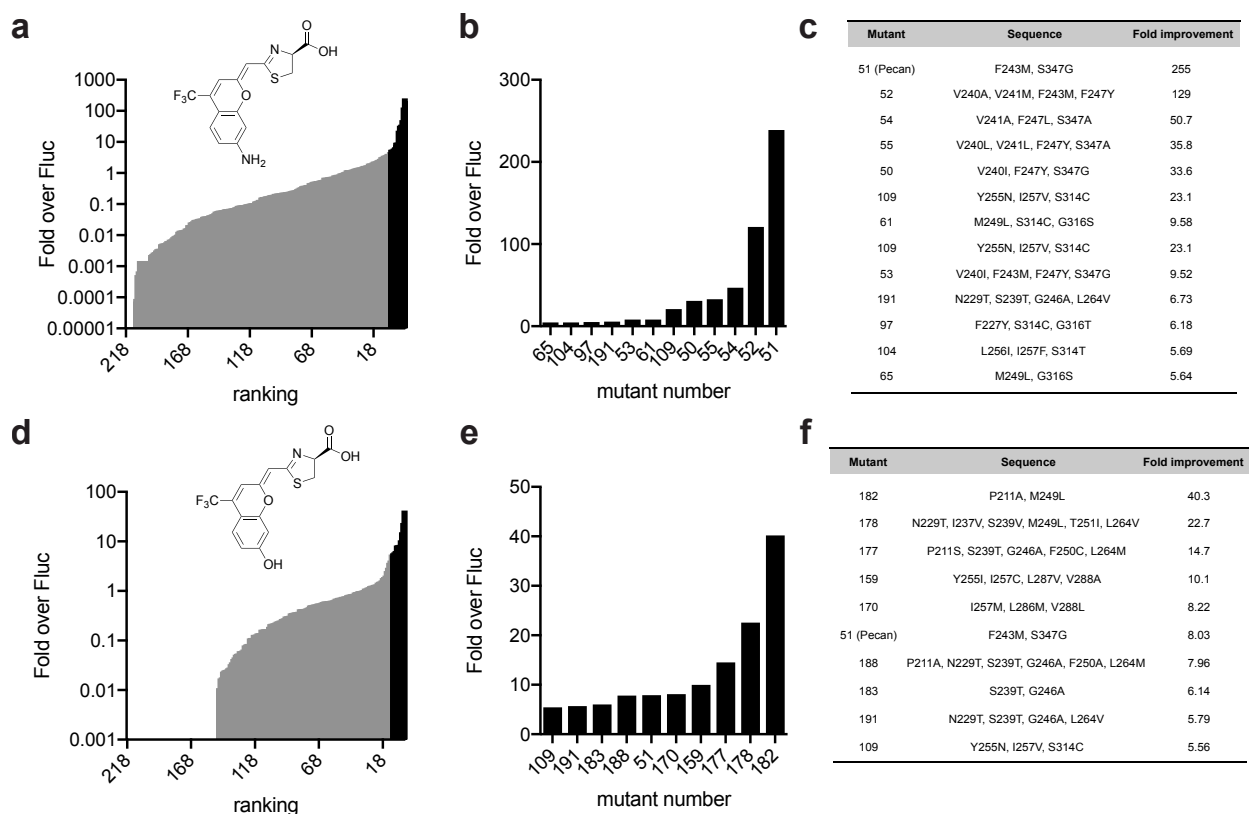


Figure S11. Identifying complementary luciferases for CouLuc-1 analogs via semi-rational library design. (a-c) CouLuc-1-NH₂ and (d-e) CouLuc-1-OH were screened against a panel of mutant luciferases using a protocol from Rathbun, *et al.*,⁴ with some modifications. Bacteria harboring the luciferase gene were induced for protein expression in a 96 deep-well plate. The cells were pelleted and resuspended in phosphate buffer (250 mM sodium phosphate, pH 8). Each luciferin was added (100 μ M) and the plate was imaged, and the luminescent values for each mutant were referenced to native Fluc. Mutants with >5-fold improvement in flux (black) with (b) CouLuc-1-NH₂ or (e) CouLuc-1-OH were classified as “hits” and their sequences were listed in (c) and (f), respectively.

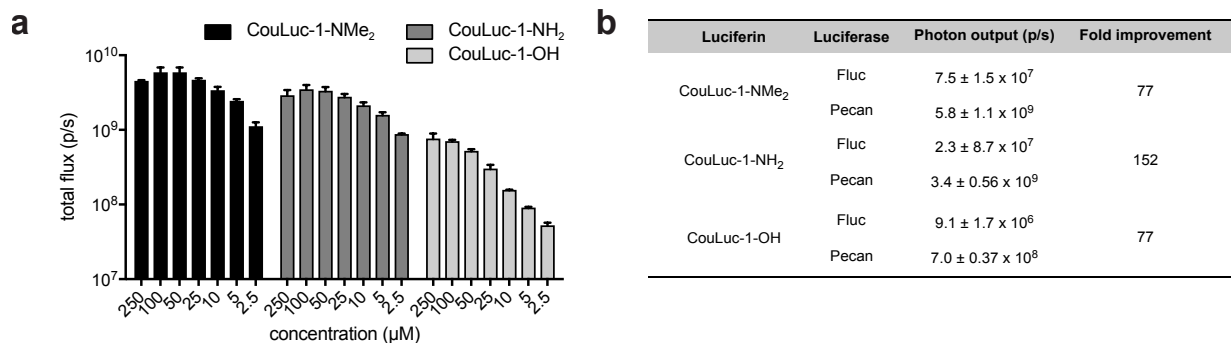


Figure S12. Improved light emission was recapitulated with recombinant Pecan (a) Light emission of CouLuc-1 analogs (250–2.5 μM) when incubated with ATP (1 mM), coenzyme A (1 mM) and recombinant Pecan (160 nM). Emission intensities are plotted as total photon flux values. Error bars represent the standard error of the mean for $n = 3$ experiments. (b) Tabulated photon outputs from (a) with [luciferin] = 100 μM . Fold improvements for each analog with Pecan (compared to Fluc) are also listed.

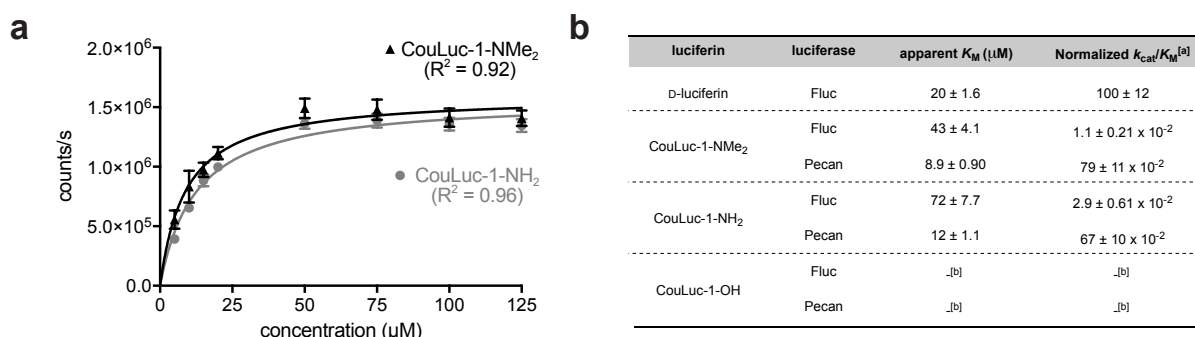


Figure S13. Biochemical analyses of Fluc with CouLuc-1 analogs. (a) Kinetics studies revealed CouLuc-1 analogs were poor binders of native luciferase. (b) Kinetic constants are apparent values, determined via measurements of initial light emission over a range of substrate concentrations. ^[a]Values were normalized to emission of Fluc/D-luciferin. Error bars represent the standard error of the mean for $n = 3$ experiments. ^[b]Kinetic parameters could not be determined due to low photon outputs.

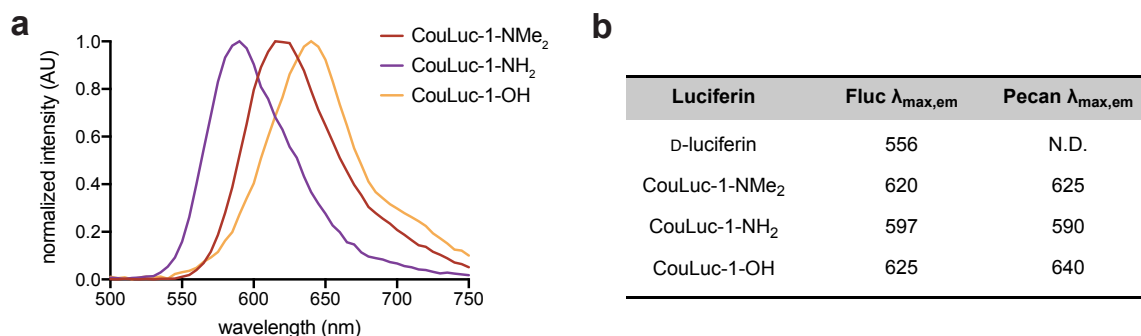


Figure S14. Red-shifted bioluminescence was maintained with Pecan. (a) Recombinant Pecan was incubated with CouLuc-1 analogs and emission spectra were recorded. (b) Emission maxima (λ_{em}) for each analog. The corresponding emission maxima with Fluc are also shown.

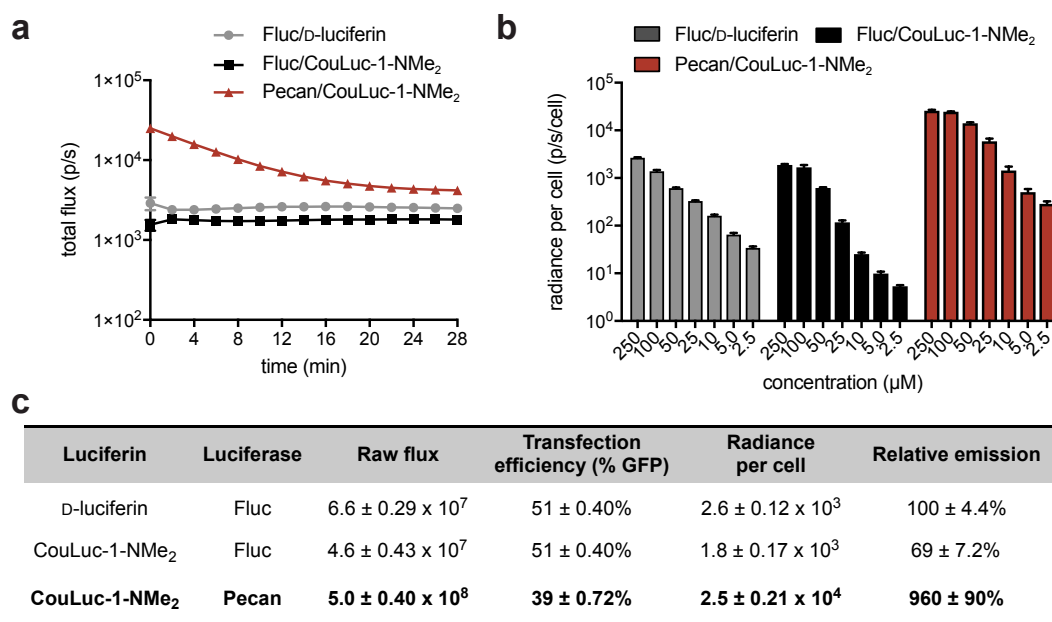
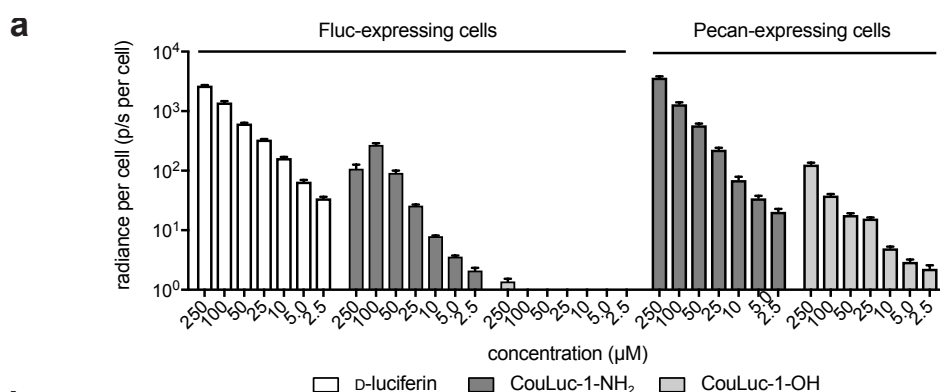


Figure S15. Cellular imaging with Pecan and CouLuc-1-NMe₂. HEK293 cells (5×10^4) expressing Fluc or Pecan were incubated with CouLuc-1-NMe₂ (250–2.5 μM) or D-luciferin (250–2.5 μM). Transfection efficiencies were determined via co-expression of GFP. (a) Maximum photon outputs ([luciferin] = 250 μM) were determined by monitoring signals over time. (b) Peak emission intensities for each probe combination are shown as photon flux values per cell. Error bars represent the standard error of the mean for $n = 3$ experiments. (c) Tabulated photon outputs from (b) with [luciferin] = 250 μM . Relative emission values for each luciferase/luciferin pair (compared to Fluc/D-luciferin) are also listed.



b

Luciferin	Luciferase	Raw flux	Transfection efficiency (% GFP)	Radiance per cell	Relative emission
D-luciferin	Fluc	$6.6 \pm 0.29 \times 10^7$	$51 \pm 0.40\%$	$2.6 \pm 0.12 \times 10^3$	$100 \pm 4.4\%$
CouLuc-1-NH ₂	Fluc	$2.7 \pm 0.48 \times 10^7$	$51 \pm 0.40\%$	$1.1 \pm 0.19 \times 10^2$	$4.1 \pm 0.74\%$
CouLuc-1-OH	Fluc	$3.5 \pm 0.40 \times 10^4$	$51 \pm 0.40\%$	1.4 ± 0.16	$0.052 \pm 0.0065\%$
CouLuc-1-NH ₂	Pecan	$7.3 \pm 0.25 \times 10^7$	$39 \pm 0.72\%$	$3.7 \pm 0.14 \times 10^3$	$142 \pm 8.3\%$
CouLuc-1-OH	Pecan	$2.6 \pm 0.13 \times 10^6$	$39 \pm 0.72\%$	$1.3 \pm 0.71 \times 10^2$	$5 \pm 0.35\%$

Figure S16. Improved light emission observed with Pecan and other CouLuc-1 analogs *in cellulo*. HEK293 cells (5×10^4) expressing Fluc or Pecan were incubated with CouLuc-1-NH₂ (250–2.5 μM), CouLuc-1-OH (250–2.5 μM) or D-luciferin (250–2.5 μM). Transfection efficiencies were determined via co-expression of GFP. (a) Peak emission intensities for each probe combination are shown as photon flux values per cell. Error bars represent the standard error of the mean for $n = 3$ experiments. (b) Tabulated photon outputs from (a) with [luciferin] = 250 μM . Relative emission values for each luciferase/luciferin pair (compared to Fluc/D-luciferin) are also listed.

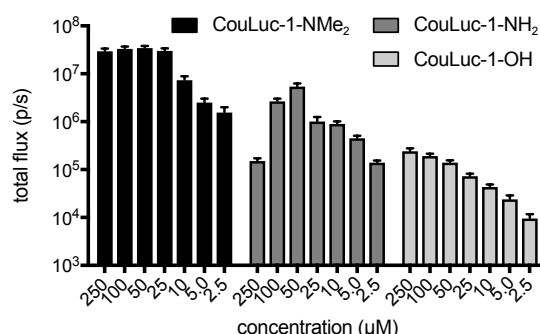


Figure S17. Robust light emission observed in DB7 cells. DB7 cells stably expressing Pecan (5×10^4) were incubated with CouLuc-1 analogs (250–2.5 μM). Photon outputs were measured immediately post substrate addition. Emission intensities are plotted as total photon flux values and error bars represent the standard error of the mean for $n = 3$ experiments.

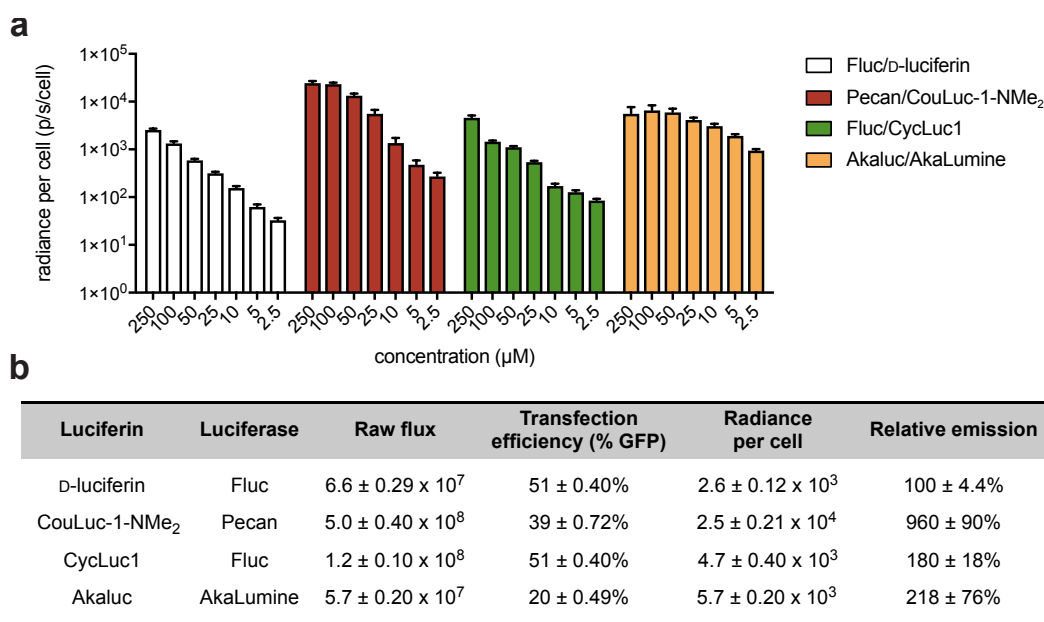


Figure S18. Cellular light emission from Pecan/CouLuc-1-NMe₂ is comparable to other red-emitting bioluminescence probes. HEK293 cells (5×10^4) expressing mutant luciferases or Fluc were incubated with either D-luciferin (250–2.5 μ M), CouLuc-1-NMe₂ (250–2.5 μ M), CycLuc1 (250–2.5 μ M) or AkaLumine (250–2.5 μ M). (a) Peak emission intensities for each probe combination are shown as photon flux values per cell. Error bars represent the standard error of the mean for $n = 3$ experiments. (b) Tabulated photon outputs from (a) with [luciferin] = 250 μ M. Relative emission values for each luciferase/luciferin pair (compared to Fluc/D-luciferin) are also listed.

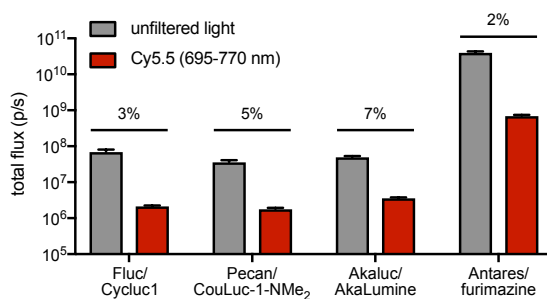


Figure S19. Pecan/CouLuc-1-NMe₂ produces a significant amount of near infrared photons. Luciferase-expressing DB7 cells (5×10^4) were treated with either CouLuc-1-NMe₂ (100 μ M), D-luciferin (100 μ M), CycLuc1 (100 μ M), AkaLumine (100 μ M) or furimazine (1:100 dilution from commercial stock). Photons produced in the near-infrared window were recorded by measuring through a Cy5.5 emission filter (695–770 nm). Emission intensities are plotted as total photon flux values and error bars represent the standard error of the mean for $n = 3$ experiments.

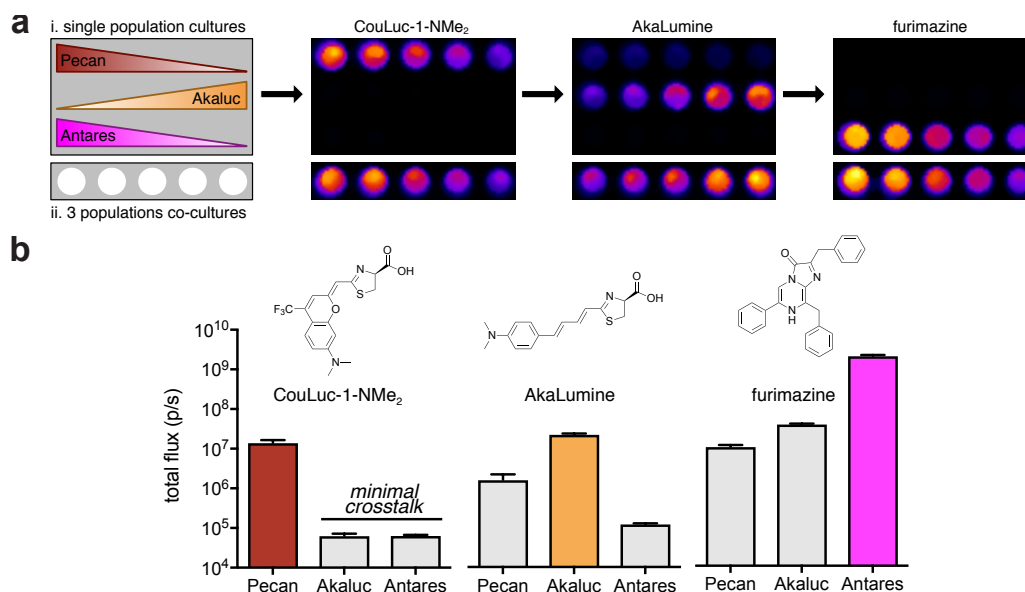


Figure S20. Multiplexed imaging with Pecan/CouLuc-1-NMe₂. Gradients of DB7 cells ($1-4 \times 10^4$) expressing Pecan, Akaluc, or Antares were plated in a 96-well plate as shown. (a) Raw luminescent images from sequential substrate administration of CouLuc-1-NMe₂ (100 μ M), AkaLumine (100 μ M), and furimazine (1:100 dilution from commercial stock). Data are representative of $n = 3$ replicates. (b) Quantified photon outputs for the images in (a). Photon flux from wells containing a single population of 4.0×10^4 luciferase-expressing cells were plotted. Minimal crosstalk was observed between Pecan/CouLuc-1-NMe₂ and Akaluc/AkaLumine. Error bars represent the standard error of the mean for $n = 3$ experiments.

General biological methods

Fluorescent spectra and assays

Absorption curves were obtained on a Shimadzu UV-2550 spectrophotometer operated by UVProbe 2.32 software. Fluorescence traces were recorded on a PTI QuantaMaster steady state spectrofluorometer operated by FelixGX 4.2.2 software, with 5 nm excitation and emission slit widths, 0.1 s integration rate, and enabled emission correction. Data analyses and curve fitting were performed using MS Excel 2019 and GraphPad Prism 8. Luciferins (10 μ M) were analyzed in a variety of solvents.

Bioluminescence emission spectra with recombinant luciferases

Emission spectra for all luciferin analogs were recorded on an Agilent Cary Eclipse Fluorescence Spectrophotometer. Each luciferin (100 μ M) was incubated in an Eppendorf tube with ATP (1 mM) and diluted to 1 mL with bioluminescence reaction buffer (20 mM Tris•HCl, 0.5 mg/mL BSA, 0.1 mM EDTA, 1 mM TCEP, 2 mM MgSO₄, pH = 7.8). Purified luciferase enzyme (6–600 μ g) was added, and an aliquot (700 μ L) was transferred to a 10 mm pathlength cuvette. The emission slit widths were set to 5–10 nm. The detector gain was set to 600 mV. Emission data were collected at 1 nm intervals from 400–850 nm at ambient temperature. The acquisition times were set to 1–60 s/wavelength depending on the amount of light produced from each sample. Light emission was recorded as relative luminescence units (RLU), and the intensities were normalized. Area under the curve was estimated via the trapezoid rule on MS Excel.

Bioluminescence emission spectra with luciferase expressing cells

For *in cellulo* emission spectra, 1×10^6 DB7 cells stably expressing the luciferase of interest⁵⁻⁶ were added to an Eppendorf tube in DMEM with 10% FBS. Cells were then incubated with luciferin (200 μ M final concentration) diluted in PBS or DMSO (7-NMe₂-CouLuc1 only, 10% DMSO final concentration) and an aliquot (700 μ L) was transferred to a 10 mm pathlength cuvette. The emission slit widths were set to 20 nm. The detector gain was set to 800 mV. Emission data were collected at 5 nm intervals from 400–850 nm at ambient temperature. The acquisition times were set to 1 s/wavelength for all samples. Light emission was recorded at relative luminescence units (RLU) and the intensities were normalized. Area under the curve was estimated via the trapezoid rule on MS Excel.

Reagents

All reagents purchased from commercial supplies were of analytical grade and used without further purification. 4'-MorphoLuc, 7'-MorpipLuc, 7'-DMAMELuc and 7'-pyrLuc, CycLuc1 were prepared and used as previously described.^{5,7-8}

General bioluminescence imaging protocol

All analyses were performed in black 96-well plates (Grenier Bio One). Plates containing luminescent reagents were allowed to sit at room temperature for 5 min post-luciferin addition, and were then imaged in a light-proof chamber with an IVIS Lumina II (Xenogen) CCD camera chilled to –90 °C. The stage was kept at 37 °C during the imaging session, and the camera was controlled using Living Image software. The exposure time was 1–60 s, and data binning levels were set to medium. Regions of interests were selected for quantification and total flux values were

analyzed using Living Image software. All data were exported to Microsoft Excel or Prism (GraphPad) for further analyses.

General cell culture methods

HEK293 and DB7 cells were cultured in complete media: DMEM (Corning) containing 10% (v/v) fetal bovine serum (FBS, Life Technologies), 4.5 g/L glucose, 2 mM L-glutamine, penicillin (100 U/mL), and streptomycin (100 µg/mL, Gibco). DB7 cells stably expressing Fluc were generated according to Jones *et al.* via transduction with ecotropic retrovirus (Phoenix packaging system).⁴⁻⁵ DB7 cells stably expressing Pecan, Akaluc, and Antares were generated according to Rathbun *et al.* via CRISPR-mediated gene insertion.⁶ For transient transfection experiments, HEK293 cells were plated 24–48 h prior to transfection in tissue culture treated 6-well dishes (Corning). Transfections were performed with luc2-IRES-eGFP or Pecan-IRES-eGFP plasmids using Lipofectamine 2000 according to the manufacturer's instructions when cells were 75–80% confluent (1–2 d post plating). Cells were manipulated 24–48 h post transfection. Expression of all transient and stable cell lines were checked via flow cytometry using an ACEA NovoCyte flow cytometer and the appropriate filter settings. Fluorescence was analyzed and quantified using the NovoExpress software (ACEA). Stably expressing luciferase cells were maintained under puromycin selection (20 µg/mL) to ensure gene incorporation was preserved. Cells were incubated at 37 °C in a 5% CO₂ humidified chamber. Cells were serially passaged using trypsin (0.25% in HBSS, Gibco).

General cloning methods

Polymerase chain reaction (PCR) methods were performed to isolate the luciferase and IRES-eGFP genes. Mutant luciferase inserts were amplified from pET vectors using the following primers:

5'- CGACTCACTATAGGGAGACCCAAGCTTATGGAAGATGCCAAAAACATTAAGAAG -3' and
5'-CACCGGCCTTATTCGAAGCGGCTTCGGCCAGTAACGTTTACACGGCGATCTTGCC-3'

IRES-eGFP insert was amplified from pcDNA vectors using the following primers:

5'- AAGGGCGGCAAGATCGCCGTGTAAACGTTACTGGCCGAAGCCGCTTGGAATAAG-3' and
5'-GCCGCCAGTGTGATGGATATCTGCAGAATTCTtaCTTGACAGCTCGTCCATGC-3'

All PCR reactions (unless otherwise stated) were performed in a BioRad C3000 Thermocycler using the following conditions: 1) 95 °C for 3 min, 2) 95 °C for 30 s, 3) T_m of primers for 30 s, 4) 72 °C for 3 min, repeat steps 2–4 twenty times, then 72 °C for 5 min, and hold at 12 °C until retrieved from the thermocycler. Linearized vectors were generated via digestion with restriction enzymes *HindIII* and *XhoI* (New England BioLabs). The linearized vectors were combined with the appropriate luciferase insert by Gibson assembly (50 °C for 60 min). A portion of the reactions (3.0 µL) was directly transformed into TOP10 competent *E. coli* cells. Colonies containing the genes of interest were expanded overnight in 5 mL LB broth supplemented with ampicillin (100 µg/mL) or kanamycin (100 µg/mL) and DNA was extracted from colonies using a Zymo Research Plasmid Mini-prep Kit. Sequencing analysis confirmed successful plasmid generation.

In cellulo bioluminescence imaging

Stably expressing luciferase cells, or transiently transfected HEKs were plated in DMEM containing 10% FBS (90 µL, 50,000 cells/well). Measurements were carried out in triplicate using black 96-well plates (Grenier Bio One). Luciferin analogs (0–250 µM) were prepared as a 10X

stock in PBS and then 10 μ L was added to assay wells. Images for all assays were acquired as described above.

Construction of combinatorial codon mutagenesis (CCM) libraries

DNA inserts for the combinatorial libraries (on average 3–4 mutations per clone) were generated as described by Belsare, *et al.*, with some modifications.⁹⁻¹⁰ The library template was first amplified using primers ZY040 and ZY041 (Table S2). The following thermal cycling conditions was used in a BioRad C3000 Thermocycler: 1) 95 °C for 3 min, 2) 95 °C for 30 s, 3) 65 °C for 30 s, 4) 72 °C for 45 s min, repeat steps 2-4 twenty times, then 72 °C for 5 min, and hold at 12 °C until retrieved from the thermocycler.

The forward fragment reactions were performed using an equimolar of mixture of mutagenic forward primers and ZY041 (Table S2). The reverse fragment reactions were performed using an equimolar mixture of mutagenic reverse primers and ZY040 (Table S2). The following thermal cycling conditions were used for the fragmentation reaction: 1) 95 °C for 3 min, 2) 95 °C for 30 s, 3) 60 °C for 30 s, 4) 72 °C for 45 s min, repeat steps 2-4 seven times, then 72 °C for 5 min, and hold at 12 °C until retrieved from the thermocycler. These reactions were used in a joining PCR reaction using the following conditions: ZY040 (1 μ L, 100 μ M), ZY041 (1 μ L, 100 μ M), 10x Q5® Reaction Buffer (6 μ L), 10x Q5® GC Enhancer Buffer, 1:4 dilution of the forward fragment reaction (4 μ L), 1:4 dilution of the reverse fragment reaction (4 μ L), dNTPs (1 μ L, 0.8 mM), and Q5® High-Fidelity DNA polymerase (0.3 μ L, 1U, New England BioLabs) totaling 30 μ L. DNA was amplified using thermal cycling conditions for insert amplification as described above. This PCR product was used as template for the second round of fragmentation (12 cycles) and joining PCRs. Mutagenesis was confirmed using Sanger sequencing (Genewiz).

Library DNA inserts were incorporated into linearized pQE vector. The linearized pQE vector was generated via digestion with restriction enzymes *Bam*HI and *Xba*I. Library inserts were assembled with the linearized pET vectors using Gibson assembly. For each assembly, 25 ng of the linearized vector was combined with insert (5:1 insert:vector ratio) and added to 5 μ L of master mix mixed with 5 μ L NanoPure H₂O. The mixtures were incubated at 50 °C for 60 min, then the entire reaction mixture was transformed into chemically competent TOP10 E. coli (70 μ L). Transformants were recovered with SOC (100 μ L) for 30 mins at 37 °C and 25 μ L plated per square, agar plate containing ampicillin.

Table S2: Primers used to construct Rosetta CCM library. The bases highlighted in red denote sites targeted for mutagenesis.

Forward CCM Primers	
ZY040	ATCGCATCACCATCACCATCACGGATCCATGGAAGATGCCAAAACATTAAGAAGG
RosCCM1-F-218	CGCTTGTGTC ^{ndt} TTCAGTCATGCCC
RosCCM1-F-221	CGATTCAGT ^{ndt} GCCCCGCG
RosCCM1-F-222	GATTCAGTCAT ^{ndt} CGCGACCCCATC
RosCCM1-F-229	GACCCCATCTTCGGC ^{ndt} CAGATCATC
RosCCM1-F-245	GCCATTTAC ^{ndt} GGCTTCGGCAT
RosCCM1-F-246	CCATTTACCAC ^{ndt} TTTCGGCATGTT
RosCCM1-F-247	CACCACGGC ^{ndt} GGCATGTTT
RosCCM1-F-250	CTTCGGCATG ^{ndt} ACCACGCTG
RosCCM1-F-251	CTTCGGCATGTT ^{ndt} ACGCTGG
RosCCM1-F-254	TCACCACGCTG ^{ndt} TACTTGATCTG
RosCCM1-F-314	GATCGCC ^{ndt} GGCGGG
RosCCM1-F-338	GCATCCGC ^{ndt} GGCTACGG
RosCCM1-F-342	AGGGCTACGGC ^{ndt} ACAGAAACAA
RosCCM1-F-343	CTACGGCCTG ^{ndt} GAAACAAGTAGTG
RosCCM1-F-347	CTGACAGAAACA ^{ndt} GCCATTCTGATCACC
RosCCM1-F-351	TGCCATTCTG ^{ndt} ACCCCCGAAG
RosCCM1-F-352	CATTCTGATC ^{ndt} CCCCGAAGGGG
RosCCM1-F-420	GGCTGCAC ^{ndt} GGCGACATCGC
RosCCM1-F-437	TCATCGTGGAC ^{ndt} CTGAAGAGCC
RosCCM1-F-519	TGACCGGC ^{ndt} TTGGACGCC

Reverse CCM Primers	
ZY041	TTTCGTTTTATTTGATGCCTCTAGATTACACGGCGATCTTGCCGCCCTTCTT
RosCCM1-R-218	GGGCATGACTGAA ^{ahn} GACACAAGCG
RosCCM1-R-221	CGCGGGC ^{ahn} ACTGAATCG
RosCCM1-R-222	GATGGGGTCGCG ^{ahn} ATGACTGAATC
RosCCM1-R-229	GATGATCTG ^{ahn} GCCGAAGATGGGGTC
RosCCM1-R-245	ATGCCGAAGCC ^{ahn} GTGAAATGGC
RosCCM1-R-246	AACATGCCGAA ^{ahn} GTGGTGAAATGG
RosCCM1-R-247	GAACATGCC ^{ahn} GCCGTGGTG
RosCCM1-R-250	CAGCGTGGT ^{ahn} CATGCCGAAG
RosCCM1-R-251	CCAGCGT ^{ahn} GAACATGCCGAAG
RosCCM1-R-254	CAGATCAAGTA ^{ahn} CAGCGTGGTGA
RosCCM1-R-314	CCCGCC ^{ahn} GGCGATC
RosCCM1-R-338	CCGTAGCC ^{ahn} GCGGATGC
RosCCM1-R-342	TTGTTTCTGT ^{ahn} GCCGTAGCCCT
RosCCM1-R-343	CACTAGTTGTTT ^{ahn} CAGGCCGTAG
RosCCM1-R-347	GGTGATCAGAATGGC ^{ahn} AGTTGTTTCTGTCTAG
RosCCM1-R-351	CTTCGGGGGT ^{ahn} CAGAATGGCA
RosCCM1-R-352	CCCCTTCGGG ^{ahn} GATCAGAATG
RosCCM1-R-420	GCGATGTCGCC ^{ahn} GTGCAGCC
RosCCM1-R-437	GGCTCTTCAG ^{ahn} GTCCACGATGA
RosCCM1-R-519	GGCGTCCAA ^{ahn} GCCGGTCA

Primary screening protocol

The aforementioned agar plates were sprayed with either a solution of CouLuc-1-NMe₂ or CouLuc-1-OH (100–500 µM, 500 µL per plate). The plates were incubated at 25 °C for 5 minutes and imaged as described above. Light emitting colonies were picked and grown for secondary screenings.

Secondary screening protocol

Hits from the primary screen were further analyzed as described in Jones, *et al.*, with some modifications.⁵ Light-emitting colonies from the agar plates were picked and expanded in LB broth containing ampicillin (100 µg/mL, LB-AMP) in a 96-well deep-well plate (500 µg/well). The plate was incubated at 37 °C overnight. An aliquot of the overnight culture (4 µL) was then used to inoculate 400 µL of auto-induction LB media, and the cells were incubated at 30 °C with shaking (250 rpm) for 24 h. The remaining starter cultures were mixed with 50% glycerol (1:1) and stored at –80 °C for subsequent plasmid recovery and sequencing analysis. The cells were pelleted by centrifugation (4000 rpm for 10 min) and resuspended in phosphate buffer (600 µL, 250 mM sodium phosphate, pH = 7.8). Bacterial culture (90 µL) was added to 96-well black plates, followed by a 10X solution of luciferin and ATP in phosphate buffer (10 µL, 250 mM phosphate, pH = 7.8, 100 µM luciferin and 1 mM ATP final concentration). The plate was then imaged as described above. Mutants with light emission 10-fold greater than wild type Fluc were considered as hits.

The panel of mutants from above was further validated in a second round of analysis. TOP10 *E. coli* cells expressing the desired mutants (glycerol stocks) were used to inoculate 5 mL LB-AMP media. The cultures were incubated at 37 °C overnight. An aliquot of the starter culture (150 µL) was used to inoculate a fresh solution of LB-AMP (5 mL) and incubated at 37 °C to mid-log phase (O.D.₆₀₀ ~0.8). The cultures were then induced with isopropyl β-D-1- thiogalactopyranoside (IPTG, 500 µM final concentration), and incubated at 23 °C for 16–18 h. The cells were harvested by centrifugation at 3600 rpm for 15 min. The cells were pelleted by centrifugation (4000 rpm for 10 min) and resuspended in phosphate buffer (600 µL, 250 mM sodium phosphate, pH = 7.8). Bacterial culture (90 µL) was added to 96-well black plates, followed by a 10X solution of luciferin and ATP in phosphate buffer (10 µL, 250 mM phosphate, pH = 7.8, 100 µM luciferin and 1 mM ATP final concentration). The plate was then imaged as described above. Mutants with reproducible improvement (>10-fold over Fluc) were sequenced.

Complete analog/mutant luciferase screen

The panel of luciferin analogs was screened against a library of functional luciferase mutants described in Rathbun, *et al.*⁴ BL21 *E. coli* cells expressing mutant luciferases (glycerol stocks) were used to inoculate LB-Kan media in a 96-well deep-well plate (500 µL/well). The plate was incubated at 37 °C overnight. An aliquot of the overnight culture (4 µL) was used to inoculate 400 µL of auto-induction LB media³, and the cells were incubated at 30 °C with shaking (250 rpm) for 24 h. The cells were pelleted by centrifugation at 4000 rpm for 10 min and resuspended in sodium phosphate buffer (600 µL, 100 mM, pH 8). Cell lysate was spread across six cells (90 µL/well) on six different 96-well black plates. Native Fluc expressing bacteria were included in each screen as a control for compound integrity. To each well, a 10X solution of luciferin and ATP in phosphate buffer (10 µL, 250 mM phosphate, pH = 7.8, 250 µM luciferin and 1 mM ATP final concentration)

was added, and the plate was imaged as described above. This process was repeated until all compounds were imaged with all 222 luciferase mutants.

Substrate unmixing analysis with orthogonal pairs

Substrate unmixing was conducted using ImageJ (installed under the FIJI package) as described in Rathbun, *et al.*⁶ Luminescence images containing raw photon counts were imported into FIJI and subjected to a 2-pixel median filter. Next, the signal at each pixel was min-max scaled to lie between 0 and 65535 (the maximum value that can be stored in a 16-bit image). Images were then stacked, and an additional image containing the maximum value of the stack was computed (as a Z projection). This new image was added to the stack, and signal was unmixed using the ImageJ plugin developed by Gammon *et al.*¹¹ Pseudocolors were assigned in FIJI through the “Merge Channels” tool.

Recombinant protein expression and purification

Luciferases were expressed and purified as described by Jones, *et al.*⁵ The pET-luciferase plasmids (WT, Pecan) were transformed into chemically competent BL21 *E. coli* cells. The transformants were plated on agar plates containing kanamycin. Cells were expanded in LB-Kan at 37 °C overnight. The overnight culture (20 mL) was used to inoculate 1 L LB-Kan and incubated at 37 °C to mid-log phase (O.D.~0.8). The culture was then induced with isopropyl β -D-1-thiogalactopyranoside (IPTG, 500 μ M final concentration), and incubated at 22 °C for 16–18 h. The cells were harvested at 4 °C by centrifugation at 4000 rpm for 15 min. Cell pellets were resuspended in 40 mL of phosphate buffer (50 mM phosphate, 300 mM NaCl, 1 mM dithiothreitol (DTT), and 1 mM phenylmethylsulfonyl fluoride, pH = 7.4). Lysozyme (2 mg) was added, and the cells were sonicated and centrifuged at 10000 rpm for 1 h at 4 °C. WT Fluc and mutant luciferases were purified from clarified supernatants using nickel affinity chromatography (BioLogic Duo Flow Chromatography System, Bio-Rad). Proteins were dialyzed into a Tris-acetate buffer (25 mM Tris-acetate, 1 mM EDTA, and 0.2 mM ammonium sulfate, pH = 7.8) at 4 °C for 16 h. DTT (1 mM final concentration) and 15% glycerol were added to the dialyzed samples prior to storage at –20°C. Final protein concentrations were determined using absorbance at 280 nm using a JASCO V730 UV-vis spectrophotometer. SDS-PAGE was also performed to verify protein purify, and gels were stained with Coomassie R-250.

Light emission assays with recombinant luciferase

Bioluminescence assays were performed as described by Jones, *et al.*⁵ Measurements were carried out in triplicate, using solid black, flat-bottom, 96-well plates (Grenier Bio One). Assay wells contained purified Fluc (0 or 1 mg), luciferin analogs (0–250 μ M), ATP (Sigma Aldrich, 1 mM), coenzyme-A (trilithium salt, NanoLight Technologies, 1 mM), and diluted with bioluminescence reaction buffer to a total volume of 100 μ L. Luciferins and ATP were premixed in the wells prior to Fluc addition. Images for all assays were acquired as described above.

Bioluminescence kinetic measurements

Bioluminescence kinetics assays were performed as described by Jones, *et al.* with some modifications.⁵ Measurements were acquired on a Tecan F200 Pro injection port luminometer with a neutral density filter. Reactions were performed in black 96-well flat-bottom plates (Greiner). Solutions of luciferin analog in bioluminescence reaction buffer were prepared (0.2–100 μ M analog), and 50 μ L were added to each well. The luminescence from each well was measured for

1.5 s prior to the addition of Fluc or mutant in bioluminescence buffer with ATP. For wells containing D-luciferin, a 1.6 μM solution of enzymes (50 μL) was used. For other compounds, a 160 μM solution of enzyme (50 μL) was administered. Following the addition of enzyme, luminescence was recorded every 0.2 s over a 60 s period. Samples were analyzed in triplicate. The peak intensities were determined by averaging the five maximum photon outputs per run. K_M and relative k_{cat} values were determined using nonlinear regression analyses in Prism (GraphPad).

General Rosetta methods

All calculations were carried out using Rosetta master version 60589 SHA1 code: 8442bff4fb7bf2ccb44655e8d15276c9bccfbbd0 using the ref15 score function.¹²

Preparing the scaffolds

A high-resolution (2.62 Å) structure of *Photinus pyralis* luciferase (PDB ID: 4G36) was processed to remove water molecules, non-proteinogenic molecules and a second copy of the protein in the asymmetric unit. Mutations present in the Pecan and Akaluc scaffold were made using the prepared 4g36 scaffold. The structures were subjected to an energy minimization using the Rosetta relax protocol to prepare them for subsequent protocols¹³ with the following command line:

```
<Path to>/Rosetta/main/source/bin/relax.default.linuxgccrelease -s
<input_file> @<Path to>/relax.flags
```

The contents of relax.flags was:

```
-nstruct 1
-relax:default_repeats 5
-relax:constrain_relax_to_start_coords
-relax:coord_constrain_sidechains
-relax:ramp_constraints false
-ex1
-ex2
-use_input_sc
-flip_HNQ
-ignore_unrecognized_res
-relax:coord_cst_stdev 0.5
```

Preparing the CouLuc-1 ligands

The CouLuc-1 ligands were built in Avogadro: an open-source molecular builder and visualization tool. Version 1.2.0. <http://avogadro.cc/>¹⁴ and subjected to an energy minimization using the UFF force field.¹⁵ The .mol2 files were converted to .params files for use in Rosetta using an internal script. The params files used in the RosettaMatch algorithm are as follows:

The CouLuc-1- NMe₂ params file where LCC stands for CouLuc-1-NMe₂ is as follows:

```
NAME LCC
IO_STRING LCC Z
TYPE LIGAND
AA UNK
ATOM N7 Ntrp X -0.50
ATOM S2 S X -0.05
ATOM O1 OOC X -0.65
ATOM O2 OOC X -0.65
ATOM O3 OH X -0.55
ATOM C5 CH2 X -0.07
```

ATOM	C6	CH1	X	0.02
ATOM	O4	OH	X	-0.55
ATOM	C9	CH1	X	0.02
ATOM	N4	Npro	X	-0.26
ATOM	C11	aroC	X	-0.01
ATOM	N3	Nhis	X	-0.42
ATOM	C10	aroC	X	-0.01
ATOM	N2	Nhis	X	-0.42
ATOM	C13	aroC	X	-0.01
ATOM	N6	NH2O	X	-0.36
ATOM	H6	Hpol	X	0.54
ATOM	H7	Hpol	X	0.54
ATOM	C12	aroC	X	-0.01
ATOM	N5	Ntrp	X	-0.50
ATOM	C14	aroC	X	-0.01
ATOM	H15	Haro	X	0.22
ATOM	H2	Hpol	X	0.54
ATOM	H14	Haro	X	0.22
ATOM	C8	CH1	X	0.02
ATOM	O6	OH	X	-0.55
ATOM	H8	Hpol	X	0.54
ATOM	C7	CH1	X	0.02
ATOM	O5	OH	X	-0.55
ATOM	H3	Hpol	X	0.54
ATOM	H11	Hapo	X	0.20
ATOM	H12	Hapo	X	0.20
ATOM	H13	Hapo	X	0.20
ATOM	H9	Hapo	X	0.20
ATOM	H4	Hapo	X	0.20
ATOM	H5	Hapo	X	0.20
ATOM	C4	COO	X	0.73
ATOM	C3	aroC	X	-0.01
ATOM	N1	Nhis	X	-0.42
ATOM	C1	aroC	X	-0.01
ATOM	C15	CH1	X	0.02
ATOM	C16	COO	X	0.73
ATOM	O8	OOC	X	-0.65
ATOM	C18	aroC	X	-0.01
ATOM	C19	aroC	X	-0.01
ATOM	C20	aroC	X	-0.01
ATOM	C17	aroC	X	-0.01
ATOM	H17	Haro	X	0.22
ATOM	C25	CH1	X	0.02
ATOM	F1	F	X	-0.14
ATOM	F2	F	X	-0.14
ATOM	F3	F	X	-0.14
ATOM	C24	aroC	X	-0.01
ATOM	C23	aroC	X	-0.01
ATOM	C22	aroC	X	-0.01
ATOM	C21	aroC	X	-0.01
ATOM	H20	Haro	X	0.22
ATOM	N8	Nhis	X	-0.42
ATOM	C26	CH3	X	-0.16
ATOM	H21	Hapo	X	0.20
ATOM	H22	Hapo	X	0.20
ATOM	H23	Hapo	X	0.20
ATOM	C27	CH3	X	-0.16
ATOM	H24	Hapo	X	0.20
ATOM	H25	Hapo	X	0.20
ATOM	H26	Hapo	X	0.20
ATOM	H19	Haro	X	0.22
ATOM	H18	Haro	X	0.22
ATOM	H16	Hapo	X	0.20
ATOM	S1	S	X	-0.05
ATOM	C2	aroC	X	-0.01
ATOM	H1	Haro	X	0.22

ATOM	O7	ONH2	X	-0.44
ATOM	H10	Hpo1	X	0.54
BOND_TYPE	C1	C15	1	
BOND_TYPE	C1	N1	4	
BOND_TYPE	N1	C3	4	
BOND_TYPE	O1	S2	2	
BOND_TYPE	C1	S1	4	
BOND_TYPE	S1	C2	4	
BOND_TYPE	C2	C3	4	
BOND_TYPE	C2	H1	1	
BOND_TYPE	N2	C10	4	
BOND_TYPE	N2	C13	4	
BOND_TYPE	O2	S2	2	
BOND_TYPE	S2	O3	1	
BOND_TYPE	S2	N7	1	
BOND_TYPE	C3	C4	1	
BOND_TYPE	N3	C10	4	
BOND_TYPE	N3	C11	4	
BOND_TYPE	O3	C5	1	
BOND_TYPE	C4	N7	1	
BOND_TYPE	C4	O7	2	
BOND_TYPE	N4	C9	1	
BOND_TYPE	N4	C11	4	
BOND_TYPE	N4	C14	4	
BOND_TYPE	O4	C6	1	
BOND_TYPE	O4	C9	1	
BOND_TYPE	C5	C6	1	
BOND_TYPE	C5	H4	1	
BOND_TYPE	C5	H5	1	
BOND_TYPE	N5	C12	4	
BOND_TYPE	N5	C14	4	
BOND_TYPE	N5	H2	1	
BOND_TYPE	O5	C7	1	
BOND_TYPE	O5	H3	1	
BOND_TYPE	C6	C7	1	
BOND_TYPE	C6	H9	1	
BOND_TYPE	N6	C13	1	
BOND_TYPE	N6	H6	1	
BOND_TYPE	N6	H7	1	
BOND_TYPE	O6	C8	1	
BOND_TYPE	O6	H8	1	
BOND_TYPE	C7	C8	1	
BOND_TYPE	C7	H11	1	
BOND_TYPE	N7	H10	1	
BOND_TYPE	C8	C9	1	
BOND_TYPE	C8	H12	1	
BOND_TYPE	N8	C26	1	
BOND_TYPE	N8	C27	1	
BOND_TYPE	O8	C18	4	
BOND_TYPE	C9	H13	1	
BOND_TYPE	C10	H14	1	
BOND_TYPE	C11	C12	4	
BOND_TYPE	C12	C13	4	
BOND_TYPE	C14	H15	1	
BOND_TYPE	C15	C16	1	
BOND_TYPE	C15	H16	1	
BOND_TYPE	O8	C16	4	
BOND_TYPE	C16	C17	4	
BOND_TYPE	C17	C20	4	
BOND_TYPE	C17	H17	1	
BOND_TYPE	C18	C19	4	
BOND_TYPE	C18	C21	4	
BOND_TYPE	C19	C20	4	
BOND_TYPE	C19	C24	4	
BOND_TYPE	C20	C25	1	
BOND_TYPE	C21	C22	4	

```

BOND_TYPE C21 H20 1
BOND_TYPE N8 C22 1
BOND_TYPE C22 C23 4
BOND_TYPE C23 C24 4
BOND_TYPE C23 H19 1
BOND_TYPE C24 H18 1
BOND_TYPE C25 F1 1
BOND_TYPE C25 F2 1
BOND_TYPE C25 F3 1
BOND_TYPE C26 H21 1
BOND_TYPE C26 H22 1
BOND_TYPE C26 H23 1
BOND_TYPE C27 H24 1
BOND_TYPE C27 H25 1
BOND_TYPE C27 H26 1
CHI 1 C8 C7 O5 H3
PROTON_CHI 1 SAMPLES 21 45 50 55 60 65 70 75 -45 -50 -55 -60 -65 -70 -75 165 170
175 180 185 190 195 EXTRA 0
CHI 2 C9 C8 O6 H8
PROTON_CHI 2 SAMPLES 21 45 50 55 60 65 70 75 -45 -50 -55 -60 -65 -70 -75 165 170
175 180 185 190 195 EXTRA 0
CHI 3 N1 C1 C15 C16
CHI 4 N7 S2 O3 C5
CHI 5 C4 N7 S2 O1
CHI 6 N7 C4 C3 N1
CHI 7 S2 O3 C5 C6
CHI 8 S2 N7 C4 C3
CHI 9 O4 C9 N4 C11
CHI 10 O3 C5 C6 O4
CHI 11 C1 C15 C16 O8
CHI 12 C19 C20 C25 F1
CHI 13 C23 C22 N8 C26
NBR_ATOM N7
NBR_RADIUS 16.480287
ICOOR_INTERNAL N7 0.000000 0.000000 0.000000 N7 S2 O1
ICOOR_INTERNAL S2 0.000000 180.000000 1.650062 N7 S2 O1
ICOOR_INTERNAL O1 0.000000 72.104658 1.437728 S2 N7 O1
ICOOR_INTERNAL O2 -110.996100 68.074449 1.445125 S2 N7 O1
ICOOR_INTERNAL O3 -129.794407 67.944568 1.509427 S2 N7 O2
ICOOR_INTERNAL C5 48.026210 59.837306 1.410874 O3 S2 N7
ICOOR_INTERNAL C6 157.652992 70.710750 1.511242 C5 O3 S2
ICOOR_INTERNAL O4 77.282034 69.984387 1.402847 C6 C5 O3
ICOOR_INTERNAL C9 125.140105 74.095561 1.413122 O4 C6 C5
ICOOR_INTERNAL N4 -109.511147 70.744428 1.445332 C9 O4 C6
ICOOR_INTERNAL C11 -150.220766 54.143952 1.365802 N4 C9 O4
ICOOR_INTERNAL N3 -0.899108 46.184845 1.342623 C11 N4 C9
ICOOR_INTERNAL C10 -179.435301 59.581414 1.325031 N3 C11 N4
ICOOR_INTERNAL N2 -0.833691 57.581285 1.332176 C10 N3 C11
ICOOR_INTERNAL C13 0.541646 58.153548 1.342096 N2 C10 N3
ICOOR_INTERNAL N6 -179.885440 60.506917 1.449335 C13 N2 C10
ICOOR_INTERNAL H6 -0.115371 59.977458 0.984393 N6 C13 N2
ICOOR_INTERNAL H7 179.945780 60.016656 0.985154 N6 C13 H6
ICOOR_INTERNAL C12 179.862428 62.184716 1.420651 C13 N2 N6
ICOOR_INTERNAL N5 -179.949517 44.621863 1.328601 C12 C13 N2
ICOOR_INTERNAL C14 179.677558 70.203038 1.324715 N5 C12 C13
ICOOR_INTERNAL H15 -179.578659 55.002841 1.032967 C14 N5 C12
ICOOR_INTERNAL H2 -179.970617 54.849045 0.984976 N5 C12 C14
ICOOR_INTERNAL H14 179.967987 61.153361 1.031699 C10 N3 N2
ICOOR_INTERNAL C8 125.386647 71.678423 1.475682 C9 O4 N4
ICOOR_INTERNAL O6 90.159142 71.814346 1.374530 C8 C9 O4
ICOOR_INTERNAL H8 -179.907404 70.535671 0.969463 O6 C8 C9
ICOOR_INTERNAL C7 -120.342024 77.546124 1.466197 C8 C9 O6
ICOOR_INTERNAL O5 150.569759 65.740398 1.379514 C7 C8 C9
ICOOR_INTERNAL H3 179.991726 70.530485 0.970413 O5 C7 C8
ICOOR_INTERNAL H11 117.079816 69.012841 1.070864 C7 C8 O5
ICOOR_INTERNAL H12 -121.174077 63.727852 1.069712 C8 C9 C7

```

ICOOR_INTERNAL	H13	117.670342	67.676021	1.069572	C9	O4	C8
ICOOR_INTERNAL	H9	-119.425559	70.515230	1.070763	C6	C5	O4
ICOOR_INTERNAL	H4	-120.035866	70.426804	1.069592	C5	O3	C6
ICOOR_INTERNAL	H5	-119.906355	70.417410	1.069976	C5	O3	H4
ICOOR_INTERNAL	C4	-83.793754	58.281421	1.467467	N7	S2	O1
ICOOR_INTERNAL	C3	178.602413	63.790977	1.496597	C4	N7	S2
ICOOR_INTERNAL	N1	171.710317	59.685217	1.308129	C3	C4	N7
ICOOR_INTERNAL	C1	179.403075	66.538537	1.363242	N1	C3	C4
ICOOR_INTERNAL	C15	178.038432	54.751568	1.475845	C1	N1	C3
ICOOR_INTERNAL	C16	-179.973359	56.742589	1.347238	C15	C1	N1
ICOOR_INTERNAL	O8	1.725866	59.229554	1.354592	C16	C15	C1
ICOOR_INTERNAL	C18	179.858798	56.623479	1.354364	O8	C16	C15
ICOOR_INTERNAL	C19	0.887588	59.212928	1.412822	C18	O8	C16
ICOOR_INTERNAL	C20	-0.844484	61.931272	1.515819	C19	C18	O8
ICOOR_INTERNAL	C17	0.091368	61.915940	1.352930	C20	C19	C18
ICOOR_INTERNAL	H17	-179.883717	59.714914	1.087586	C17	C20	C19
ICOOR_INTERNAL	C25	-179.669554	53.469135	1.526954	C20	C19	C17
ICOOR_INTERNAL	F1	-0.147422	65.088860	1.374607	C25	C20	C19
ICOOR_INTERNAL	F2	-120.743410	70.959525	1.384707	C25	C20	F1
ICOOR_INTERNAL	F3	-118.465114	70.887590	1.383661	C25	C20	F2
ICOOR_INTERNAL	C24	-179.813659	62.667377	1.407529	C19	C18	C20
ICOOR_INTERNAL	C23	0.444229	58.666119	1.396868	C24	C19	C18
ICOOR_INTERNAL	C22	0.207422	58.151002	1.413573	C23	C24	C19
ICOOR_INTERNAL	C21	-0.508039	63.430140	1.413587	C22	C23	C24
ICOOR_INTERNAL	H20	179.170241	57.531909	1.075128	C21	C22	C23
ICOOR_INTERNAL	N8	-179.834487	58.360800	1.454020	C22	C23	C21
ICOOR_INTERNAL	C26	-15.367154	57.151155	1.459721	N8	C22	C23
ICOOR_INTERNAL	H21	-4.544141	65.075936	1.099691	C26	N8	C22
ICOOR_INTERNAL	H22	-118.257943	70.626381	1.111531	C26	N8	H21
ICOOR_INTERNAL	H23	-119.101486	70.203809	1.111081	C26	N8	H22
ICOOR_INTERNAL	C27	-179.704739	56.873654	1.458277	N8	C22	C26
ICOOR_INTERNAL	H24	-3.336325	65.036189	1.098860	C27	N8	C22
ICOOR_INTERNAL	H25	-118.846485	70.514855	1.110651	C27	N8	H24
ICOOR_INTERNAL	H26	-119.305614	70.093290	1.110606	C27	N8	H25
ICOOR_INTERNAL	H19	-179.115566	64.471844	1.076073	C23	C24	C22
ICOOR_INTERNAL	H18	-179.865470	56.842756	1.072154	C24	C19	C23
ICOOR_INTERNAL	H16	-179.288691	62.704338	1.086883	C15	C1	C16
ICOOR_INTERNAL	S1	-178.645915	71.214035	1.654766	C1	N1	C15
ICOOR_INTERNAL	C2	0.064084	84.137315	1.751848	S1	C1	N1
ICOOR_INTERNAL	H1	-179.571667	51.154423	1.031194	C2	S1	C1
ICOOR_INTERNAL	O7	179.926420	56.571828	1.227619	C4	N7	C3
ICOOR_INTERNAL	H10	179.925774	60.889832	0.984604	N7	S2	C4

The contents of the CouLuc-1-NH₂ ligand params file where LCD stands for CouLuc-1-NH₂ are as follows:

```

NAME LCD
IO_STRING LCD Z
TYPE LIGAND
AA UNK
ATOM N7 Ntrp X -0.51
ATOM S2 S X -0.06
ATOM O1 OOC X -0.66
ATOM O2 OOC X -0.66
ATOM O3 OH X -0.56
ATOM C5 CH2 X -0.08
ATOM C6 CH1 X 0.01
ATOM O4 OH X -0.56
ATOM C9 CH1 X 0.01
ATOM N4 Npro X -0.27
ATOM C11 aroC X -0.01
ATOM N3 Nhis X -0.43
ATOM C10 aroC X -0.01
ATOM N2 Nhis X -0.43
ATOM C13 aroC X -0.01

```


ATOM	N6	NH2O	X	-0.37
ATOM	H6	Hpol	X	0.53
ATOM	H7	Hpol	X	0.53
ATOM	C12	aroC	X	-0.01
ATOM	N5	Ntrp	X	-0.51
ATOM	C14	aroC	X	-0.01
ATOM	H15	Haro	X	0.22
ATOM	H2	Hpol	X	0.53
ATOM	H14	Haro	X	0.22
ATOM	C8	CH1	X	0.01
ATOM	O6	OH	X	-0.56
ATOM	H8	Hpol	X	0.53
ATOM	C7	CH1	X	0.01
ATOM	O5	OH	X	-0.56
ATOM	H3	Hpol	X	0.53
ATOM	H11	Hapo	X	0.20
ATOM	H12	Hapo	X	0.20
ATOM	H13	Hapo	X	0.20
ATOM	H9	Hapo	X	0.20
ATOM	H4	Hapo	X	0.20
ATOM	H5	Hapo	X	0.20
ATOM	C4	COO	X	0.72
ATOM	C3	aroC	X	-0.01
ATOM	N1	Nhis	X	-0.43
ATOM	C1	aroC	X	-0.01
ATOM	C15	CH1	X	0.01
ATOM	C16	COO	X	0.72
ATOM	O8	OOC	X	-0.66
ATOM	C18	aroC	X	-0.01
ATOM	C19	aroC	X	-0.01
ATOM	C20	aroC	X	-0.01
ATOM	C17	aroC	X	-0.01
ATOM	H17	Haro	X	0.22
ATOM	C25	CH1	X	0.01
ATOM	F1	F	X	-0.15
ATOM	F2	F	X	-0.15
ATOM	F3	F	X	-0.15
ATOM	C24	aroC	X	-0.01
ATOM	C23	aroC	X	-0.01
ATOM	C22	aroC	X	-0.01
ATOM	C21	aroC	X	-0.01
ATOM	H20	Haro	X	0.22
ATOM	N8	NH2O	X	-0.37
ATOM	H21	Hpol	X	0.53
ATOM	H22	Hpol	X	0.53
ATOM	H19	Haro	X	0.22
ATOM	H18	Haro	X	0.22
ATOM	H16	Hapo	X	0.20
ATOM	S1	S	X	-0.06
ATOM	C2	aroC	X	-0.01
ATOM	H1	Haro	X	0.22
ATOM	O7	ONH2	X	-0.45
ATOM	H10	Hpol	X	0.53
BOND_TYPE	C1	C15	1	
BOND_TYPE	C1	N1	4	
BOND_TYPE	N1	C3	4	
BOND_TYPE	O1	S2	2	
BOND_TYPE	C1	S1	4	
BOND_TYPE	S1	C2	4	
BOND_TYPE	C2	C3	4	
BOND_TYPE	C2	H1	1	
BOND_TYPE	N2	C10	4	
BOND_TYPE	N2	C13	4	
BOND_TYPE	O2	S2	2	
BOND_TYPE	S2	O3	1	
BOND_TYPE	S2	N7	1	

BOND_TYPE	C3	C4	1															
BOND_TYPE	N3	C10	4															
BOND_TYPE	N3	C11	4															
BOND_TYPE	O3	C5	1															
BOND_TYPE	C4	N7	1															
BOND_TYPE	C4	O7	2															
BOND_TYPE	N4	C9	1															
BOND_TYPE	N4	C11	4															
BOND_TYPE	N4	C14	4															
BOND_TYPE	O4	C6	1															
BOND_TYPE	O4	C9	1															
BOND_TYPE	C5	C6	1															
BOND_TYPE	C5	H4	1															
BOND_TYPE	C5	H5	1															
BOND_TYPE	N5	C12	4															
BOND_TYPE	N5	C14	4															
BOND_TYPE	N5	H2	1															
BOND_TYPE	O5	C7	1															
BOND_TYPE	O5	H3	1															
BOND_TYPE	C6	C7	1															
BOND_TYPE	C6	H9	1															
BOND_TYPE	N6	C13	1															
BOND_TYPE	N6	H6	1															
BOND_TYPE	N6	H7	1															
BOND_TYPE	O6	C8	1															
BOND_TYPE	O6	H8	1															
BOND_TYPE	C7	C8	1															
BOND_TYPE	C7	H11	1															
BOND_TYPE	N7	H10	1															
BOND_TYPE	C8	C9	1															
BOND_TYPE	C8	H12	1															
BOND_TYPE	N8	H21	1															
BOND_TYPE	N8	H22	1															
BOND_TYPE	O8	C18	4															
BOND_TYPE	C9	H13	1															
BOND_TYPE	C10	H14	1															
BOND_TYPE	C11	C12	4															
BOND_TYPE	C12	C13	4															
BOND_TYPE	C14	H15	1															
BOND_TYPE	C15	C16	1															
BOND_TYPE	C15	H16	1															
BOND_TYPE	O8	C16	4															
BOND_TYPE	C16	C17	4															
BOND_TYPE	C17	C20	4															
BOND_TYPE	C17	H17	1															
BOND_TYPE	C18	C19	4															
BOND_TYPE	C18	C21	4															
BOND_TYPE	C19	C20	4															
BOND_TYPE	C19	C24	4															
BOND_TYPE	C20	C25	1															
BOND_TYPE	C21	C22	4															
BOND_TYPE	C21	H20	1															
BOND_TYPE	N8	C22	1															
BOND_TYPE	C22	C23	4															
BOND_TYPE	C23	C24	4															
BOND_TYPE	C23	H19	1															
BOND_TYPE	C24	H18	1															
BOND_TYPE	C25	F1	1															
BOND_TYPE	C25	F2	1															
BOND_TYPE	C25	F3	1															
CHI 1	C8	C7	O5	H3														
PROTON_CHI 1	SAMPLES	21	45	50	55	60	65	70	75	-45	-50	-55	-60	-65	-70	-75	165	170
175	180	185	190	195	EXTRA	0												
PROTON_CHI 2	SAMPLES	21	45	50	55	60	65	70	75	-45	-50	-55	-60	-65	-70	-75	165	170
175	180	185	190	195	EXTRA	0												
CHI 3	N1	C1	C15	C16														

CHI 4 N7 S2 O3 C5
 CHI 5 C4 N7 S2 O1
 CHI 6 N7 C4 C3 N1
 CHI 7 S2 O3 C5 C6
 CHI 8 S2 N7 C4 C3
 CHI 9 O4 C9 N4 C11
 CHI 10 O3 C5 C6 O4
 CHI 11 C1 C15 C16 O8
 CHI 12 C19 C20 C25 F1

NBR_ATOM N7

NBR_RADIUS 15.401802

ICOOR_INTERNAL	N7	0.000000	0.000000	0.000000	N7	S2	O1
ICOOR_INTERNAL	S2	0.000000	180.000000	1.649480	N7	S2	O1
ICOOR_INTERNAL	O1	0.000000	72.115214	1.437728	S2	N7	O1
ICOOR_INTERNAL	O2	-110.979907	68.095120	1.445125	S2	N7	O1
ICOOR_INTERNAL	O3	-129.796485	67.884564	1.508898	S2	N7	O2
ICOOR_INTERNAL	C5	47.972804	59.847207	1.411561	O3	S2	N7
ICOOR_INTERNAL	C6	157.660576	70.738957	1.511080	C5	O3	S2
ICOOR_INTERNAL	O4	77.333973	70.005558	1.402847	C6	C5	O3
ICOOR_INTERNAL	C9	125.086234	74.080093	1.413900	O4	C6	C5
ICOOR_INTERNAL	N4	-109.502643	70.720185	1.445332	C9	O4	C6
ICOOR_INTERNAL	C11	-150.229052	54.143952	1.365802	N4	C9	O4
ICOOR_INTERNAL	N3	-0.892936	46.223588	1.342216	C11	N4	C9
ICOOR_INTERNAL	C10	-179.432403	59.624923	1.326020	N3	C11	N4
ICOOR_INTERNAL	N2	-0.848435	57.610071	1.331554	C10	N3	C11
ICOOR_INTERNAL	C13	0.552053	58.120141	1.342096	N2	C10	N3
ICOOR_INTERNAL	N6	-179.890730	60.506917	1.449335	C13	N2	C10
ICOOR_INTERNAL	H6	-0.115371	59.977458	0.984393	N6	C13	N2
ICOOR_INTERNAL	H7	179.952772	59.961946	0.984831	N6	C13	H6
ICOOR_INTERNAL	C12	179.862428	62.184716	1.420651	C13	N2	N6
ICOOR_INTERNAL	N5	-179.949517	44.621863	1.328601	C12	C13	N2
ICOOR_INTERNAL	C14	179.677558	70.203038	1.324715	N5	C12	C13
ICOOR_INTERNAL	H15	-179.517871	55.041066	1.032119	C14	N5	C12
ICOOR_INTERNAL	H2	-179.976464	54.922095	0.984330	N5	C12	C14
ICOOR_INTERNAL	H14	-179.959018	61.152494	1.031712	C10	N3	N2
ICOOR_INTERNAL	C8	125.404314	71.733653	1.475916	C9	O4	N4
ICOOR_INTERNAL	O6	90.149730	71.799851	1.374530	C8	C9	O4
ICOOR_INTERNAL	H8	179.999645	70.557415	0.969220	O6	C8	C9
ICOOR_INTERNAL	C7	-120.391196	77.527376	1.465575	C8	C9	O6
ICOOR_INTERNAL	O5	150.567803	65.743236	1.380198	C7	C8	C9
ICOOR_INTERNAL	H3	179.981880	70.545702	0.969832	O5	C7	C8
ICOOR_INTERNAL	H11	117.168004	68.989317	1.070413	C7	C8	O5
ICOOR_INTERNAL	H12	-121.158644	63.838599	1.069836	C8	C9	C7
ICOOR_INTERNAL	H13	117.674596	67.713631	1.070064	C9	O4	C8
ICOOR_INTERNAL	H9	-119.374097	70.454273	1.069969	C6	C5	O4
ICOOR_INTERNAL	H4	-119.990464	70.450854	1.069592	C5	O3	C6
ICOOR_INTERNAL	H5	-119.938832	70.434132	1.070190	C5	O3	H4
ICOOR_INTERNAL	C4	-83.828030	58.301695	1.468382	N7	S2	O1
ICOOR_INTERNAL	C3	178.603415	63.816343	1.496095	C4	N7	S2
ICOOR_INTERNAL	N1	171.714611	59.715820	1.309092	C3	C4	N7
ICOOR_INTERNAL	C1	179.404452	66.574660	1.362844	N1	C3	C4
ICOOR_INTERNAL	C15	179.343162	54.627824	1.477523	C1	N1	C3
ICOOR_INTERNAL	C16	179.978262	56.646772	1.345610	C15	C1	N1
ICOOR_INTERNAL	O8	0.981830	59.223614	1.354162	C16	C15	C1
ICOOR_INTERNAL	C18	179.745138	56.639084	1.351881	O8	C16	C15
ICOOR_INTERNAL	C19	0.484766	59.068241	1.419987	C18	O8	C16
ICOOR_INTERNAL	C20	-0.558169	62.167587	1.515074	C19	C18	O8
ICOOR_INTERNAL	C17	0.167837	61.905154	1.351574	C20	C19	C18
ICOOR_INTERNAL	H17	-179.921795	59.732081	1.088256	C17	C20	C19
ICOOR_INTERNAL	C25	-179.891720	53.582674	1.526174	C20	C19	C17
ICOOR_INTERNAL	F1	-0.070420	65.114755	1.374596	C25	C20	C19
ICOOR_INTERNAL	F2	-120.759332	70.951926	1.385320	C25	C20	F1
ICOOR_INTERNAL	F3	-118.384368	70.903342	1.383675	C25	C20	F2
ICOOR_INTERNAL	C24	-179.946722	62.419046	1.414589	C19	C18	C20
ICOOR_INTERNAL	C23	0.010362	59.023358	1.398205	C24	C19	C18
ICOOR_INTERNAL	C22	0.193614	59.392855	1.396772	C23	C24	C19

ICOOR_INTERNAL	C21	-0.022927	60.637687	1.395543	C22	C23	C24
ICOOR_INTERNAL	H20	179.999029	60.022004	1.082887	C21	C22	C23
ICOOR_INTERNAL	N8	-179.722109	59.603023	1.416893	C22	C23	C21
ICOOR_INTERNAL	H21	179.543056	59.258297	1.030065	N8	C22	C23
ICOOR_INTERNAL	H22	-179.490041	59.252862	1.031163	N8	C22	H21
ICOOR_INTERNAL	H19	-179.986643	60.635697	1.083038	C23	C24	C22
ICOOR_INTERNAL	H18	-179.867044	56.526093	1.071263	C24	C19	C23
ICOOR_INTERNAL	H16	-179.940476	62.786240	1.087599	C15	C1	C16
ICOOR_INTERNAL	S1	-179.929034	71.177075	1.654766	C1	N1	C15
ICOOR_INTERNAL	C2	0.061092	84.158025	1.751119	S1	C1	N1
ICOOR_INTERNAL	H1	-179.547396	51.165815	1.032145	C2	S1	C1
ICOOR_INTERNAL	O7	179.981870	56.614562	1.227206	C4	N7	C3
ICOOR_INTERNAL	H10	179.984530	60.814997	0.984262	N7	S2	C4

The contents of the CouLuc-1-OH ligand params file where LCE stands for CouLuc-1-OH are as follows:

```

NAME LCE
IO_STRING LCE Z
TYPE LIGAND
AA UNK
ATOM N7 Ntrp X -0.50
ATOM S2 S X -0.05
ATOM O1 OOC X -0.65
ATOM O2 OOC X -0.65
ATOM O3 OH X -0.55
ATOM C5 CH2 X -0.07
ATOM C6 CH1 X 0.02
ATOM O4 OH X -0.55
ATOM C9 CH1 X 0.02
ATOM N4 Npro X -0.26
ATOM C11 aroC X -0.00
ATOM N3 Nhis X -0.42
ATOM C10 aroC X -0.00
ATOM N2 Nhis X -0.42
ATOM C13 aroC X -0.00
ATOM N6 NH2O X -0.36
ATOM H6 Hpol X 0.54
ATOM H7 Hpol X 0.54
ATOM C12 aroC X -0.00
ATOM N5 Ntrp X -0.50
ATOM C14 aroC X -0.00
ATOM H15 Haro X 0.23
ATOM H2 Hpol X 0.54
ATOM H14 Haro X 0.23
ATOM C8 CH1 X 0.02
ATOM O6 OH X -0.55
ATOM H8 Hpol X 0.54
ATOM C7 CH1 X 0.02
ATOM O5 OH X -0.55
ATOM H3 Hpol X 0.54
ATOM H11 Hapo X 0.21
ATOM H12 Hapo X 0.21
ATOM H13 Hapo X 0.21
ATOM H9 Hapo X 0.21
ATOM H4 Hapo X 0.21
ATOM H5 Hapo X 0.21
ATOM C4 COO X 0.73
ATOM C3 aroC X -0.00
ATOM N1 Nhis X -0.42
ATOM C1 aroC X -0.00
ATOM C15 CH1 X 0.02
ATOM C16 COO X 0.73
ATOM O8 OOC X -0.65

```

ATOM	C18	aroC	X	-0.00
ATOM	C19	aroC	X	-0.00
ATOM	C20	aroC	X	-0.00
ATOM	C17	aroC	X	-0.00
ATOM	H17	Haro	X	0.23
ATOM	C25	CH1	X	0.02
ATOM	F1	F	X	-0.14
ATOM	F2	F	X	-0.14
ATOM	F3	F	X	-0.14
ATOM	C24	aroC	X	-0.00
ATOM	C23	aroC	X	-0.00
ATOM	C22	aroC	X	-0.00
ATOM	C21	aroC	X	-0.00
ATOM	H20	Haro	X	0.23
ATOM	O9	OH	X	-0.55
ATOM	H21	Hpol	X	0.54
ATOM	H19	Haro	X	0.23
ATOM	H18	Haro	X	0.23
ATOM	H16	Hapo	X	0.21
ATOM	S1	S	X	-0.05
ATOM	C2	aroC	X	-0.00
ATOM	H1	Haro	X	0.23
ATOM	O7	ONH2	X	-0.44
ATOM	H10	Hpol	X	0.54
BOND_TYPE	C1	C15	1	
BOND_TYPE	C1	N1	4	
BOND_TYPE	N1	C3	4	
BOND_TYPE	O1	S2	2	
BOND_TYPE	C1	S1	4	
BOND_TYPE	S1	C2	4	
BOND_TYPE	C2	C3	4	
BOND_TYPE	C2	H1	1	
BOND_TYPE	N2	C10	4	
BOND_TYPE	N2	C13	4	
BOND_TYPE	O2	S2	2	
BOND_TYPE	S2	O3	1	
BOND_TYPE	S2	N7	1	
BOND_TYPE	C3	C4	1	
BOND_TYPE	N3	C10	4	
BOND_TYPE	N3	C11	4	
BOND_TYPE	O3	C5	1	
BOND_TYPE	C4	N7	1	
BOND_TYPE	C4	O7	2	
BOND_TYPE	N4	C9	1	
BOND_TYPE	N4	C11	4	
BOND_TYPE	N4	C14	4	
BOND_TYPE	O4	C6	1	
BOND_TYPE	O4	C9	1	
BOND_TYPE	C5	C6	1	
BOND_TYPE	C5	H4	1	
BOND_TYPE	C5	H5	1	
BOND_TYPE	N5	C12	4	
BOND_TYPE	N5	C14	4	
BOND_TYPE	N5	H2	1	
BOND_TYPE	O5	C7	1	
BOND_TYPE	O5	H3	1	
BOND_TYPE	C6	C7	1	
BOND_TYPE	C6	H9	1	
BOND_TYPE	N6	C13	1	
BOND_TYPE	N6	H6	1	
BOND_TYPE	N6	H7	1	
BOND_TYPE	O6	C8	1	
BOND_TYPE	O6	H8	1	
BOND_TYPE	C7	C8	1	
BOND_TYPE	C7	H11	1	
BOND_TYPE	N7	H10	1	

```

BOND_TYPE C8 C9 1
BOND_TYPE C8 H12 1
BOND_TYPE O8 C18 4
BOND_TYPE C9 H13 1
BOND_TYPE O9 H21 1
BOND_TYPE C10 H14 1
BOND_TYPE C11 C12 4
BOND_TYPE C12 C13 4
BOND_TYPE C14 H15 1
BOND_TYPE C15 C16 1
BOND_TYPE C15 H16 1
BOND_TYPE O8 C16 4
BOND_TYPE C16 C17 4
BOND_TYPE C17 C20 4
BOND_TYPE C17 H17 1
BOND_TYPE C18 C19 4
BOND_TYPE C18 C21 4
BOND_TYPE C19 C20 4
BOND_TYPE C19 C24 4
BOND_TYPE C20 C25 1
BOND_TYPE C21 C22 4
BOND_TYPE C21 H20 1
BOND_TYPE O9 C22 1
BOND_TYPE C22 C23 4
BOND_TYPE C23 C24 4
BOND_TYPE C23 H19 1
BOND_TYPE C24 H18 1
BOND_TYPE C25 F1 1
BOND_TYPE C25 F2 1
BOND_TYPE C25 F3 1
CHI 1 C8 C7 O5 H3
PROTON_CHI 1 SAMPLES 21 45 50 55 60 65 70 75 -45 -50 -55 -60 -65 -70 -75 165 170
175 180 185 190 195 EXTRA 0
CHI 2 C9 C8 O6 H8
PROTON_CHI 2 SAMPLES 21 45 50 55 60 65 70 75 -45 -50 -55 -60 -65 -70 -75 165 170
175 180 185 190 195 EXTRA 0
CHI 3 C23 C22 O9 H21
CHI 4 N1 C1 C15 C16
CHI 5 N7 S2 O3 C5
CHI 6 C4 N7 S2 O1
CHI 7 N7 C4 C3 N1
CHI 8 S2 O3 C5 C6
CHI 9 S2 N7 C4 C3
CHI 10 O4 C9 N4 C11
CHI 11 O3 C5 C6 O4
CHI 12 C1 C15 C16 O8
CHI 13 C19 C20 C25 F1
NBR_ATOM N7
NBR_RADIUS 15.401802
ICOOR_INTERNAL N7 0.000000 0.000000 0.000000 N7 S2 O1
ICOOR_INTERNAL S2 0.000000 180.000000 1.649480 N7 S2 O1
ICOOR_INTERNAL O1 0.000000 72.115214 1.437728 S2 N7 O1
ICOOR_INTERNAL O2 -110.979907 68.095120 1.445125 S2 N7 O1
ICOOR_INTERNAL O3 -129.796485 67.884564 1.508898 S2 N7 O2
ICOOR_INTERNAL C5 47.972804 59.847207 1.411561 O3 S2 N7
ICOOR_INTERNAL C6 157.660576 70.738957 1.511080 C5 O3 S2
ICOOR_INTERNAL O4 77.333973 70.005558 1.402847 C6 C5 O3
ICOOR_INTERNAL C9 125.086234 74.080093 1.413900 O4 C6 C5
ICOOR_INTERNAL N4 -109.502643 70.720185 1.445332 C9 O4 C6
ICOOR_INTERNAL C11 -150.229052 54.143952 1.365802 N4 C9 O4
ICOOR_INTERNAL N3 -0.892936 46.223588 1.342216 C11 N4 C9
ICOOR_INTERNAL C10 -179.432403 59.624923 1.326020 N3 C11 N4
ICOOR_INTERNAL N2 -0.848435 57.610071 1.331554 C10 N3 C11
ICOOR_INTERNAL C13 0.552053 58.120141 1.342096 N2 C10 N3
ICOOR_INTERNAL N6 -179.890730 60.506917 1.449335 C13 N2 C10
ICOOR_INTERNAL H6 -0.115371 59.977458 0.984393 N6 C13 N2

```


ICOOR_INTERNAL	H7	179.952772	59.961946	0.984831	N6	C13	H6
ICOOR_INTERNAL	C12	179.862428	62.184716	1.420651	C13	N2	N6
ICOOR_INTERNAL	N5	-179.949517	44.621863	1.328601	C12	C13	N2
ICOOR_INTERNAL	C14	179.677558	70.203038	1.324715	N5	C12	C13
ICOOR_INTERNAL	H15	-179.517871	55.041066	1.032119	C14	N5	C12
ICOOR_INTERNAL	H2	-179.976464	54.922095	0.984330	N5	C12	C14
ICOOR_INTERNAL	H14	-179.959018	61.152494	1.031712	C10	N3	N2
ICOOR_INTERNAL	C8	125.404314	71.733653	1.475916	C9	O4	N4
ICOOR_INTERNAL	O6	90.149730	71.799851	1.374530	C8	C9	O4
ICOOR_INTERNAL	H8	179.999645	70.557415	0.969220	O6	C8	C9
ICOOR_INTERNAL	C7	-120.391196	77.527376	1.465575	C8	C9	O6
ICOOR_INTERNAL	O5	150.567803	65.743236	1.380198	C7	C8	C9
ICOOR_INTERNAL	H3	179.981880	70.545702	0.969832	O5	C7	C8
ICOOR_INTERNAL	H11	117.168004	68.989317	1.070413	C7	C8	O5
ICOOR_INTERNAL	H12	-121.158644	63.838599	1.069836	C8	C9	C7
ICOOR_INTERNAL	H13	117.674596	67.713631	1.070064	C9	O4	C8
ICOOR_INTERNAL	H9	-119.374097	70.454273	1.069969	C6	C5	O4
ICOOR_INTERNAL	H4	-119.990464	70.450854	1.069592	C5	O3	C6
ICOOR_INTERNAL	H5	-119.938832	70.434132	1.070190	C5	O3	H4
ICOOR_INTERNAL	C4	-83.828030	58.301695	1.468382	N7	S2	O1
ICOOR_INTERNAL	C3	178.603415	63.816343	1.496095	C4	N7	S2
ICOOR_INTERNAL	N1	171.714611	59.715820	1.309092	C3	C4	N7
ICOOR_INTERNAL	C1	179.404452	66.574660	1.362844	N1	C3	C4
ICOOR_INTERNAL	C15	179.223421	54.664545	1.476648	C1	N1	C3
ICOOR_INTERNAL	C16	-179.989679	56.710153	1.346762	C15	C1	N1
ICOOR_INTERNAL	O8	0.912521	59.265165	1.353938	C16	C15	C1
ICOOR_INTERNAL	C18	179.613843	56.700286	1.353045	O8	C16	C15
ICOOR_INTERNAL	C19	0.696119	58.989698	1.419737	C18	O8	C16
ICOOR_INTERNAL	C20	-0.534929	62.229493	1.516594	C19	C18	O8
ICOOR_INTERNAL	C17	-0.014746	61.919117	1.352467	C20	C19	C18
ICOOR_INTERNAL	H17	-179.863883	59.795042	1.088156	C17	C20	C19
ICOOR_INTERNAL	C25	-179.760539	53.572574	1.525937	C20	C19	C17
ICOOR_INTERNAL	F1	-0.152786	65.152910	1.374488	C25	C20	C19
ICOOR_INTERNAL	F2	-120.702945	70.924488	1.383259	C25	C20	F1
ICOOR_INTERNAL	F3	-118.504269	70.882734	1.383434	C25	C20	F2
ICOOR_INTERNAL	C24	-179.969607	62.368500	1.414553	C19	C18	C20
ICOOR_INTERNAL	C23	0.083722	59.067642	1.398551	C24	C19	C18
ICOOR_INTERNAL	C22	0.123564	59.352531	1.393135	C23	C24	C19
ICOOR_INTERNAL	C21	-0.006879	60.580877	1.397258	C22	C23	C24
ICOOR_INTERNAL	H20	179.995074	60.167720	1.083846	C21	C22	C23
ICOOR_INTERNAL	O9	-179.830419	60.331140	1.346965	C22	C23	C21
ICOOR_INTERNAL	H21	179.547800	57.851533	0.967795	O9	C22	C23
ICOOR_INTERNAL	H19	-179.995294	60.475787	1.083563	C23	C24	C22
ICOOR_INTERNAL	H18	179.968998	56.552726	1.071404	C24	C19	C23
ICOOR_INTERNAL	H16	-179.899585	62.673003	1.087086	C15	C1	C16
ICOOR_INTERNAL	S1	-179.809293	71.177075	1.654766	C1	N1	C15
ICOOR_INTERNAL	C2	0.061092	84.158025	1.751119	S1	C1	N1
ICOOR_INTERNAL	H1	-179.547396	51.165815	1.032145	C2	S1	C1
ICOOR_INTERNAL	O7	179.981870	56.614562	1.227206	C4	N7	C3
ICOOR_INTERNAL	H10	179.984530	60.814997	0.984262	N7	S2	C4

The Fluc structure was used as input to the RosettaMatch protocol.¹⁶ This algorithm identifies potential binding modes of input ligands based on user-defined constraints. A binding interaction is considered a “hit” if the ligand atoms do not collide with the protein backbone atoms. The following command line was used to call the RosettaMatch application.

```
<Path to>/Rosetta/main/source/bin/match.linuxgccrelease -s <input_file> @<Path
to>//general_match.flags -match:scaffold_active_site_residues_for_geomcsts <Path
to>/pos_file <Path to>/CouLuc-1_ligand.flags
```

Where the contents of the pos_file was as follows.

```
N_CST 1
1: 308
```

The contents of the constraint file were as follows.

```
CST::BEGIN
NATIVE
  TEMPLATE::  ATOM_MAP: 1 atom_name: O7 C4 C3
  TEMPLATE::  ATOM_MAP: 1 residue3: LCC/LCD/LCE

  TEMPLATE::  ATOM_MAP: 2 atom_name: N CA C ,
  TEMPLATE::  ATOM_MAP: 2 residue1: G
  TEMPLATE::  ATOM_MAP: 2 is_backbone

  CONSTRAINT:: distanceAB: 4.30 1.50 80.0 1 1
  CONSTRAINT:: angle_A: 135.3 10.0 10.0 360. 1
  CONSTRAINT:: angle_B: 43.6 10.0 10.0 360. 1
  CONSTRAINT:: torsion_A: 10.7 10.0 10.0 360. 1
  CONSTRAINT:: torsion_AB: -160.7 10.0 10.0 360. 1
  CONSTRAINT:: torsion_B: -134.1 10.0 10.0 360. 1

  ALGORITHM_INFO:: match
    CHI_STRATEGY:: CHI 1 EX_THREE_THIRD_STEP_STDDEVS
    CHI_STRATEGY:: CHI 2 EX_THREE_THIRD_STEP_STDDEVS
  ALGORITHM_INFO::END
CST::END
```

The contents of the CouLuc-1_ligand.flags files were as follows.

```
-extra_res_fa <Path to>/CouLuc-1_ligand.params
-match:geometric_constraint_file <Path to>/CouLuc-1_ligand.cst
-match:lig_name LCC/LCD/LCE
```

The contents of the general_match.flags files was as follows.

```
-packing
-ex1
-ex2
-ex2aro
-exlaro
-extrachi_cutoff 0
-use_input_sc true
-database <Path to>/Rosetta/main/database/
-match:filter_colliding_upstream_residues
-match:filter_upstream_downstream_collisions
-match:upstream_residue_collision_tolerance 0.95
-match:updown_collision_tolerance 0.3
-match::bump_tolerance 0.3
-match_grouper SameSequenceAndDSPositionGrouper
-match:grouper_downstream_rmsd 0.5
-match:euclid_bin_size 0.5
-match:euler_bin_size 5.0
-output_format PDB
-exclude_patches N_acetylated
-consolidate_matches 1
-output_matches_per_group 1
-output_matchres_only false
-enumerate_ligand_rotamers
-only_enumerate_non_match_redundant_ligand_rotamers
-out::file::output_virtual
```

The pdb files generated in the matching run were then used as inputs for RosettaDesign calculations. The RosettaDesign algorithm is used to re-sculpt the pocket surrounding the docked luciferin analogue in order to remove clashing side chains and introduce new, productive

interactions with the ligand. The RosettaDesign application was called with the following command line:

```
<Path to>/Rosetta/main/source/bin/rosetta_scripts.linuxgccrelease -s <input_file> -  
parser:protocol <Path to>/enzdes.xml -nstruct 1 -jd2:ntrials 1 -database <Path  
to>/Rosetta/main/database/ @<Path to>/CouLuc-1_ligand.flags @<Path to>/general.flags
```

The contents of the RosettaDesign general.flags file was as follows:

```
-run::preserve_header  
-enzdes::minimize_ligand_torsions 7.0  
-enzdes::detect_design_interface  
-unmute protocols.enzdes.EnzRepackMinimize  
-packing::use_input_sc  
-packing::extrachi_cutoff 1  
-packing::ex1  
-packing::ex2  
-linmem_ig 10  
-in:ignore_unrecognized_res  
-ligand::old_estat  
-jd2:enzdes_out  
-nblast_autoupdate  
-score:weights <Path to>/Rosetta/main/database/scoring/weights/ref2015.wts  
-enzdes::bb_min_allowed_dev 0.05  
-no_his_his_pairE
```

The contents of the RosettaDesign enzdes.xml file was as follows:

```
<ROSETTASCRIPTS>  
  
  <TASKOPERATIONS>  
    <DetectProteinLigandInterface name="dsgn_cuts_on" cut1="6" cut2="8"  
cut3="10" cut4="12" design="1"/>  
    <DetectProteinLigandInterface name="dsgn_cuts_off" cut1="6" cut2="8"  
cut3="10" cut4="12" design="0"/>  
    <RestrictResiduesToRepacking name="pack_only" residues="210,221"/>  
  </TASKOPERATIONS>  
  
  <SCOREFXNS>  
    <ScoreFunction name="ref2015" weights="ref2015.wts"/>  
  </SCOREFXNS>  
  
  <MOVERS>  
    #Add constraints to file  
    AddOrRemoveMatchCsts name="addcst" cst_instruction=add_new  
cstfile="../../inputs/FAB.cst"/>  
    <AddOrRemoveMatchCsts name="addcst" cst_instruction="add_new"/>  
    <AddOrRemoveMatchCsts name="rmvcst" cst_instruction="remove"  
keep_covalent="1"/>  
    <AddOrRemoveMatchCsts name="addprg" cst_instruction=add_pregenerated/>  
    #Optimize the pose per the cst file  
    <EnzRepackMinimize name="cstopt" scorefxn_minimize="ref2015" cst_opt="1"  
design="0" repack_only="0" fix_catalytic="0" minimize_rb="1" minimize_bb="1"  
minimize_sc="1" minimize_lig="1" min_in_stages="1" cycles="1"  
task_operations="dsgn_cuts_off"/>  
    #Design and repacking around the catalytic residues; keep the catalytic  
residues fixed in this instance.  
    <EnzRepackMinimize name="dsgn" scorefxn_minimize="ref2015" cst_opt="0"  
design="1" repack_only="0" fix_catalytic="1" minimize_rb="1" minimize_bb="1"  
minimize_sc="1" minimize_lig="1" min_in_stages="1" backrub="0" cycles="1"  
task_operations="dsgn_cuts_on,pack_only"/>
```

```

        #Minimize after each design.
        <EnzRepackMinimize name="min" scorefxn_minimize="ref2015" cst_opt="0"
design="0" repack_only="0" fix_catalytic="1" minimize_rb="1" minimize_bb="1"
minimize_sc="1" minimize_lig="1" min_in_stages="1" backrub="0" cycles="1"
task_operations="dsgn_cuts_off"/>

        #Perform a final repacking step.
        <EnzRepackMinimize name="rpkmmin" scorefxn_minimize="ref2015" cst_opt="0"
design="0" repack_only="1" fix_catalytic="0" minimize_rb="1" minimize_bb="1"
minimize_sc="1" minimize_lig="0" min_in_stages="1" backrub="0" cycles="1"
task_operations="dsgn_cuts_off"/>

        #Monte Carlo movers for each step in the enzdes process (helps to
generate )
        <GenericMonteCarlo name="multi_cstopt" mover_name="cstopt"
scorefxn_name="ref2015" trials="10" sample_type="low" temperature="0.6" drift="1"
recover_low="1" preapply="0"/>
    </MOVERS>

    <PROTOCOLS>
        <Add mover_name="addcst"/>
        <Add mover_name="multi_cstopt"/>
        <Add mover_name="dsgn"/>
        <Add mover_name="min"/>
        <Add mover_name="dsgn"/>
        <Add mover_name="min"/>
        <Add mover_name="dsgn"/>
        <Add mover_name="min"/>
        Add mover=rmvcst/>
        Add mover=rpkmmin/>
        Add mover=des_min/>
        Add mover=des_min/>
        Add mover=des_min/>
        Add mover_name="rmvcst"/>
        Add mover_name="rpkmmin"/>
        Add mover=finmin_rpkmin/>
    </PROTOCOLS>

</ROSETTASCRIPTS>

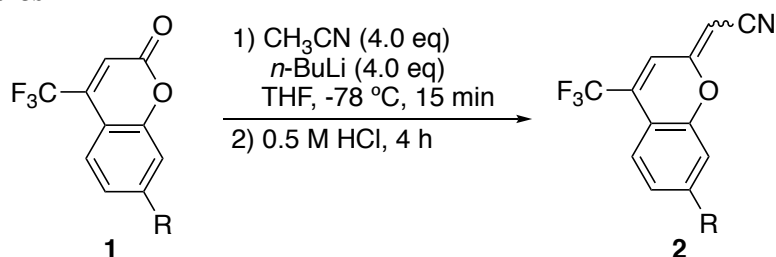
```

Synthetic materials and methods

Unless stated otherwise, reactions were conducted in oven-dried glassware under an atmosphere of nitrogen using anhydrous solvents. All commercially obtained reagents were used as received. Flash column chromatography was performed using reversed phase (100 Å, 20-40 micron particle size, RediSep® Rf Gold® Reversed-phase C18 or C18Aq) on a CombiFlash® Rf 200i (Teledyne Isco, Inc.). High-resolution LC/MS analyses were conducted on a Thermo-Fisher LTQ-Orbitrap-XL hybrid mass spectrometer system with an Ion MAX API electrospray ion source in negative ion mode. Analytical LC/MS was performed using a Shimadzu LCMS-2020 Single Quadrupole utilizing a Kinetex 2.6 µm C18 100 Å (2.1 x 50 mm) column obtained from Phenomenex, Inc. Runs employed a gradient of 0→90% MeCN/0.1% aqueous formic acid over 4.5 min at a flow rate of 0.2 mL/min. ¹H NMR and ¹³C NMR spectra were recorded on Bruker spectrometers (at 400 or 500 MHz or at 100 or 125 MHz) and are reported relative to deuterated solvent signals. Data for ¹H NMR spectra are reported as follows: chemical shift (δ ppm), multiplicity, coupling constant (Hz), and integration. Data for ¹³C NMR spectra are reported in terms of chemical shift. Absorption curves were obtained on a Shimadzu UV-2550 spectrophotometer operated by UVProbe 2.32 software. Fluorescence traces were recorded on a PTI QuantaMaster steady-state spectrofluorometer operated by FelixGX 4.2.2 software, with 5 nm excitation and emission slit

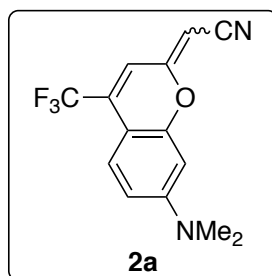
widths, 0.1 s integration rate, and enabled emission correction. Data analysis and curve fitting were performed using MS Excel 2019 and GraphPad Prism 8.

Synthetic procedures



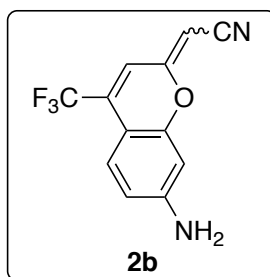
General procedure for the synthesis of nitrile (2)

To a solution of CH_3CN (8.0 mmol, 4.0 eq) in THF (20 mL) was added $n\text{-BuLi}$ (8.0 mmol, 2.5 M, 4.0 eq) at -78°C . The solution was stirred at -78°C 10 minutes, after which a solution of coumarin (**1**) (2.0 mmol, 1.0 eq) in 5 mL of THF was added slowly. The reaction was stirred at -78°C for 10-15 min and quenched with 15 mL aqueous NH_4Cl solution. The mixture was warmed to room temperature and extracted with EtOAc and concentrated. To the crude oil was added 125 mL of 0.5 M HCl and stirred vigorously for 1-4 h. The precipitate was extracted with EtOAc, dried Na_2SO_4 and concentrated to give nitrile **2** as a mixture of isomers. Based on ^1H NMR spectroscopic analysis, the resulting product was typically $>90\%$ pure and was typically used in the next step without further purification. Silica gel column chromatography could be performed using EtOAc/hexanes to obtain high purity material ($>95\%$).



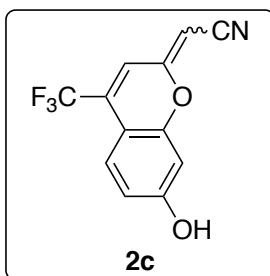
(Z/E)-2-(7-Dimethylamino)-4-(trifluoromethyl)-2H-chromen-2-ylideneacetonitrile (2a).

Following the general procedure using commercial 7-(dimethylamino)-4-(trifluoromethyl)coumarin (**1a**) (514 mg, 2.0 mmol). Purification by flash chromatography on silica gel (hexanes/EtOAc, 0% to 20%) afforded **2a** as an orange solid (358 mg, 64% yield). ^1H NMR (CDCl_3 , 400 MHz, compound exists as a mixture of isomers, *Z*-isomer denoted by *, *E*-isomer denoted by §) δ 7.32 – 7.26 (m, 1H^* , 1H^\S), 6.85 (s, 1H^\S), 6.50 – 6.47 (m, 2H^* , 1H^\S), 6.38 (s, 1H^*), 6.33 (d, $J = 2.6$ Hz, 1H^\S), 4.78 (s, 1H^\S), 4.48 (s, 1H^*), 3.05 (s, 6H^*), 3.04 (s, 6H^\S); ^{13}C NMR (CDCl_3 , 100 MHz) δ 164.1 § , 162.6*, 154.6 § , 153.1*, 131.7 (q, $J = 33.0$ Hz) § , 131.1 (q, $J = 33.0$ Hz)*, 125.8 (q, $J = 2.2$ Hz) § , 125.6 (q, $J = 2.2$ Hz)*, 122.3 (q, $J = 272.8$ Hz) § , 122.2 (q, $J = 272.6$ Hz)*, 117.7 § , 116.9*, 112.6 (q, $J = 6.3$ Hz)*, 111.2 (q, $J = 6.3$ Hz) § , 108.7 § , 108.7*, 103.4*, 103.3 § , 98.7*, 98.1 § , 73.6 § , 72.3*, 40.2*, 40.2 § ; ^{19}F NMR (CDCl_3 , 377 MHz) δ -64.5 § , -64.6*; HRMS (ESI) calculated for *Z*-isomer $\text{C}_{14}\text{H}_{12}\text{F}_3\text{N}_2\text{O}$ ($\text{M}+\text{H}$) $^+$ 290.0896, observed 290.0900; *E*-isomer $\text{C}_{14}\text{H}_{12}\text{F}_3\text{N}_2\text{O}$ ($\text{M}+\text{H}$) $^+$ 290.0896, observed 290.0901.



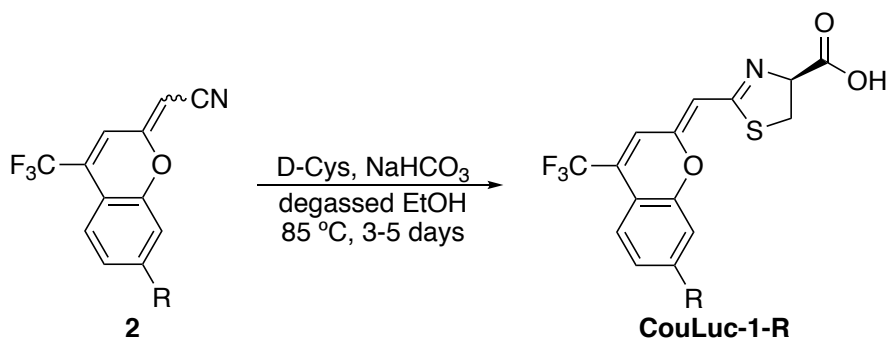
(Z/E)-2-(7-Amino-4-(trifluoromethyl)-2H-chromen-2-ylidene)acetonitrile (2b).

Following the general procedure using commercial 7-amino-4-(trifluoromethyl)coumarin (**1b**) (458 mg, 2.0 mmol). Purification by flash chromatography on silica gel (hexanes/EtOAc, 0% to 30%) afforded **2b** as an orange solid (308 mg, 61% yield). ¹H NMR (CD₃CN, 400 MHz, compound exists as a mixture of isomers, *Z*-isomer denoted by *, *E*-isomer denoted by §) δ 7.24 – 7.18 (m, 1H*, 1H§), 6.77 (dd, *J* = 2.4, 1.2 Hz, 1H§), 6.62 (dd, *J* = 2.4, 1.2 Hz, 1H*), 6.51 – 6.49 (m, 1H*, 1H§), 6.44 (d, *J* = 2.3 Hz, 1H*), 6.37 (d, 1H§), 5.00 – 4.92 (m, 2H*, 2H§), 4.91 (s, 1H§), 4.73 (s, 1H*); ¹³C NMR (CD₃CN, 125 MHz) δ 164.6§, 163.3*, 155.6§, 155.4*, 153.7§, 153.5*, 131.8 (q, *J* = 32.1 Hz)§, 130.7 (q, *J* = 32.1 Hz)*, 126.8 (q, *J* = 2.2 Hz)§, 126.6 (q, *J* = 2.2 Hz)*, 123.3 (q, *J* = 273.7 Hz)§, 123.3 (q, *J* = 273.5 Hz)*, 118.1§, 117.3*, 114.8 (q, *J* = 6.5 Hz)*, 112.2 (q, *J* = 6.5 Hz)§, 112.1*, 112.0§, 104.8*, 104.5§, 101.1*, 100.9§, 74.7§, 73.5*; ¹⁹F NMR (CD₃CN, 377 MHz) δ -64.6*, -64.7§; HRMS (ESI) calculated for C₁₂H₈F₃N₂O (M+H)⁺ 253.0583, observed 253.0582.



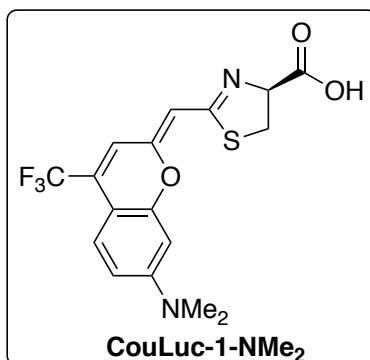
(Z/E)-2-(7-Hydroxy-4-(trifluoromethyl)-2H-chromen-2-ylidene)acetonitrile (2c).

Following the general procedure using commercial 7-hydroxy-4-(trifluoromethyl)coumarin (**1c**) (460 mg, 2.0 mmol). Purification by flash chromatography on silica gel (hexanes/EtOAc, 0% to 50%) afforded **2c** as a yellow solid (354 mg, 70% yield). ¹H NMR (CD₃OD, 400 MHz, compound exists as a mixture of isomers, *Z*-isomer denoted by *, *E*-isomer denoted by §) δ 7.37 – 7.31 (m, 1H*, 1H§), 6.93 – 6.92 (m, 1H§), 6.86 – 6.84 (m, 1H*), 6.71 – 6.66 (m, 2H*, 1H§), 6.60 (d, *J* = 2.4 Hz, 1H§), 5.11 (s, 1H§), 4.96 (s, 1H*); ¹³C NMR (CD₃OD, 100 MHz) δ 164.7§, 163.5*, 163.4§, 163.1*, 155.9§, 155.6*, 132.3 (q, *J* = 323.0 Hz)§, 131.1 (q, *J* = 323.0 Hz)*, 127.6*, 127.6§, 127.2 (q, *J* = 1.8 Hz)§, 127.0 (q, *J* = 1.8 Hz)*, 124.9*, 124.8§, 122.1*, 122.1§, 117.9*, 117.1 (q, *J* = 6.5 Hz)*, 117.0§, 114.3 (q, *J* = 6.4 Hz)§, 114.0§, 114.0*, 107.6*, 107.3§, 104.1§, 104.0*, 75.9§, 74.4*; ¹⁹F NMR (CD₃OD, 377 MHz) δ -66.1§, -66.2*; HRMS (ESI) calculated for C₁₂H₅F₃NO₂ (M-H)⁻ 252.0278, observed 252.0270.



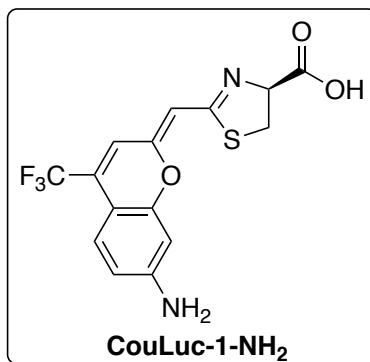
General procedure for the synthesis of CouLuc-1-R

To a microwave vial containing nitrile (**2**) (0.15 mmol, 1.0 eq), D-cysteine hydrochloride monohydrate (0.23 mmol, 1.5 eq) and NaHCO₃ (0.60 mmol, 4.0 eq) was added N₂-sparged EtOH (1.5 mL). The suspension was heated at 85 °C under N₂ and monitored by LC/MS. After 3-5 days the consumption of **2** is greater than 75%. The reaction mixture was cooled to room temperature and EtOH was evaporated under vacuum. The crude solid was triturated with Et₂O (3 x 5 mL), acidified to pH 1.0, filtered and wash with cold water (3 x 5 mL). The crude mixture was purified directly by reversed phase chromatography (C₁₈, 0-100% MeOH/water). The solvent was removed *in vacuo* to afford **CouLuc-1-R**.



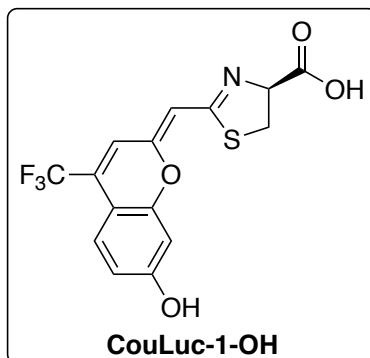
(Z)-2-((7-(Dimethylamino)-4-(trifluoromethyl)-2H-chromen-2-ylidene)methyl)-4,5-dihydrothiazole-4-carboxylic acid (CouLuc-1-NMe₂).

Following the general procedure using **2a** (42 mg, 0.15 mmol), **CouLuc-1-NMe₂** was obtained as a red solid (23 mg, 40% yield). ¹H NMR (CD₃OD + TFA-*d*₁, 500 MHz) δ 7.56 – 7.53 (m, 1H), 6.93 (s, 1H), 6.89 (dd, *J* = 9.3, 2.6 Hz, 1H), 6.76 (d, *J* = 2.6 Hz, 1H), 6.18 (s, 1H), 5.16 (dd, *J* = 9.4, 5.6 Hz, 1H), 4.00 – 3.90 (m, 2H), 3.14 (s, 6H); ¹³C NMR (125 MHz, DMSO-*d*₆ + TFA-*d*₁) δ 186.3, 179.5, 173.0, 164.0, 163.1, 143.1 (q, *J* = 32.5 Hz), 135.0, 131.6 (q, *J* = 275.6 Hz), 128.3, 122.4 (q, *J* = 6.1 Hz), 121.1, 112.9, 106.7, 102.8, 72.0, 43.4; ¹⁹F NMR (DMSO-*d*₆, 377 MHz) δ - 63.4; HRMS (ESI) calculated for C₁₇H₁₅F₃N₂O₃S (M+H)⁺ 385.0828, observed 385.0833.



(Z)-2-((7-Amino-4-(trifluoromethyl)-2H-chromen-2-ylidene)methyl)-4,5-dihydro-thiazole-4-carboxylic acid (CouLuc-1-NH₂).

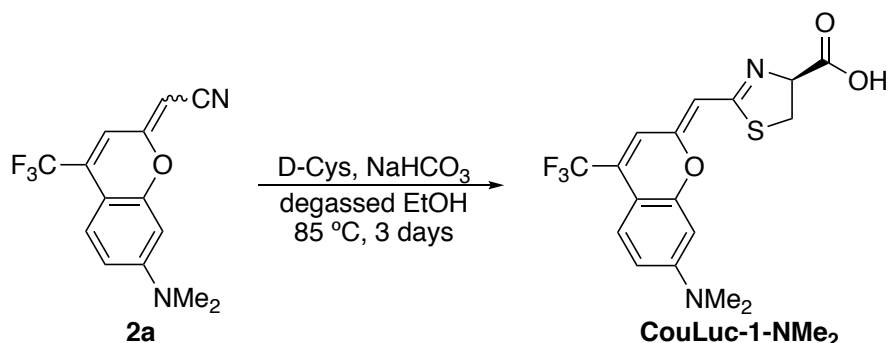
Following the general procedure using **2b** (37 mg, 0.15 mmol), **CouLuc-1-NH₂** was obtained as an orange solid (28 mg, 52% yield). ¹H NMR (400 MHz, DMSO-*d*₆) δ 7.09 – 7.02 (m, 1H), 6.87 (s, 1H), 6.45 – 6.38 (m, 2H), 6.14 (s, 2H), 5.94 (s, 1H), 4.96 (t, *J* = 9.0 Hz, 1H), 3.49 (dd, *J* = 11.1, 9.5 Hz, 1H), 3.41 (dd, *J* = 11.1, 8.5 Hz, 1H); ¹³C NMR (125 MHz, DMSO-*d*₆) δ 172.3, 162.5, 153.8, 152.8, 152.7, 126.5 (q, *J* = 30.6 Hz), 124.9, 122.5 (q, *J* = 271.9 Hz), 115.9 (q, *J* = 6.3 Hz), 110.3, 102.2, 101.8, 99.3, 76.2, 32.2; ¹⁹F NMR (DMSO-*d*₆, 377 MHz) δ -63.4; HRMS (ESI) calculated for C₁₅H₁₂F₃N₂O₃S (M+H)⁺ 357.0515, observed 357.0523.



(Z)-2-((7-hydroxy-4-(trifluoromethyl)-2H-chromen-2-ylidene)methyl)-4,5-dihydro-thiazole-4-carboxylic acid (CouLuc-1-OH).

Following the general procedure using **2c** (38 mg, 0.15 mmol), **CouLuc-1-OH** was obtained as an orange solid (24 mg, 45% yield). ¹H NMR (500 MHz, CD₃OD + TFA-*d*₁) δ 7.63 – 7.61 (m, 1H), 7.25 (s, 1H), 7.03 (d, *J* = 2.4 Hz, 1H), 6.97 (dd, *J* = 8.9, 2.4 Hz, 1H), 6.32 (s, 1H), 5.29 (dd, *J* = 9.8, 5.7 Hz, 1H), 4.06 (dd, *J* = 12.1, 9.8 Hz, 1H), 4.01 (dd, *J* = 12.0, 5.7 Hz, 1H); ¹³C NMR (125 MHz, CD₃OD + TFA-*d*₁) δ 180.3, 170.6, 165.3, 164.7, 156.1, 136.4 (q, *J* = 33.2 Hz), 127.9 (q, *J* = 2.4 Hz), 123.2 (q, *J* = 272.3 Hz), 116.8 (q, *J* = 5.9 Hz), 116.4, 108.4, 104.3, 64.4, 35.1; ¹⁹F NMR (CD₃OD + TFA-*d*₁, 377 MHz) δ -65.5; HRMS (ESI) calculated for C₁₅H₁₁F₃NO₄S (M+H)⁺ 358.0355, observed 358.0358.

Synthesis of CouLuc-1-NMe₂ with chromatography-free procedure



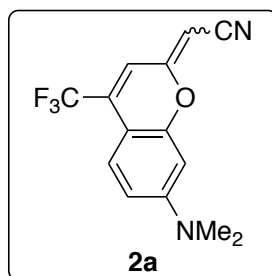
To a reaction flask containing nitrile (**2a**) (1.25 g, 4.49 mmol), D-cysteine hydrochloride monohydrate (1.18 g, 6.73 mmol) and NaHCO₃ (1.51 g, 17.94 mmol) was N₂-sparged EtOH (45 mL) was heated at 85 °C under N₂. After heating for 3 days the EtOH was evaporated under vacuum. The yellow solid was triturated with Et₂O (3 x 20 mL), acidified to pH 1.0 with 1M HCl to give a red solid that was separated by centrifugation and the supernatant was discarded. The precipitates were suspended in 15 mL water and then centrifuged. The washing process was repeated twice. The precipitate was dried under reduced pressure to afford **CouLuc-1-NMe₂** as a red solid (468 mg, 27% yield) to provide high purity material by NMR (>95%).

References

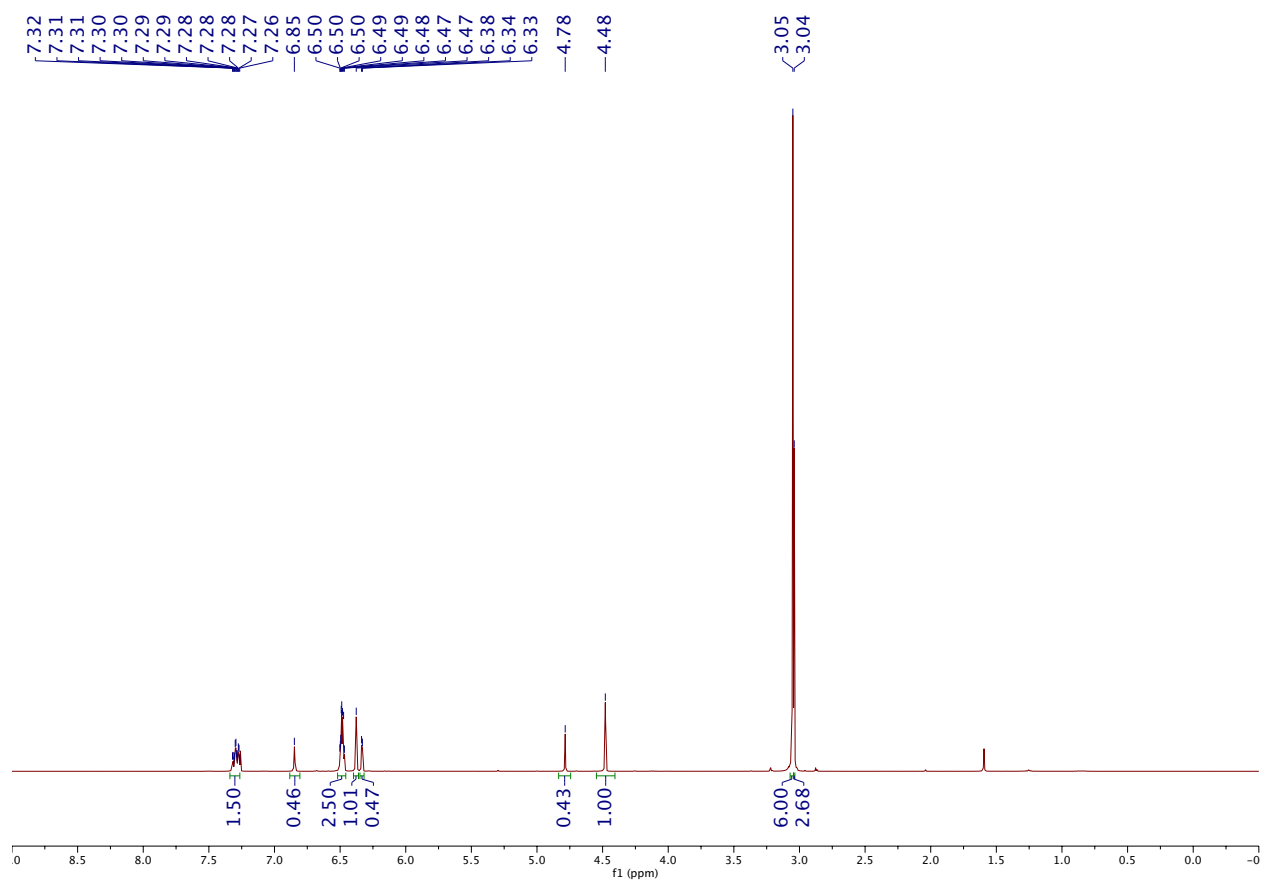
1. Tinberg, C. E.; Khare, S. D.; Dou, J.; Doyle, L.; Nelson, J. W.; Schena, A.; Jankowski, W.; Kalodimos, C. G.; Johnsson, K.; Stoddard, B. L.; Baker, D. Computational design of ligand-binding proteins with high affinity and selectivity. *Nature* **2013**, *501*, 212.
2. Zanghellini, A.; Jiang, L.; Wollacott, A. M.; Cheng, G.; Meiler, J.; Althoff, E. A.; R  thlisberger, D.; Baker, D. New algorithms and an in silico benchmark for computational enzyme design. *Protein Sci.* **2006**, *15*, 2785.
3. Studier, F. W. Protein production by auto-induction in high-density shaking cultures. *Protein Expr. Purif.* **2005**, *41*, 207.
4. Rathbun, C. M.; Porterfield, W. B.; Jones, K. A.; Sagoe, M. J.; Reyes, M. R.; Hua, C. T.; Prescher, J. A. Parallel screening for rapid identification of orthogonal bioluminescent tools. *ACS Cent. Sci.* **2017**, *3*, 1254.
5. Jones, K. A.; Porterfield, W. B.; Rathbun, C. M.; McCutcheon, D. C.; Paley, M. A.; Prescher, J. A. Orthogonal luciferase–luciferin pairs for bioluminescence imaging. *J. Am. Chem. Soc.* **2017**, *139*, 2351.
6. Rathbun, C. M.; Ionkina, A. A.; Yao, Z.; Jones, K. A.; Porterfield, W. B.; Prescher, J. A. Rapid multicomponent bioluminescence imaging via substrate unmixing. *ACS Chem. Biol.* **2021**, *16*, 682.
7. Zhang, B. S.; Jones, K. A.; McCutcheon, D. C.; Prescher, J. A. Pyridone luciferins and mutant luciferases for bioluminescence imaging. *ChemBioChem* **2018**, *19*, 470–477.
8. Harwood, K. R.; Mofford, D. M.; Reddy, G. R.; Miller, S. C. Identification of mutant firefly luciferases that efficiently utilize aminoluciferins. *Chem. Biol.* **2011**, *18*, 1649.

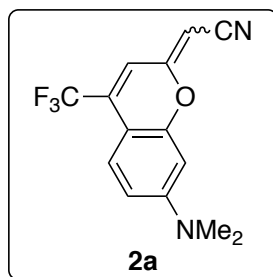
9. Belsare, K. D.; Andorfer, M. C.; Cardenas, F. S.; Chael, J. R.; Park, H. J.; Lewis, J. C. A simple combinatorial codon mutagenesis method for targeted protein engineering. *ACS Synth. Biol.* **2017**, *6*, 416.
10. Yao, Z.; Zhang, B. S.; Steinhardt, R. C.; Mills, J. H.; Prescher, J. A. Multicomponent bioluminescence imaging with a π -extended luciferin. *J. Am. Chem. Soc.* **2020**, *142*, 14080.
11. Gammon, S. T.; Leevy, W. M.; Gross, S.; Gokel, G. W.; Piwnica-Worms, D. Spectral unmixing of multicolored bioluminescence emitted from heterogeneous biological sources. *Anal. Chem.* **2006**, *78*, 1520.
12. Alford, R. F.; Leaver-Fay, A.; Jeliazkov, J. R.; O'Meara, M. J.; DiMaio, F. P.; Park, H.; Shapovalov, M. V.; Renfrew, P. D.; Mulligan, V. K.; Kappel, K.; Labonte, J. W.; Pacella, M. S.; Bonneau, R.; Bradley, P.; Dunbrack, R. L.; Das, R.; Baker, D.; Kuhlman, B.; Kortemme, T.; Gray, J. J. The Rosetta all-atom energy function for macromolecular modeling and design. *J. Chem. Theory Comput.* **2017**, *13*, 3031.
13. Nivón, L. G.; Moretti, R.; Baker, D. A pareto-optimal refinement method for protein design scaffolds. *PLoS One* **2013**, *8*, e59004.
14. Hanwell, M. D.; Curtis, D. E.; Lonie, D. C.; Vandermeersch, T.; Zurek, E.; Hutchison, G. R. Avogadro: an advanced semantic chemical editor, visualization, and analysis platform. *J. Cheminformatics* **2012**, *4*, 17.
15. Rappe, A. K.; Casewit, C. J.; Colwell, K. S.; Goddard, W. A.; Skiff, W. M. UFF, a full periodic table force field for molecular mechanics and molecular dynamics simulations. *J. Am. Chem. Soc.* **1992**, *114*, 10024–10035.
16. Richter, F.; Leaver-Fay, A.; Khare, S. D.; Bjelic, S.; Baker, D. De novo enzyme design using Rosetta3. *PLoS One* **2011**, *6*, e19230.

NMR Spectra

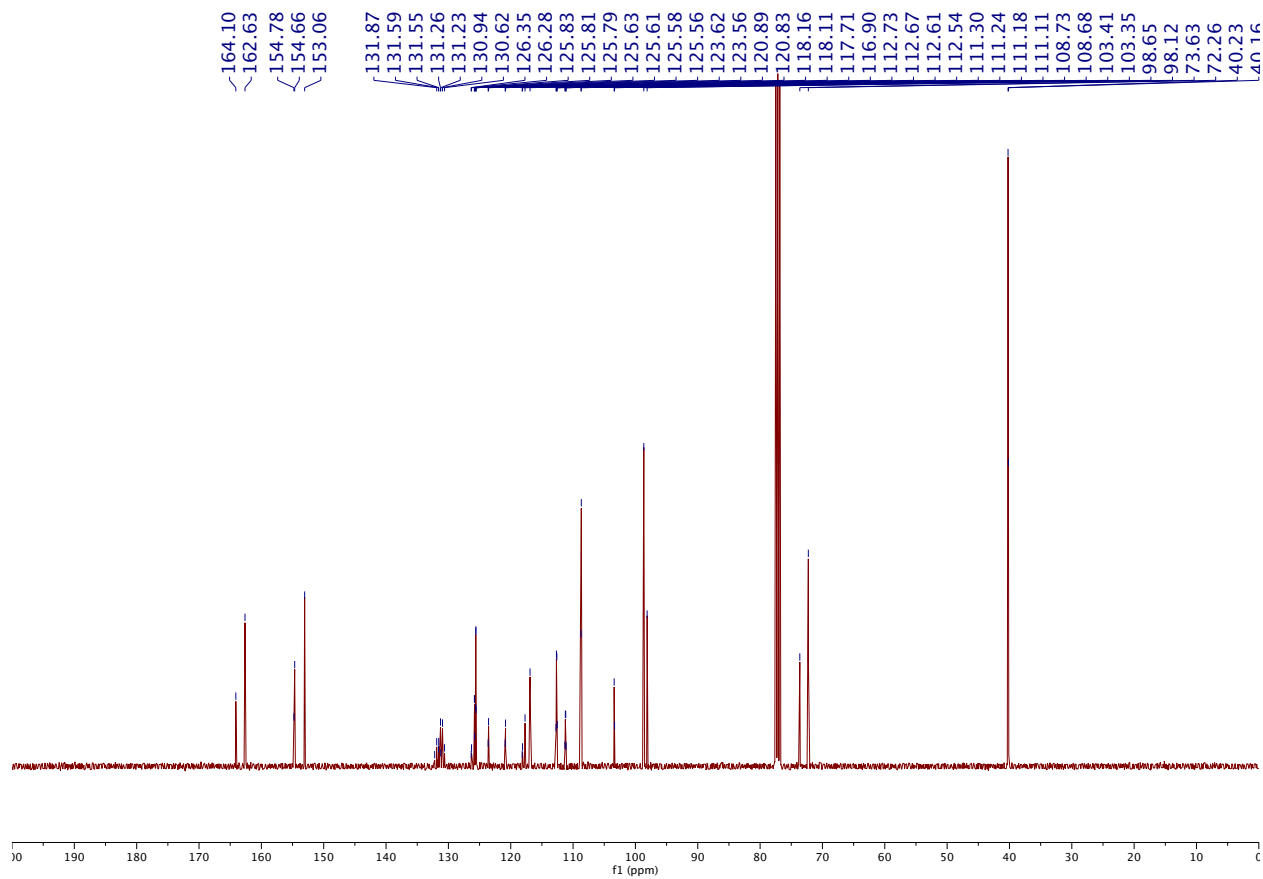


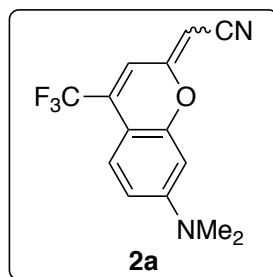
¹H NMR



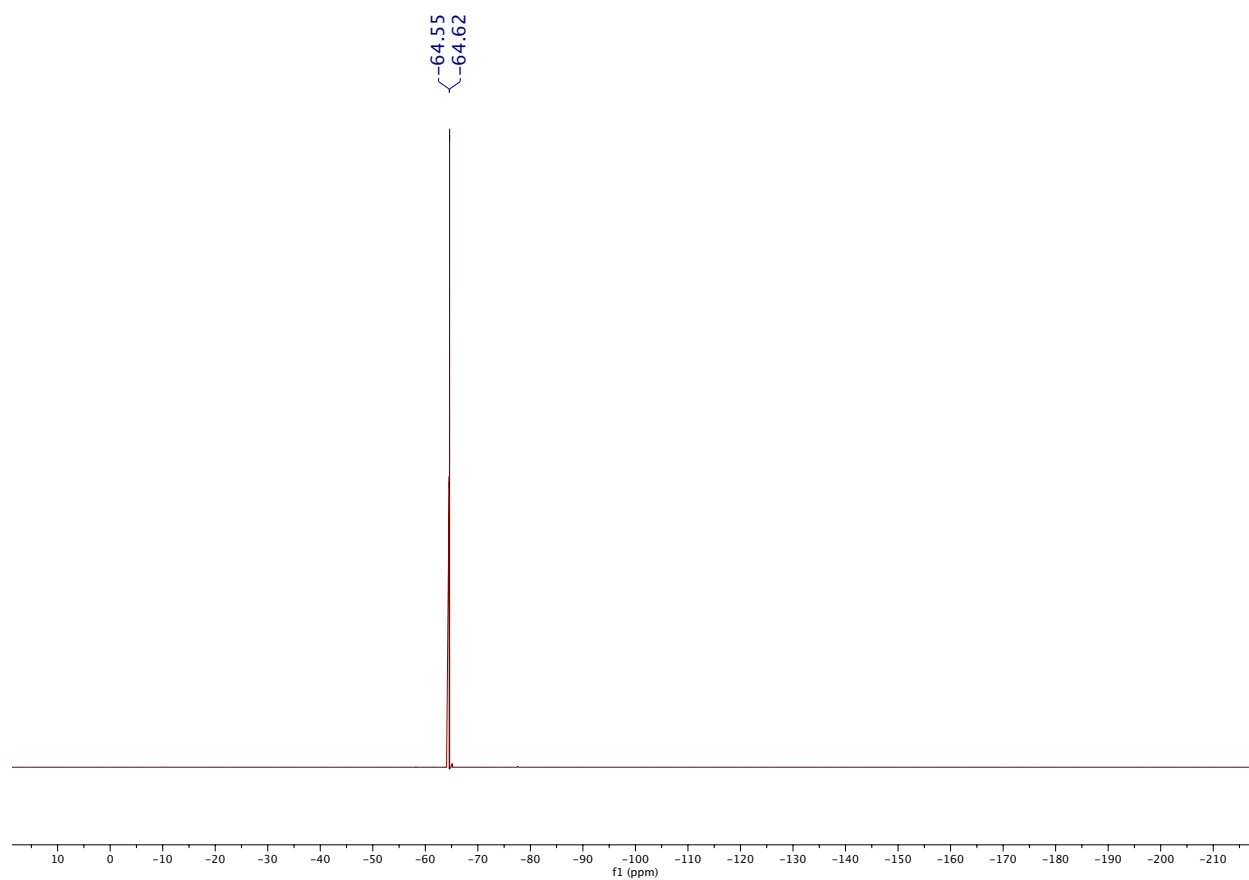


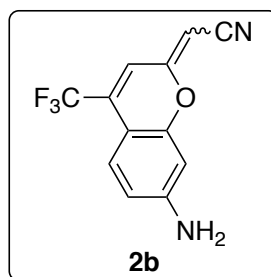
¹³C NMR



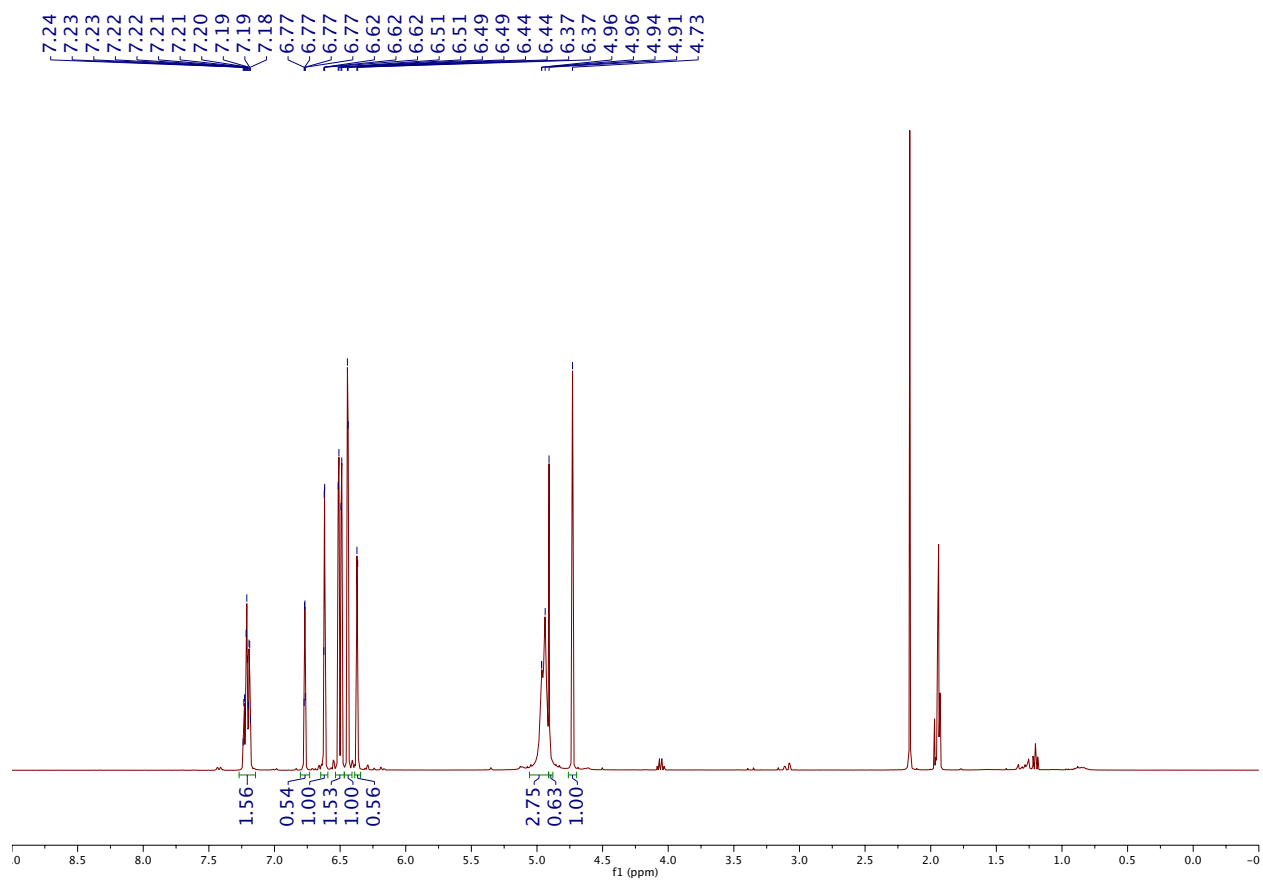


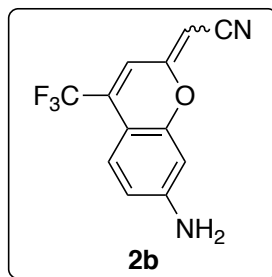
¹⁹F NMR



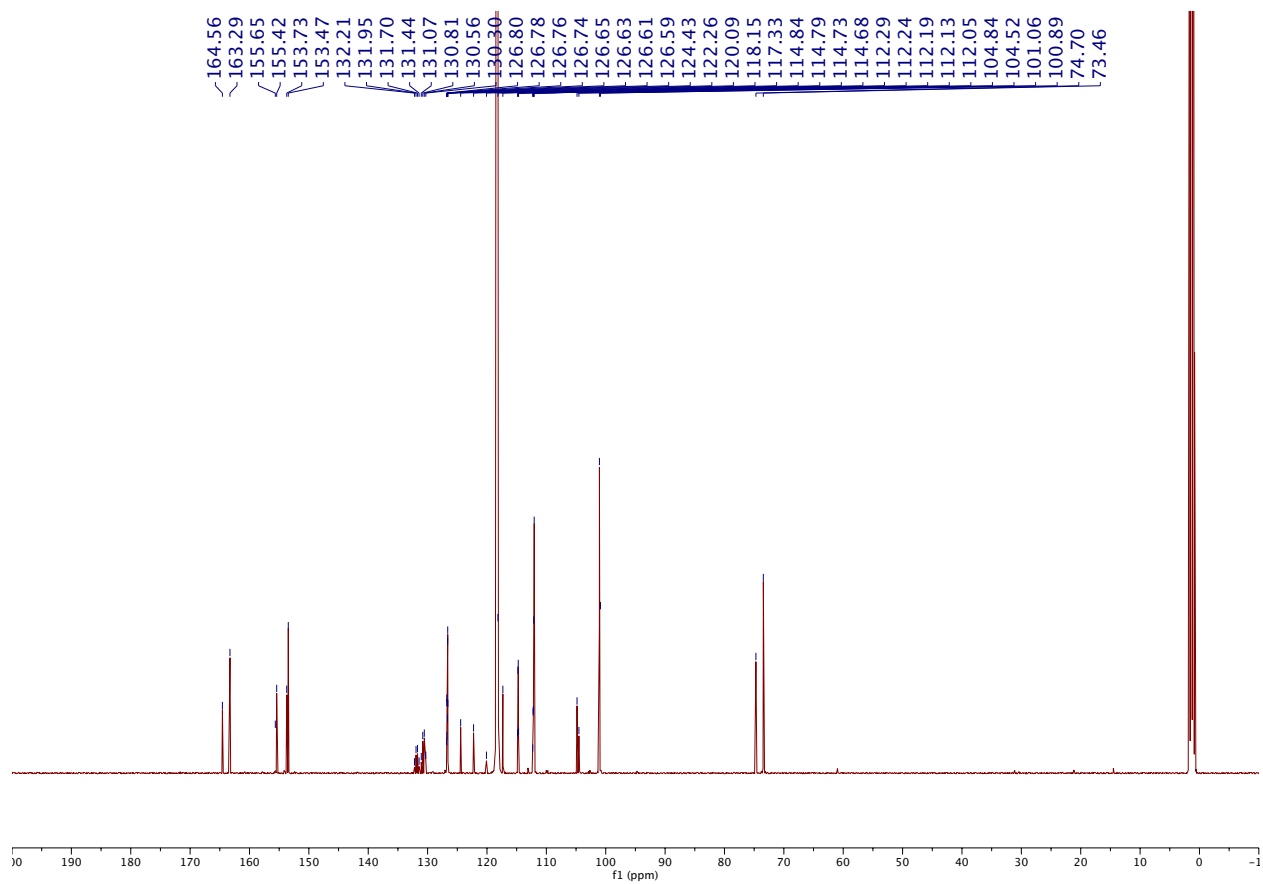


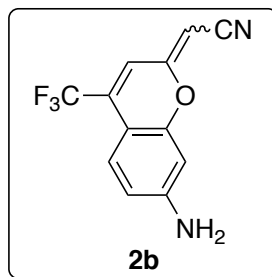
¹H NMR



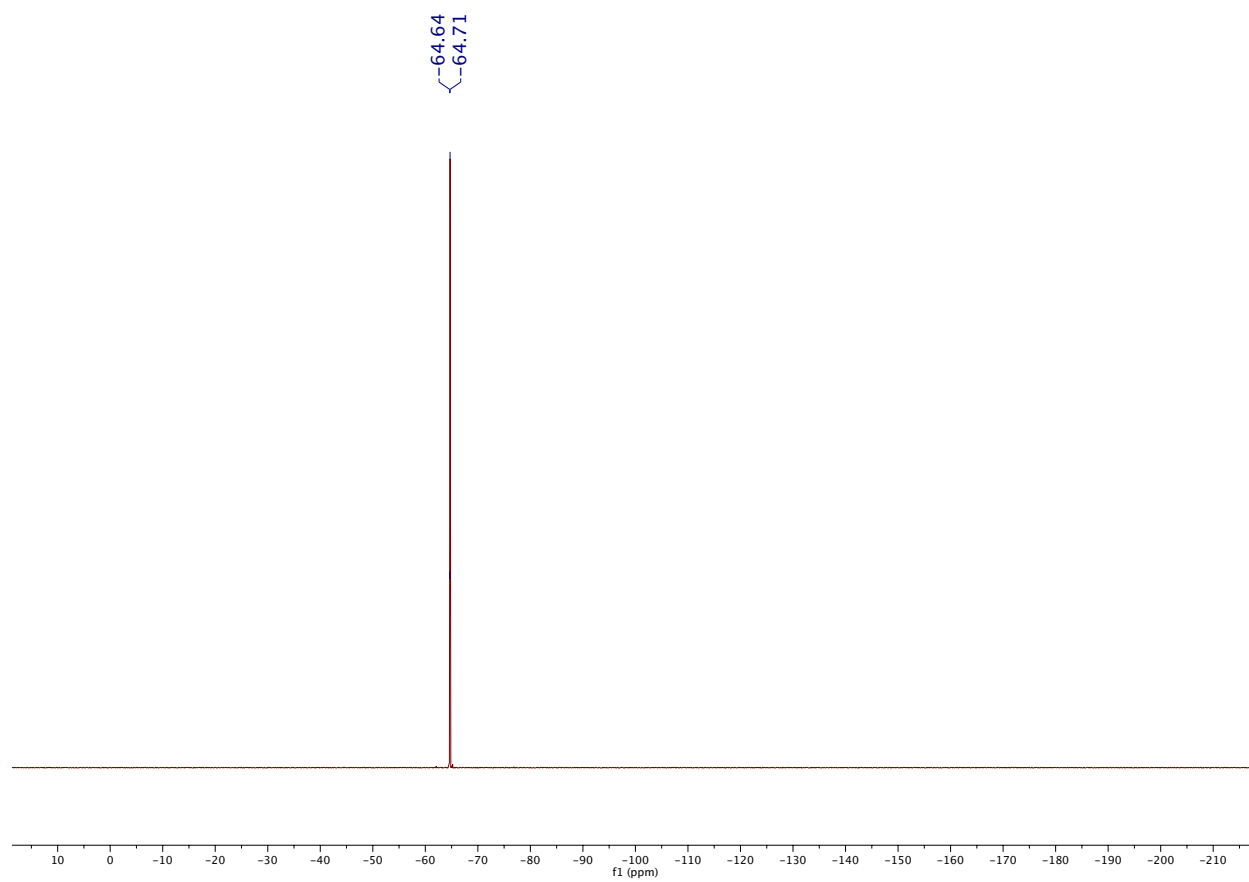


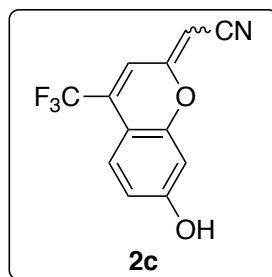
¹³C NMR



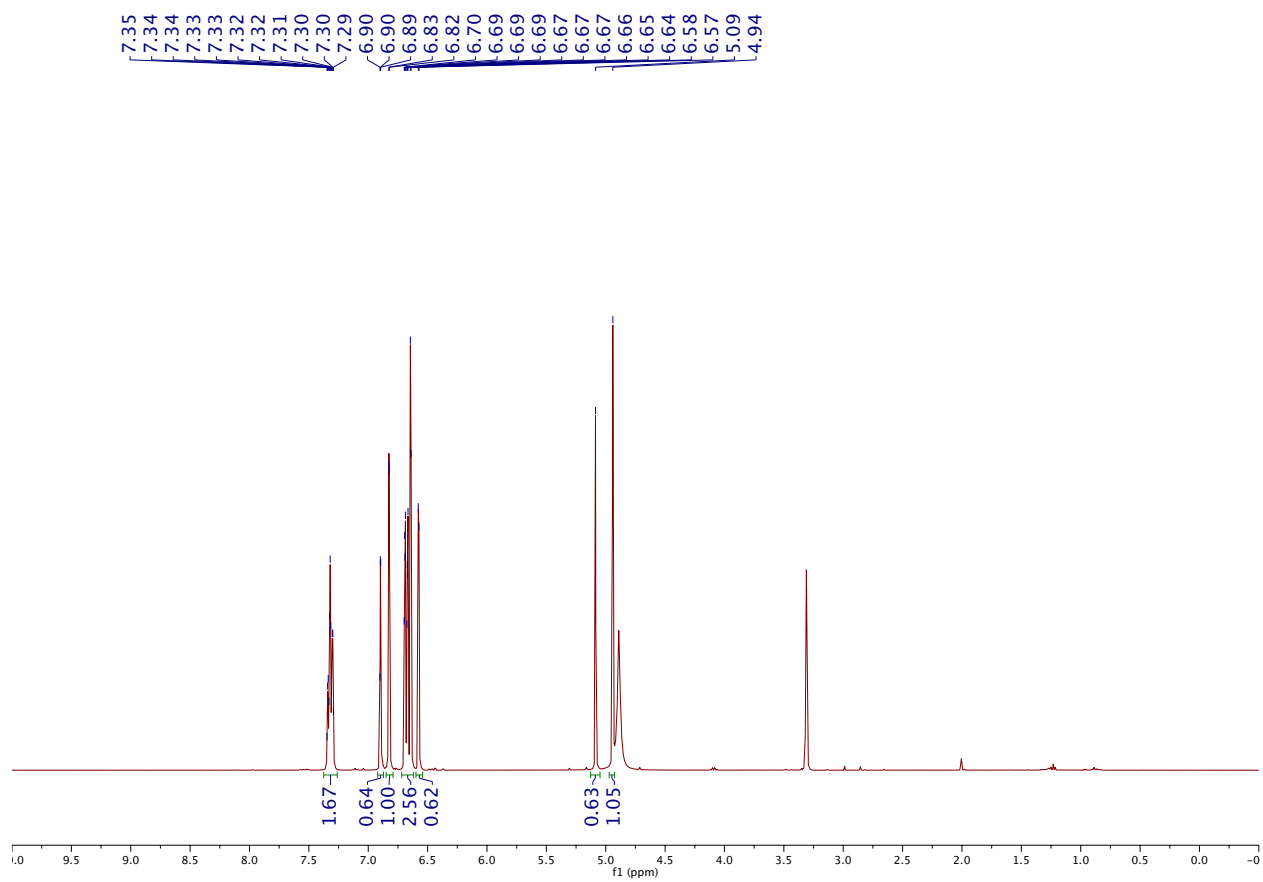


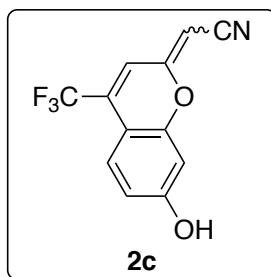
¹⁹F NMR



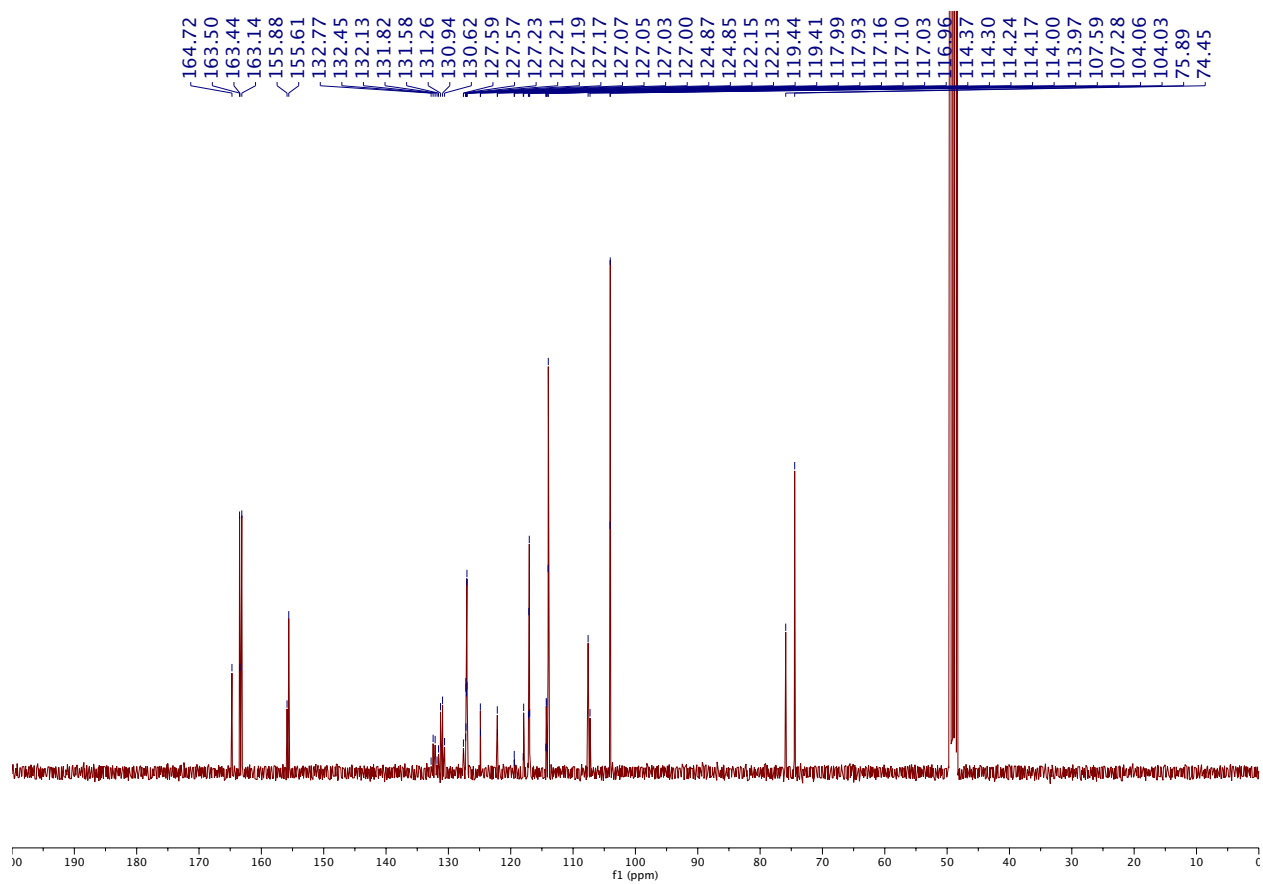


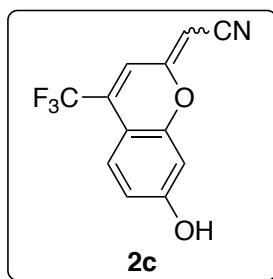
¹H NMR



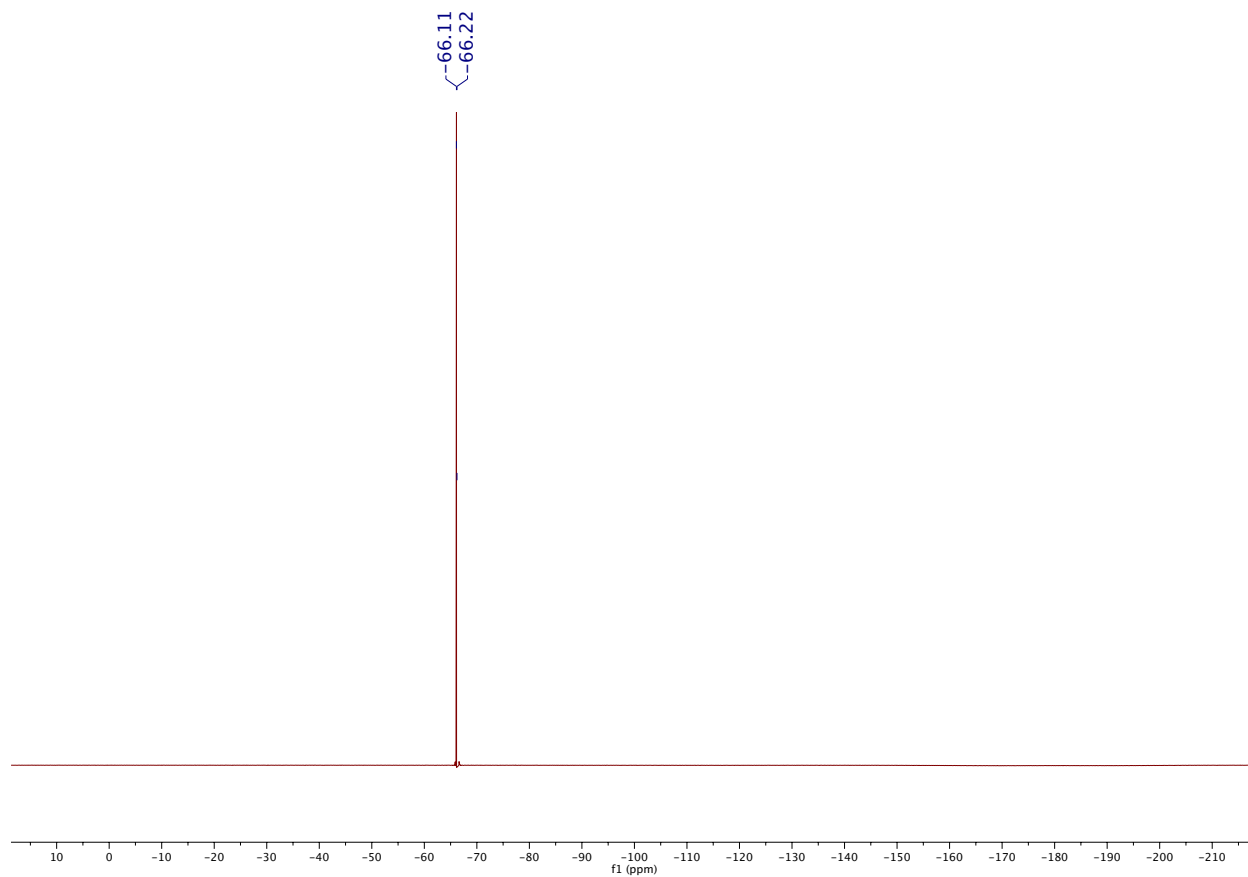


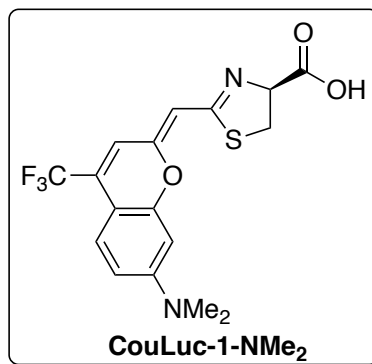
¹³C NMR



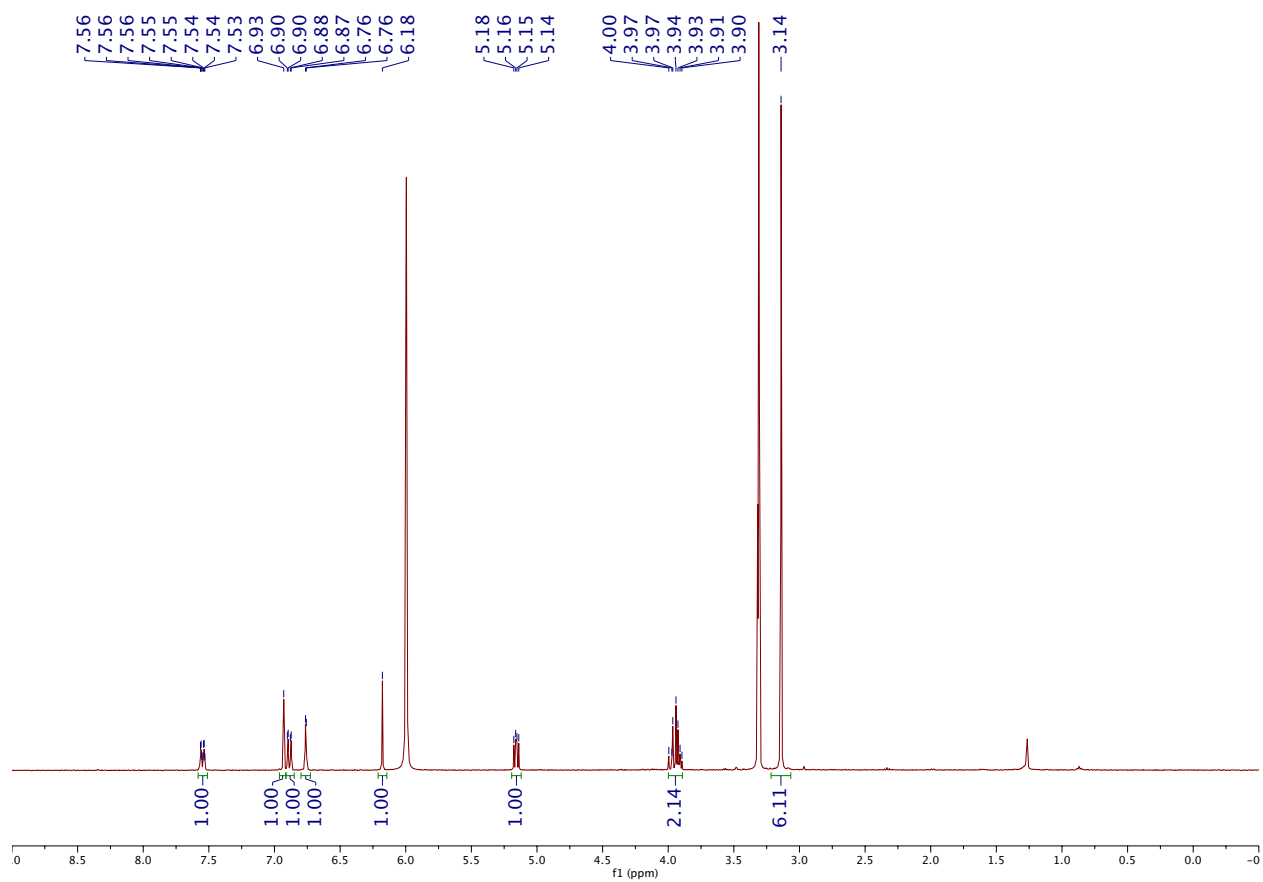


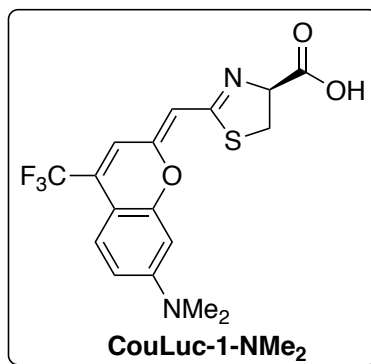
¹⁹F NMR



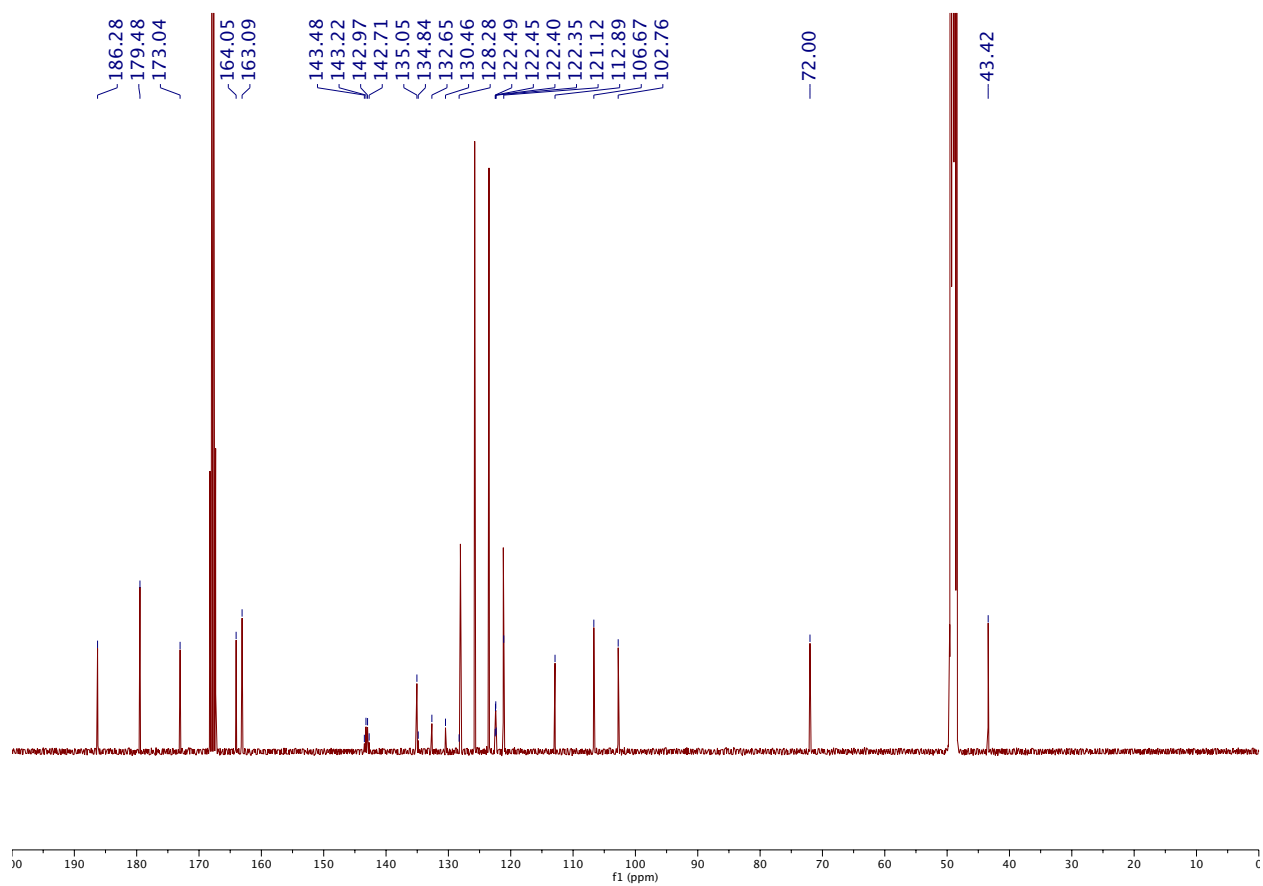


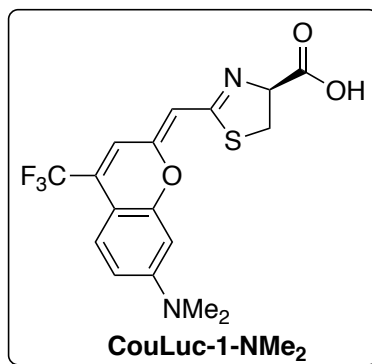
¹H NMR



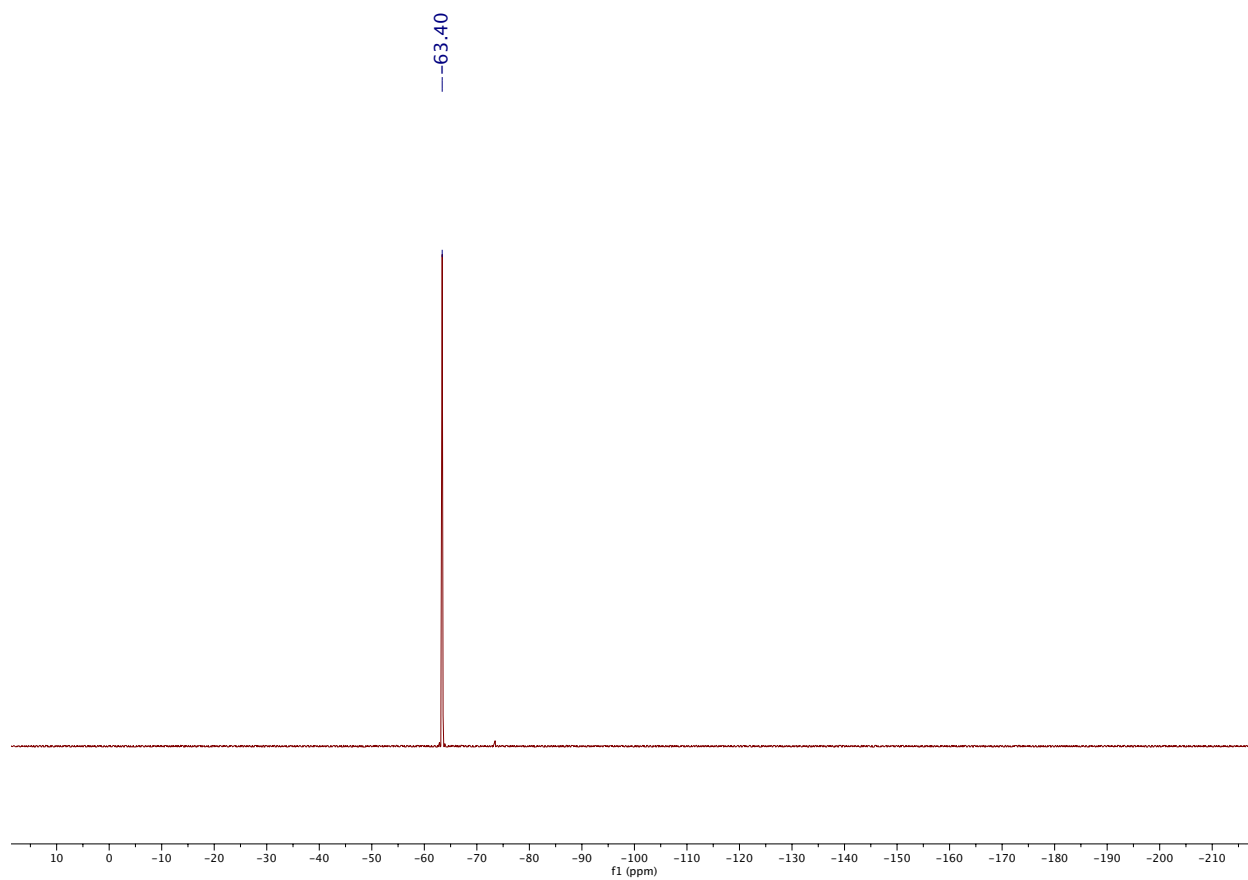


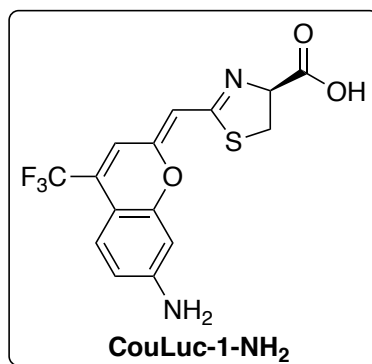
¹³C NMR



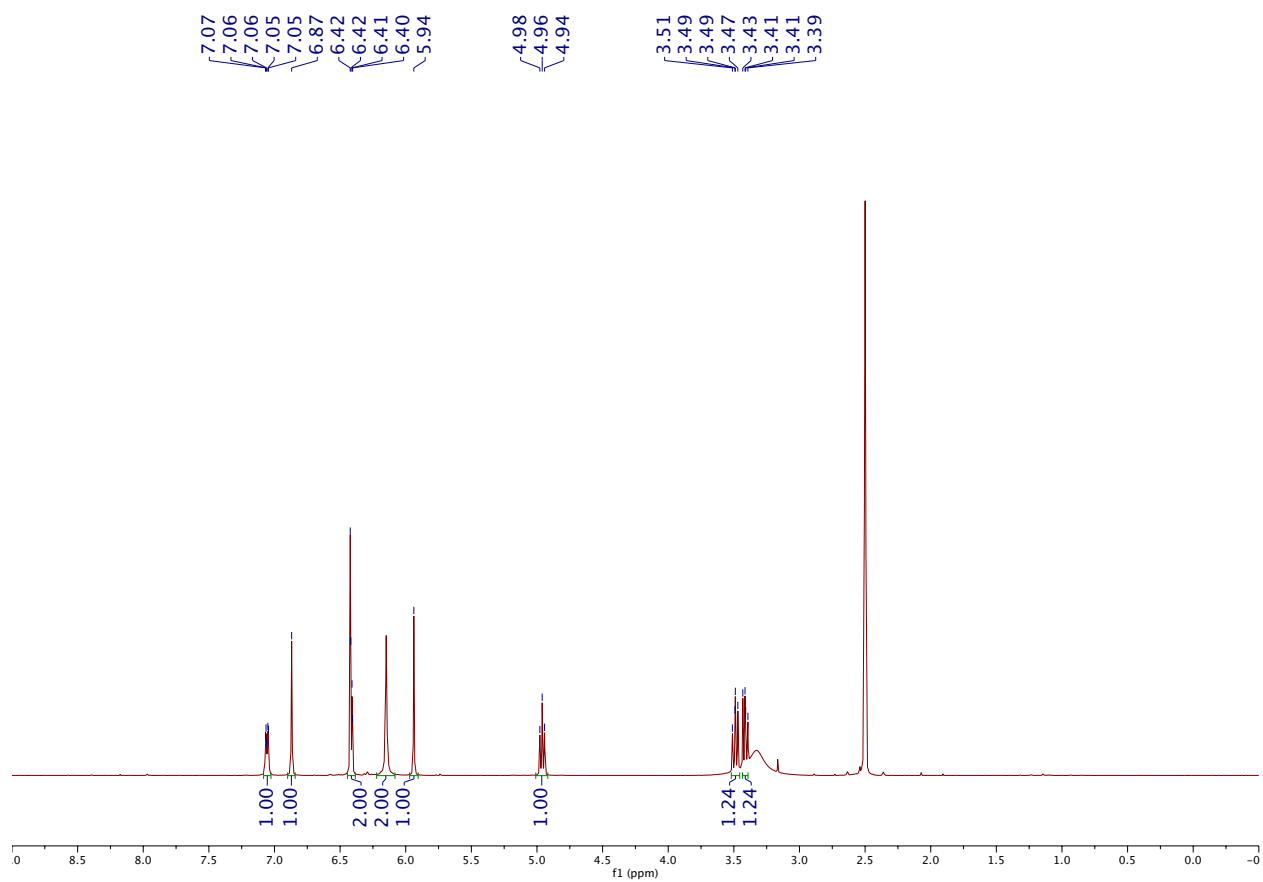


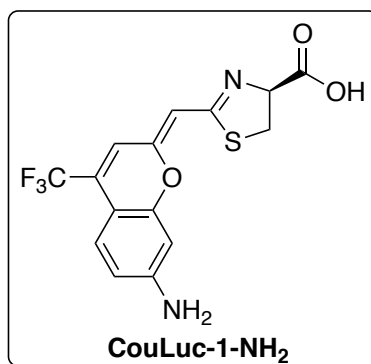
¹⁹F NMR



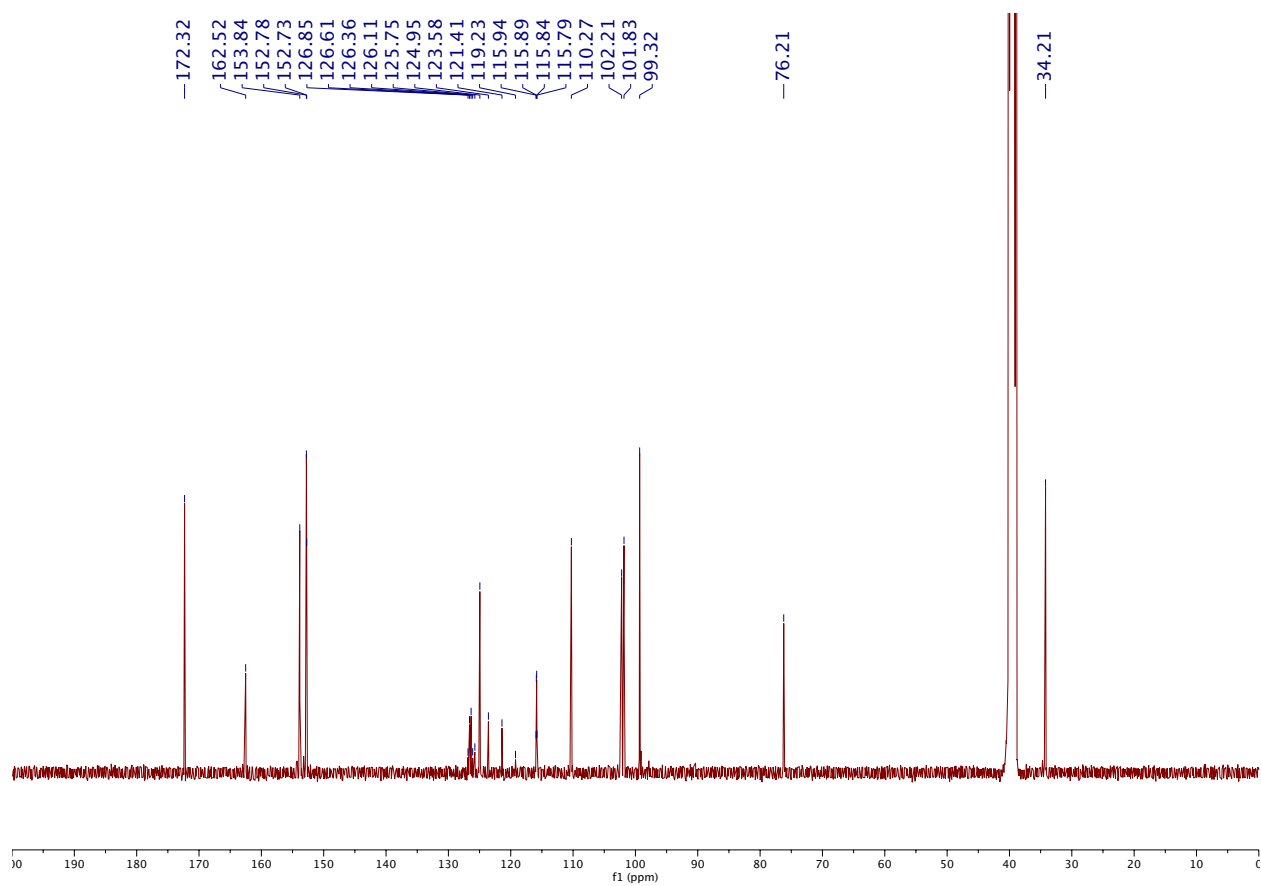


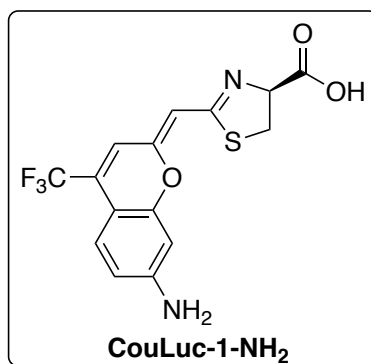
¹H NMR



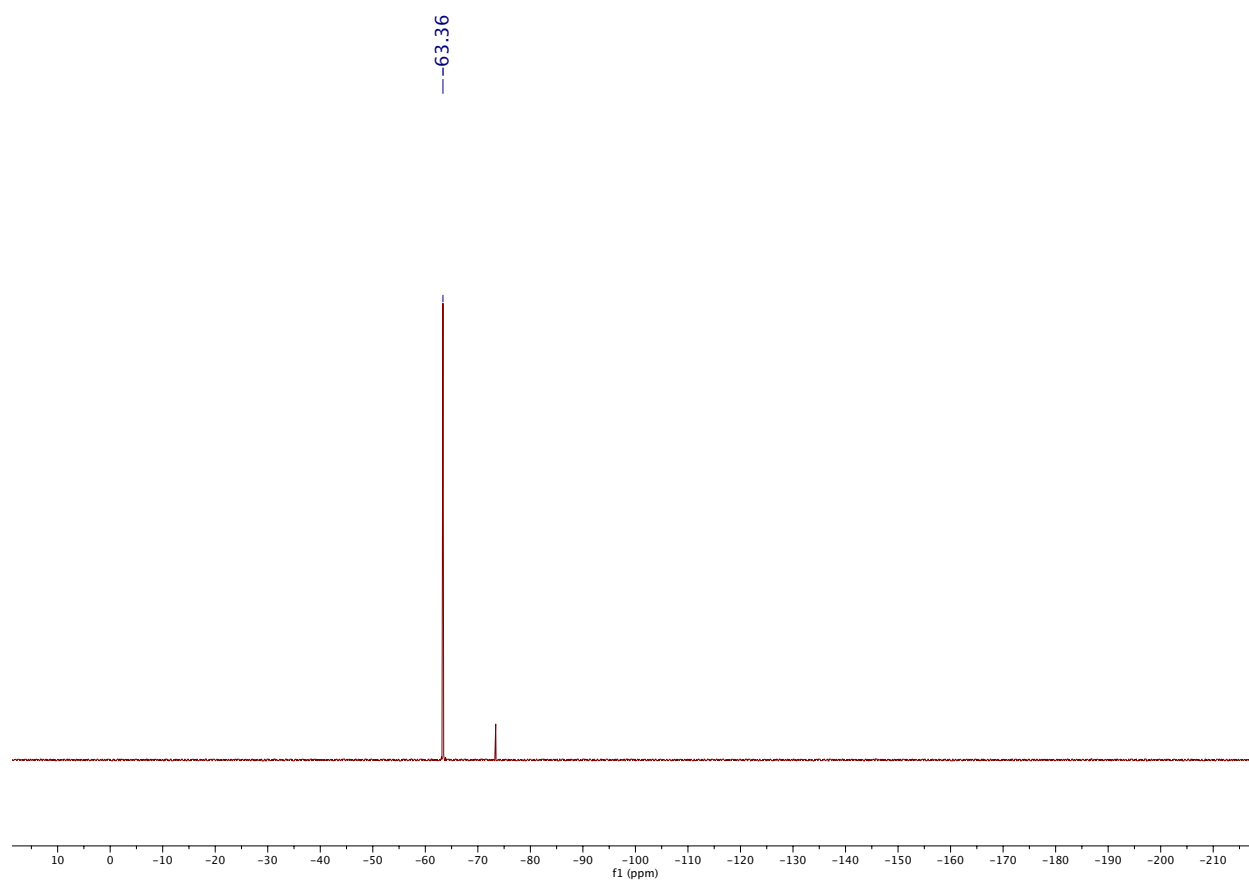


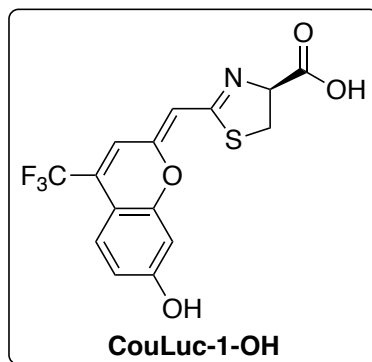
¹³C NMR



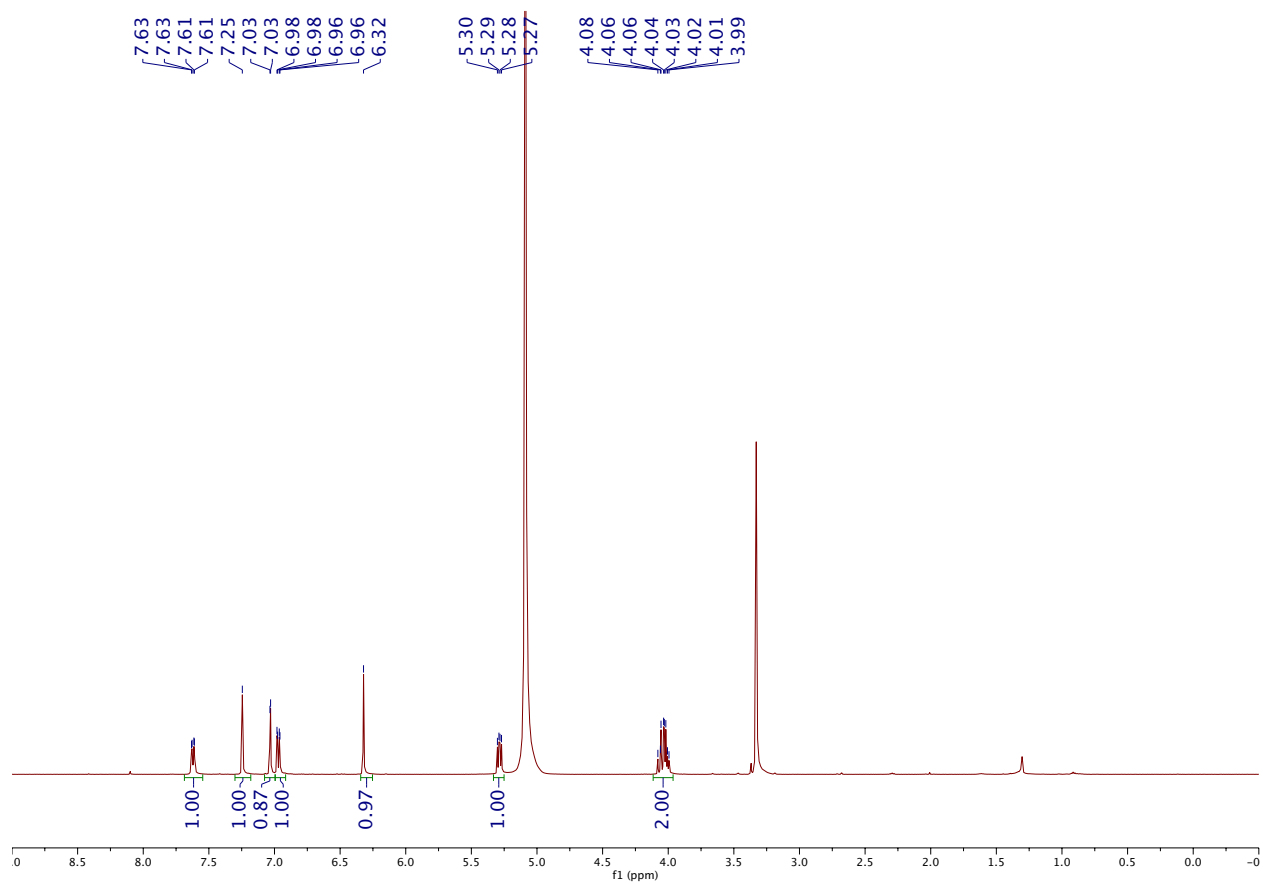


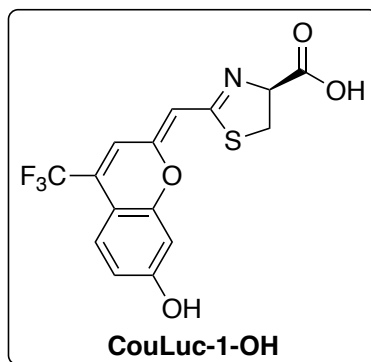
¹⁹F NMR



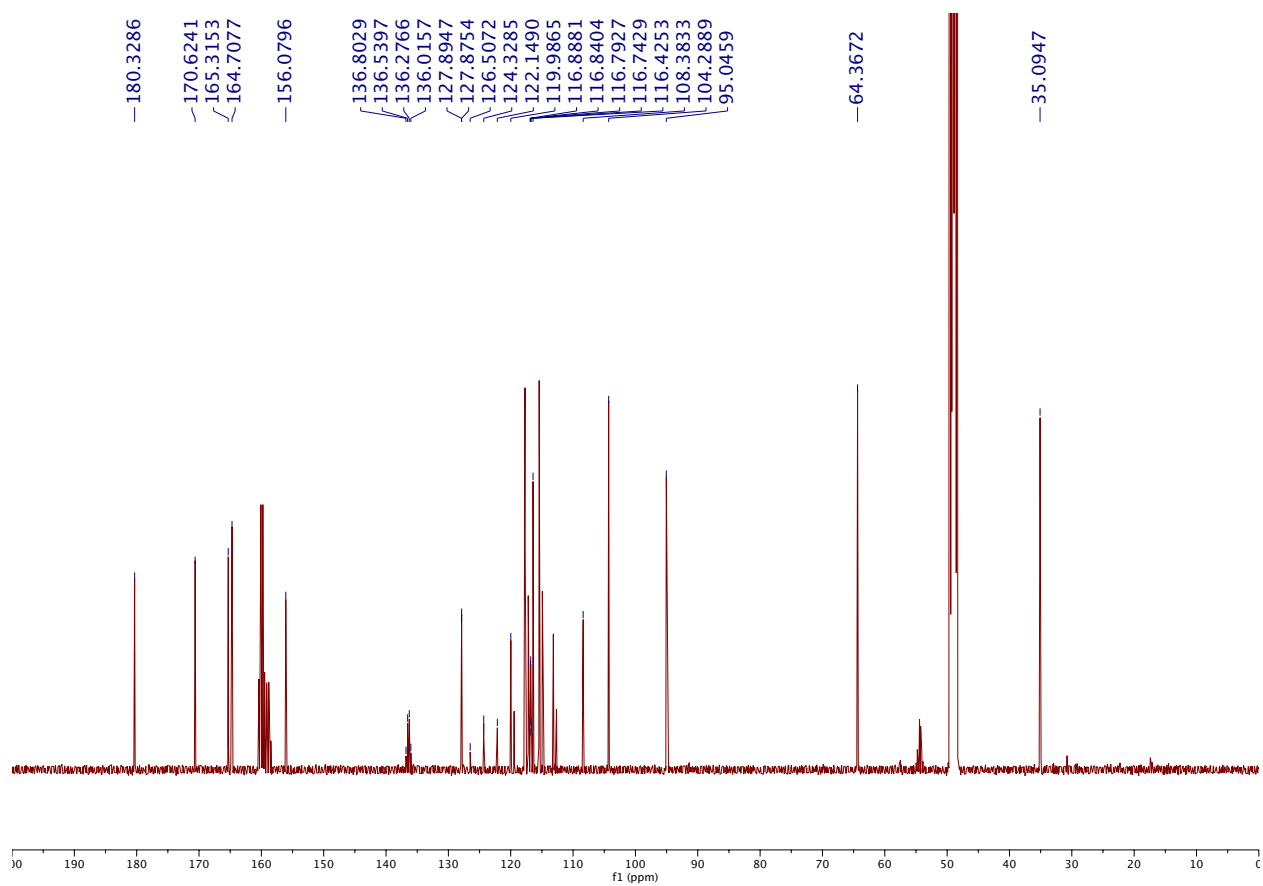


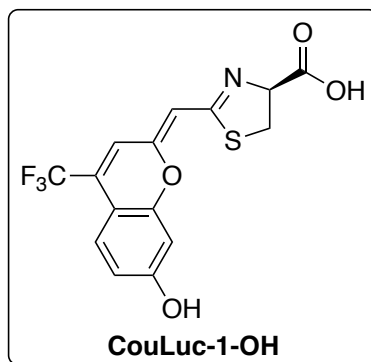
¹H NMR





¹³C NMR





¹⁹F NMR
CD₃OD + TFA-*d*₁

